A SOCIO-ECOLOGICAL UNDERSTANDING OF EXTREME HEAT VULNERABILITY IN MARICOPA COUNTY, ARIZONA

by

Juan Declet-Barreto

A Dissertation Presented in Partial Fulfillment
of the Requirements for the Degree
Doctor of Philosophy

Approved October 2013 by the
Graduate Supervisory Committee:

Sharon Harlan, Co-Chair
Bob Bolin, Co-Chair
Paul Hirt
Christopher Boone

ARIZONA STATE UNIVERSITY

December 2013

ABSTRACT

This dissertation explores vulnerability to extreme heat hazards in the Maricopa County, Arizona metropolitan region. By engaging an interdisciplinary approach, I uncover the epidemiological, historical-geographical, and mitigation dimensions of human vulnerability to extreme heat in a rapidly-urbanizing region characterized by an intense urban heat island and summertime heat waves. I first frame the overall research within global climate change and hazards vulnerability research literature, and then present three case studies. I conclude with a synthesis of the findings and lessons learned from my interdisciplinary approach using an urban political ecology framework. In the first case study I construct and map a predictive index of sensitivity to heat health risks for neighborhoods, compare predicted neighborhood sensitivity to heat-related hospitalization rates, and estimate relative risk of hospitalizations for neighborhoods. In the second case study, I unpack the history and geography of land use/land cover change, urban development and marginalization of minorities that created the metropolitan region's urban heat island and consequently, the present conditions of extreme heat exposure and vulnerability in the urban core. The third study uses computational microclimate modeling to evaluate the potential of a vegetation-based intervention for mitigating extreme heat in an urban core neighborhood. Several findings relevant to extreme heat vulnerability emerge from the case studies. First, two main socio-demographic groups are found to be at higher risk for heat illness: low-income minorities in sparsely-vegetated neighborhoods in the urban core, and the elderly and socially-isolated in the expansive suburban fringe of Maricopa County. The second case study reveals that current conditions of heat exposure in the region's urban heat island are the legacy of historical marginalization of minorities and large-scale land-use/land cover transformations of natural desert land covers into heat-retaining urban surfaces of the built environment. Third, summertime air temperature reductions in the range 0.9-1.9 °C and of up to 8.4 °C in surface temperatures in the urban core can be achieved through desert-adapted canopied vegetation, suggesting that, at the microscale, the urban heat island can be mitigated by creating vegetated park cool islands. A synthesis of the three case studies using the urban political ecology framework argues that climate changed-induced heat hazards in cities must be problematized within the socio-ecological transformations that produce and reproduce urban landscapes of risk. The interdisciplinary approach to heat hazards in this dissertation advances understanding of the social and ecological drivers of extreme heat by drawing on multiple theories and methods from sociology, urban and Marxist geography, microclimatology, spatial epidemiology, environmental history, political economy and urban political ecology.

DEDICATION

A mi Abuelo Juan, por enseñarme a distinguir la Verdad de la Mentira. A mi Bertha Lilia, por su amor, paciencia, cariño, y por siempre apoyarme en todos mis afanes. A mi Sophia Ximena, por enseñarme el significado del amor incondicional.

ACKNOWLEDGEMENTS

This dissertation is the fruit of five years of interdisciplinary research; its scope and breadth continuously expanded the boundaries of my original domains of theoretical and methodological knowledge. The diverse group of mentors, colleagues, and fellow researchers with whom I have been involved greatly influenced the present attempt at a holistic understanding of heat vulnerabilities. First among these is the essential mentoring of my dissertation committee, especially Sharon Harlan and Bob Bolin. Sharon helped me both broaden and deepen my understanding of scholarly and scientific research, and provided financial support and sagely advice every step of the way. Bob always helped steer the work's theoretical underpinning and relevance to the broader justice and societal issues ("theoretical theory", as he likes to say) in which environmental vulnerability scholarship must necessarily be framed. The many conversations I had with Paul Hirt during the early stages of this work made me realize that geographers interested in history are not so different from environmental historians, and that it's not true–as I thought at some point and now stand corrected–that the latter don't care for theory. Paul also helped to make the often dense theoretical foundations more accessible to broader audiences. Finally, Chris Boone helped locate my research within current environmental justice and urbanism theories.

The substance of the work presented here developed under the generous auspices of the Urban Vulnerability to Climate Change: A System Dynamics Analysis (UVCC), a Coupled Natural and Human Systems National Science Foundation grant (GEO-0816168). The support of the NSF is greatly appreciated. Continuous collaboration with friends and colleagues in the UVCC research group helped shape the interdisciplinary character of this work. Special thanks go once again to Sharon Harlan for giving me the opportunity to be part of this excellent team of researchers. Thanks also to Tony Brazel, Darren Ruddell, Diana Petitti, Chris Martin, Darrel Jenerette, Susanne Grossman-Clarke, Gerardo Chowell-Puente, Will Stefanov, Shuo Yang, Tommy Bleasdale, and Tim Lant for providing data and helping to resolve methodological issues in their particular fields of knowledge. To Ben Ruddell and Winston Chow, collaborators of the UVCC grant who joined us along the way, I thank them for providing their climatological and computational modeling knowledge; I incorporated their insights into this work as much as possible. I'd like also to recognize the assistance of Tiffany Halperin and Juan Brenes García, two landscape architecture practitioners who provided essential visions of what landscape forms for urban heat island mitigation could look like.

Evidence of the past is often buried among the papers and photographs of those with enough vision–or privilege–to be able to document it. Christine Marín and Rebekah Tabah, historical data archivists at Arizona State University who assisted me in locating hard-to-find data sources from Phoenix's past, also deserve my thanks for helping find and make sense of such evidence, critical to reconstruct the past.

To my friends and colleagues in the Environmental Social Science program, especially to Tommy Bleasdale and Katelyn Parady, I'd like to say thank you for sharing the journey of discovery into Phoenix's social and environmental past, and also for the dense and at times testy theoretical discussions and argumentation in class. It is perhaps what I will miss the most from post-graduate school. Too bad we never got around to organizing that Harvey reading group.

To the people of Sherman Park, especially Chug, Art, Joe, and Emma: the dedication you show for your neighborhood helps shape a more equitable and environmentally-sound future; it continuously inspires me to imagine better futures.

Lastly, I have to thank my wonderful wife Bertha Declet-Arroyo for her love and patience, and also for giving me the greatest gift I could ever hope for: our daughter Sophia Ximena. She came into our lives halfway through this dissertation process, boosting my impetus for articulating a better tomorrow.

TABLE OF CONTENTS

LIST OF TABLES

LIST OF FIGURES

Chapter 1

PRESENTATION OF THE RESEARCH PROBLEM

1.1 Introduction

Environmental hazards in the context of global climate change

There is consensus within the scientific community that climate change is occurring and affecting socio-ecological systems (IPCC Working Group I 2013). Climate change is increasing the frequency, duration, and intensity of environmental hazards like floods, droughts, storms, and cold and heat waves, in addition to contributing to sea-level rise. The Intergovernmental Panel for Climate Change (IPCC) estimates that the 0.5 °C increase registered in mean global temperatures since the 1970s is largely attributable to accumulation of greenhouse gases concentrations (IPCC Working Group I 2013). Future projections predict that by mid-century, global temperatures will increase in the range of 0.3 to 0.7 °C (IPCC Working Group I 2013), also increasing the variability–and thus unpredictability–of extreme climatic events (McMichael et al. 2006). In its latest Assessment Report, the IPCC states with "very high confidence" that regional temperature increases in all continents and most oceans are affecting physical and biological systems (IPCC Working Group I 2013). For example, in the global hydrological system, glaciers are melting, lakes and rivers are becoming warmer and water quality is being affected, contributing to the disappearance of coastal wetlands and elevating sea levels. Changes in faunal and floral species abundance and elevational shifts and poleward migration of certain faunal species suggest that global warming is triggering adaptation responses in terrestrial ecosystems.

Social systems within and across national boundaries are being affected as well: in underdeveloped countries in particular, changes in the spatial and temporal extent of climate events are driving rural-urban national and international migration in response to hazards (Wisner 2004). Although identifying the contribution of anthropogenic practices to climate change is often confounded by natural climatic variability and non-climatic drivers of global change, climate change research has linked responses to changes in biophysical systems to human action (IPCC Working Group I 2013); furthermore, research shows that changing variability in the global climate system cannot be explained alone by natural fluctuations. Economic expansion, urban development and land use/land cover change are among the anthropocentric, non-climatic processes that are bringing changes to socio-ecological systems across global, regional, and local scales, and adversely affecting human health and livelihoods (Terrain Group 2007; Carnesale and Chameides 2011).

Human health impacts are some of the most concerning outcomes of environmental hazards and climate change, receiving ample attention by researchers. Among these are mortality and morbidity from thermal stress (Patz et al. 2000; Meehl and Tebaldi 2004; Stott et al. 2004), heat waves (Harlan et al. 2006; Meehl and Tebaldi 2004; Anderson and Bell 2011) and increased concentrations of particulate matter, ozone, and other air contaminants (Kinney 2008; Mills 2009), loss of life from cyclones, floods, storms, and droughts (Milly et al. 2002; Bronstert 2003; Pilkey and Cooper 2004), infectious disease and microbial proliferation (Reeves et al. 1994), food yield and nutrition reductions due to impaired crops, livestock, and fisheries (McMichael 2001; Parry et al. 2004), and livelihoods disruptions due to poverty and outcomes related to these hazards.

Climate change-induced health impacts are unequally distributed, not only between developed and underdeveloped countries, but also among different demographic groups within countries, regions, and locales. Small island states, for example, are more vulnerable to sea-level rise and other disruptions than countries with higher standing in the global political economy (Ebi et al. 2006). Within nations or regions, different demographic groups experience climate change impacts differentially. Women, the very young or very old, and those with mental or physical disabilities, for example, are at higher risk for adverse climate change impacts (Cutter 1995; Fothergill and Peek 2004; Sheffield and Landrigan 2011). In addition, these demographic groups may already be disadvantaged socially, economically, or politically, magnifying their vulnerability to climate change effects (Balbus and Malina 2009). In both developed and underdeveloped countries, vulnerable populations are often urban and poor (Kovats and Akhtar 2008; Feiden 2011). Past research recognized the unequal nature of climate change impacts, and that inequalities in vulnerabilities arise out of the social, economic, and institutional circumstances enveloping countries, regions, locales, and the populations within (Adger 1999; Wisner 1978). Current vulnerability research continues this framing, focusing on socio-economic and structural inequalities in the production of climate change-related hazards (e.g., Adger 2006; Brooks et al. 2005;Collins 2010; Mustafa 2005).

The regional and local contexts of environmental hazards: Climate change in cities in the United States

In the United States, the main observed impacts of climate change include a 2°F increase in mean air temperatures over the last 50 years, sea-level rise, erosion, and disappearing wetlands along the coastal regions, snowpack melting, and increases in the frequency and intensity of precipitation, droughts, and wildfires (Carnesale and Chameides 2011). The western and southwestern United States are predicted to continue the trend towards dryer conditions due to increased greenhouse gas

concentrations (Seager and Vecchi 2010). As a result, these regions have seen an increase in the number of heatwaves in the early 21st century (Peterson et al. 2013).

Global and regional changes in hydrologic and climatic systems are the backdrop for the rapid demographic, economic, and ecological changes that cities in the southwestern United States are experiencing. Climate change in cities operates not only through the global-scale processes described above, but also have regional/local manifestations due to socio-ecological processes like rapid population growth, urban expansion, and land use/land cover change. These changes are exerting regional and local pressures on natural and urban ecosystems already under stress due to climate change-induced alterations, and are presenting challenges to the viability of continued human occupation (Theobald et al. 2013).

Understanding the socio-ecological production of climate change-related hazards vulnerability: Urban Heat Islands and extreme heat in cities

The effects of global climate change in cities are magnified by increases in the intensity and frequency of heatwaves and extreme heat due to urban heat island (UHI) magnitudes, one of the most evident consequences of localized climate change in cities (Oke 1982). UHIs are characterized by significantly higher nighttime temperatures in the built environment in comparison to surrounding rural environments (Lowry 1967; Balling and Brazel 1987; Oke 1997).

Extreme heat in urban environments is the result of processes of urban development and local and global climate change that operate on coupled human-ecological systems through alterations to surface and atmospheric energy balances (Jenerette et al. 2007; Brazel et al. 2000). Extreme heat hazards occur in seasonally hot climates and during summer heat waves, and are amplified by city-specific UHIs and localized climate change effects. Heat waves linked to global and regional climate change have increased in frequency and intensity over the 20th century as high temperatures exceed normal ranges of temperature variability (Meehl and Tebaldi 2004; IPCC Working Group I 2013). Among weather-related hazards, extreme heat accounts for the majority of fatalities in the United States (CDC 2006). Extreme heat is a summertime phenomenon and prolonged events during the season are common. Additionally, intra-urban exposure varies according to ecological and built environment structure (Harlan et al. 2006; Jenerette et al. 2007). Extreme heat affects human health by disrupting the thermoregulation capacity of the body, which shifts blood away from vital organs in the body's effort to cool itself (Basu and Samet 2002; Bouchama and Knochel 2002). Decreased blood flow in organs

like the heart and lungs can increase heat-related morbidity (e.g., hospitalizations), and mortality (i.e., death). Morbidity and mortality related to excessive heat are mediated in human bodies by physiological characteristics of individuals, such as increased blood pressure, respiratory or cardiovascular diseases, diet, and obesity (Yip et al. 2008;Cutter 2002; Uejio et al. 2011; Romero-Lankao et al. 2012).

In naturally-hot urban environments like Maricopa County, Arizona, UHIs are creating increasingly high and unequally-distributed human health burdens. The spatial heterogeneity of UHI magnitudes shapes a landscape of unequal heat burdens at the urban scale. Heat burdens are distributed unequally in cities due to social and ecological resource disparities created by the process of urbanization. Urbanization alters the distribution of natural resources and ecosystem services that regulate and mitigate urban temperatures. For example, exposure to the UHI is typically highest in central business districts (CBDs), where high rates of solar energy absorption into vertical and horizontal impervious surfaces, and dense concentrations of heat-emitting vehicular and industrial activities occur. Sensitive populations include the urban poor and ethnic minorities, who possess little in the way of social or economic resources to protect themselves from the health effects of heat; their neighborhoods are devoid of ecological coping resources like heat-mitigating vegetation, but abundant in heat-retaining impervious surfaces.

Heat hazards created or exacerbated by global and local climate change effects are the outcome of multiple and complex socio-ecological processes operating at multiple spatial scales (Blaikie 1994; Adger 1999; Cutter 2002). Understanding how human groups are differentially affected by environmental hazards, uncovering how they are produced, and formulating interventions to reduce human vulnerability to their effects requires an approach that recognizes the interactions between anthropogenic and biogenic processes in shaping hazards.

The localized impacts of climate change are increasing heat-related and other environmental stresses in cities, adversely affecting human health and the biophysical environment (IPCC Working Group I 2013; Wilhelmi and Hayden 2010). Vulnerability to extreme heat is an unevenly-distributed outcome of socio-economic and ecological processes in urban environments. In order to understand and devise solutions to minimize human and ecosystem impacts, it is critical first to understand inequality in present conditions of heat-related vulnerability among human populations. It is essential also to reveal the trajectories of urban development and land use/land cover change that produce

present-day vulnerability because understanding the history and geography of heat-related vulnerability can help prepare for the next step of informing equitable and sustainable mitigation interventions.

A research program that engages the complexity of socio-ecological factors that shape extreme heat vulnerability in cities is critical to 1) assess the uneven socio-spatial distribution of heat vulnerability among human groups; 2) uncover the trajectories of urban development in the production of hazards related to increasing temperatures; and 3) formulate and evaluate interventions to mitigate extreme heat. This dissertation focuses on these three research activities to achieve an integrative, interdisciplinary understanding of extreme heat vulnerability in cities. The dissertation is structured around three case studies that draw on various theoretical and methodological frameworks to illustrate different dimensions of extreme heat vulnerability. I draw on social and health sciences, critical geography, urban political ecology, environmental history, and urban climatology. Finally, I reflect on the contributions of the three case studies to understanding heat-related risks and the strengths and weaknesses of my interdisciplinary approach.

This dissertation makes three main contributions to understanding heat-related hazards. First, the modeling of heat-related vulnerability includes human health outcomes data from heat-related hospital visits. The hospital visits records allow me to evaluate a proposed heat vulnerability model against individual health-based outcomes, a methodology frequently absent in vulnerability research. Second, uncovering the trajectories of urban development in creating hazardous environments provides a structural, historico-geographical framework in which to understand the production of current climate change vulnerabilities to environmental hazards like extreme heat. Third, the evaluation of a heat mitigation intervention assesses the potential of vegetation in reducing extreme heat exposure. Taken as a whole, this study contributes to an integrative and interdisciplinary approach to understanding heat-related hazards by considering the historical, geographical, sociological, and microclimatological dimensions of extreme heat.

In this dissertation, I answer the following questions to increase understanding of heat-related vulnerability in cities:

1.2 Research Question 1: How does vulnerability to heat-related health outcomes vary according to socio-economic and ecological differences in neighborhoods in the urbanized area of Maricopa County, Arizona?

To answer this question, I evaluate the socio-spatial variability of health outcomes, sensitivity, and exposure that shapes present heat-related vulnerability in neighborhoods in Maricopa County, Arizona. I first estimate rates of summertime heat-related hospitalizations as a function of exposure to maximum daily air temperature. Second, I construct and map a predictive heat sensitivity index from socio-economic and biophysical environment variables identified in the climate change vulnerability and public health literature as influencing sensitivity to heat-related hazards. Third, I combine the hospitalizations data with the sensitivity and exposure components to estimate how sensitivity affects heat-related health outcomes. Fourth, I describe typical vulnerability profiles of neighborhoods to understand the factors that differentiate vulnerability in neighborhoods. Finally, I use the quantitative assessment of heat health-related exposure, sensitivity, and health outcomes to engage a more profound, place-based discussion of the conditions at the neighborhood and community scales that create different outcomes for heat-related vulnerability across urban Maricopa County.

1.3 Research Question 2: How has urban development in Maricopa County shaped the uneven landscape of socio-ecological heat hazards vulnerability during the 20th century?

Phoenix, the largest city in Arizona, was founded in the late 19th century as an isolated agricultural settlement. The original townsite has since grown into a conurbated metropolis of more than 4 million inhabitants through large-scale land use transformations brought on by agricultural, industrial, and suburban development. As urban development converts more land and industrial, commercial, residential, and transportation activities increase, multiple technological, industrial, and weather-related hazards have concentrated in the urban core, an area known informally as South Phoenix. The historical concentration of unwanted land uses like railroads and service railyards, highways, degraded housing stock, toxic emissions, manufacturing and other industrial activities in South Phoenix has created an urban landscape of uneven socio-ecological vulnerability. This landscape is characterized by human vulnerability to the deleterious impacts of air pollution, toxic substances, and extreme heat, exacerbated by race and class-based marginalization of low income and ethnic minorities in South Phoenix. The processes of large-scale, sustained land use transformation and segregation of

minorities have continuously shaped socio-ecological vulnerability in Phoenix. I refer to this socio-spatial distribution of vulnerability as a *riskscape*, or a landscape of uneven social and environmental risk vulnerability. I unpack in detail the history and geography of the production of the riskscape in Maricopa County and what it has signified for extreme heat risks.

1.4 Research Question 3: What is the potential impact of increased vegetation in mitigating extreme heat in an urban core neighborhood in Phoenix?

Increased vegetation can help reduce extreme temperatures, and research has shown that arid urban cores can receive more cooling benefits than other areas. The heat-mitigating ecosystem services that vegetation can provide in arid cities can help address environmental justice concerns of low-income communities. I use microclimate modeling to evaluate potential air and surface temperature differences between existing low vegetation conditions in an urban core neighborhood park and a proposed vegetation regime informed by Urban Heat Island mitigation goals. I also use spatial autocorrelation analysis to estimate the spatial footprint of an extreme heat-mitigating effect known as the Park Cool Island.

Chapter 2

AN INTERDISCIPLINARY THEORETICAL FRAMEWORK TO UNDERSTAND HEAT-RELATED VULNERABILITIES

Concern with the human health impacts of climate change has spurred considerable interest among vulnerability researchers. A focus on vulnerability is important in order to define threat magnitudes and inform remedial action aimed at limiting climate change impacts through coping strategies and adaptation (Smit and Wandel 2006). Lack of concrete action to reduce greenhouse gas emissions through international agreements (e.g., the lack of progress resulting from the 1997 Kyoto Agreement), has locked the globe into increased emissions through at least the first part of the 21st century, curtailing the possibility that reductions in vulnerability will occur through mitigation of climate change effects. In light of unmitigated warming emissions levels, informing strategies and policies for adaptation and coping capacities are currently the most relevant foci of vulnerability research (Neil Adger et al. 2005; Adger et al. 2007).

Human impacts from climate change-induced hazards emerge out of complex and dynamic socio-ecological processes that occur at multiple spatial and temporal scales. For example, emissions outputs from industrial activities operate at the global scale, increasing greenhouse gas circulation in the atmosphere and warming the planet. Socio-economic processes like economic development, migration, and international trade drive land-use changes that in turn drive climate change at local, regional, and global scales (Rosenzweig et al. 2007). At the local scale, the best-understood effect of land-use changes–the urban heat island–is observable over a 24-hour period as a day/night cycle of air temperature fluctuations in the urban canopy layer. At the same spatial scale, the regional urban development and land conversion processes that create urban heat islands unfold over a time scale most often measured in decades. The socio-ecological processes and practices engaged in by humans that create climate change are unequally distributed in urban space, and have unequal social and spatial outcomes, resulting in disparities in human health and livelihoods impacts. Understanding the spatio-temporal, multi-scalar complexities and socio-ecological dimensions of climate hazards requires scholarly and scientific knowledge developed across multiple research domains. These can encompass epidemiology, sociology, and geospatial technologies (to describe present human health vulnerabilities), historical geography, political ecology/political economy, urban geography, environmental history, and environmental justice (to excavate the historical and geographical transformations that create hazards

and vulnerable people), and urban ecology, climatology, and computational modeling of air-surface energy exchanges (to evaluate the effectiveness of adaptation and mitigation strategies).

This seemingly disparate ensemble of research disciplines can be harnessed into a coherent theoretical framework to leverage the explanatory power of each discipline's theory and methods in understanding present and past conditions, and, moving forward, formulate adaptation strategies. Vulnerability research and practice provide the most sophisticated framework for this task because of its consistent focus on socio-ecological systems, a concept that recognizes that human practice is deeply embedded in the ecological–or biophysical–realm (Hewitt 1983; Hewitt 1997; Wisner 2004; Cutter et al. 2000; Turner et al. 2003; Adger 2006; Kasperson and Kasperson 2013). Insights from the vulnerability literature resonate with political ecology perspectives that locate anthropogenic practices and processes in the biophysical environment along a milieu of "socio-environmental metabolic circulation", continuously transforming both the social and biophysical realms (Swyngedouw 2006, 13).

Vulnerability describes how susceptible social and ecological systems are to risks, and is focused on increasing human well-being through risk reduction. The integration of the concept into environmental hazards and risk research emerged as a progression from applied models focused on disaster events and post-event mitigation to integrative, holistic models encompassing the anthropogenic (e.g., cultural, political, economic) and biogenic (e.g., climatological, hydrologic) dimensions of human activity that create differential conditions of risk (Turner et al. 2003; Romero Lankao and Qin 2011). I now present important working definitions of vulnerability, and follow with a discussion of the evolution of vulnerability research that lends it a unique integrative perspective to understand heat hazards.

2.1 Definitions of vulnerability

Vulnerability is defined in many different ways. As mentioned above, a foundational definition frames vulnerability as describing "states of susceptibility to harm, powerlessness, and marginality" for socio-ecological systems (Adger 2006, 268). It has also been defined as the likelihood of a coupled human-environment system, or any of its components, to be harmed due to exposure to a hazard (Turner et al. 2003). In this definition, hazards are composed of *perturbations* (increased pressure outside the normal range of variability for the system, typically an externality), *stress/stressors* (gradually increasing or sustained pressure within the range of variability for a system, typically endemic to the system), and *risk* (the likelihood and magnitude of post-hazard event consequences). Cutter provides a similar definition of vulnerability as "potential for loss" (Cutter et al. 2003, 242) that

varies both spatio-temporally and among different groups, integrating exposure conditions that create vulnerability to extreme events with the social resilience of people and places to withstand loss. Following an extensive review of vulnerability terminology, Füssel (2007) proposed a common language to specify vulnerabilities along several dimensions: *temporal reference* (past, present, dynamic), *sphere* (or *scale*) of factors affecting vulnerability (internal, external, cross-scale), *domain of knowledge* of vulnerability factors (socio-economic, biophysical, integrated), the *vulnerable system* (the bounded geographical, ecological, or human population unit of analysis), the *attributes of concern* (the vulnerable system's attributes under threat, like human well-being or biodiversity), and the *hazard* itself (the actual or potential biophysical event that can cause damage).

Other definitions focused on social vulnerability take into account changing historical and environmental conditions, along with the institutional and political-economic arrangements that create resource insecurity and exacerbate vulnerabilities. For example, Adger (1996, 1999) frames vulnerability as a state of well-being experienced differently by populations according to environmental conditions, social norms, political institutions, resource endowments, technology, and social disparities. Bohle et al. (1994) present a structural framework where vulnerability is configured according to dynamic relationships among the three key elements of human ecology, political economy, and expanded entitlements. In this context, human ecology refers to anthropogenic transformation of biophysical environment properties like climates and land covers; the class and production relations that regulate distribution of surpluses as resources are contained in the political economy component; finally, the legal, extra-legal, or cultural arrangements through which individuals appropriate coping resources are captured by expanded entitlements.

Some of the definitions of vulnerability presented here highlight biophysical hazard events, while others focus on the social, political, and economic factors that make people vulnerable; however, the vulnerability concept brings these disparate definitions together in an attempt to describe a reality that is both dynamic and complex (Romero-Lankao et al. 2012). The complex dynamics of environmental change have led to the recognition that an adequate unit of analysis must simultaneously consider the human and ecological domains. An integrative ecological focus of analysis was originally conceived at the planetary scale as an "Earth System" by Schellnhuber (1998). As the concept became integrated in the natural and social sciences, it was applied at various spatio-temporal scales and referred to as socio-ecological system (Gallopín 2006), social-ecological system (Berkes et al. 2000), or coupled human-environmental system (Turner et al. 2003). These iterations of the term highlight not

only the inseparability of the human and ecological domains, but also posit that the interactions between these domains are critical to understanding conditions of vulnerability, resilience, and adaptive capacity (Turner et al. 2003; Walker et al. 2004).

2.2 Lineages of vulnerability research

The evolution of vulnerability research theory and practice over time provides increasingly cohesive frameworks that integrate previously isolated dimensions of social and environmental hazards, reflecting the range of research programs and paradigms in the literature (Eakin and Luers 2006). Three lineages focused on different dimensions of environmental change can be identified: one centered on risks and natural hazards, a second one focused on social vulnerability viewed through a political ecology/political economy lens, and finally, a perspective that emphasizes the ecological resilience of vulnerable systems (Eakin and Luers 2006; Romero Lankao and Qin 2011).

The risk-hazards tradition

Vulnerability research originated with the work of Gilbert White and others, and was instrumental in informing flood mitigation policy in the United States in the early 20th century (White 1974; Burton et al. 1978). Often termed the impacts tradition–but also called natural or risk-hazards–, this research originated as a branch of human geography and human ecology that emphasized biophysical exposure (e.g., floods), sensitivity (determining who is vulnerable), and potential consequences (assessing potential impacts). In this tradition, hazards are modeled as probabilistic events, while the magnitude of potential consequences to humans is dependent on physical proximity to an event's location (Tobin and Montz 1997). The Risk Hazards model is a hallmark of this tradition, moving causally from a hazard event (exposure) to human and ecological impacts (Burton et al. 1978; Kates 1985; Turner et al. 2003). The central agency given to biophysical events in this tradition has been critiqued for placing the event at the start of the causal chain of events that produce vulnerability (Hewitt 1997). Others have argued that emphasizing post-event responses of improving prediction and regulation (e.g., forecasting and flood control) is at best a mitigation effort that ignores the social contexts through which different populations become vulnerable and cope with hazards (Mustafa 1998, Bankoff 2001). The dominant theme of control over the biophysical environment in the impacts tradition views hazards as a disruption of otherwise stable biophysical systems.

The social vulnerability tradition

In response to the biophysical event focus of the impacts/risk-hazards tradition, neo-Marxist political economists argued for structural interpretations of the inherent vulnerability of populations (Hewitt 1983; Blaikie 1994; Bohle et al. 1994). Sen's (1981) seminal work on entitlements and capabilities was critical in shifting attention from biophysical impacts to the social, economic, cultural, and political processes that enable or hamper adaptive capacities to mitigate climate change vulnerability. These works brought human-environment relations to the forefront of vulnerability research, opening up the field to a more dynamic understanding of vulnerability as a condition arising out of historical and geographical processes. Political ecologists have further balanced the field by giving equal explanatory power to both biophysical processes and social dynamics (Eakin and Luers 2006). For political ecologists, vulnerabilities emerge as the outcome of existing structural, socio-economic and political inequalities among actors (e.g., government bureaucracies, peasants, landowners) that sort out environmental winners and losers on multiple scales (e.g., local, regional, national, global). For example, rural villagers in Pakistan are vulnerable to flood hazards due to social disempowerment created by the state bureaucracy through urban/rural disparities in the distribution of entitlements like access to finance capital for agricultural inputs and the concentration of large landholdings in fewer hands. National-scale structural conditions are exacerbated by policies attendant to the exigencies of cash crop production for global markets, increasing vulnerability for the rural poor who live in flood-prone areas. (Mustafa 1998).

The ecological resilience tradition

Shifting away from the emphasis on biophysical impacts, inherent social vulnerability, and socio-political conflict, some researchers have turned attention to the ability to bounce back from the impacts of hazards. Populations and other systems possess–researchers argue–varying degrees of ecological resilience that allow for recovery from hazards (Cutter et al. 2008; Leichenko 2011). Ecologist C.S. Holling (1973) introduced the term to characterize a system's ability to absorb disturbance and change while maintaining the relationships that govern the system's behavior, and has been recently expanded to describe a system's ability to preserve both structure and function in the face of change (Walker et al. 2004). Vulnerability research has incorporated the term resilience to describe the ability of socio-ecological systems (i.e., populations, communities, or ecosystems) to recover from disturbances brought on by socio-environmental or political change (Adger 2006). The ecological resilience perspective contributes to changing views of ecological systems as exhibiting non- and

multi-equilibrium characteristics that are influenced by non-deterministic factors, shifting a system's condition along a continuum of stable states. This is a shift away from previous, more rigid conceptualizations of systems as deterministic, single-state entities prone to collapse once an arbitrary tipping point is reached (Eakin and Luers 2006).

Three key dimensions of vulnerability

The three traditions of vulnerability research converge in an integrated framework to understand hazards. The socio-ecological system facilitates "systemic research on integrated social and ecological processes, nested spatial and temporal scales, feedback loops, and complex processes" (SOURCE 2007, 62). This interdisciplinary framework requires that vulnerability and its operational dimensions be specified in ways that are useful to social and biophysical environment scientists (Gallopín 2006). Three key dimensions of vulnerability are identified as part of the socio-ecological vulnerability framework, which I describe below.

Vulnerability occurs within a socio-spatially differentiated spectrum of exposure, sensitivity, and adaptive (or coping) capacity that can mitigate or exacerbate the impacts of environmental hazards like extreme heat (Romero Lankao and Qin 2011; Turner et al. 2003). Exposure usually refers to the biophysical environment's manifestation of hazards (e.g., extreme temperatures, flood, drought), and is usually expressed as a probability, duration, and spatial magnitude of occurrence (Cutter 1996; Luers et al. 2003; Mustafa et al. 2011). Sensitivity describes the degree to which populations are susceptible to the deleterious effects of exposure. Adaptive capacity encompasses the mechanisms through which populations cope with environmental hazards (Adger 2006). This tri-partite framework is commonly used throughout climate change vulnerability literature.

2.3 Synthesis of vulnerability research traditions for heat-hazards research

Although the vulnerability field in general is said to be fragmented (Eakin and Luers 2006), recent studies have argued for a synthesis of its lineages into an integrative framework that places more balanced attention on biophysical impacts, structural drivers and mechanisms, and ecological resilience factors that mediate vulnerability to temperature-related hazards (Romero Lankao and Qin 2011; Romero-Lankao et al. 2012). A recent meta-analysis of temperature hazards studies reveals that current research is mostly focused on biophysical impacts, often emphasizing the quantitative relationship between temperature and adverse health outcomes. The most consistent findings of these studies are that temperature-related mortality increases as "temperatures fall below or rise above certain threshold-values", that the elderly and those with pre-existing medical conditions are especially

vulnerable, and that higher levels of education–often an income and socio-economic status correlate–are associated with reduced vulnerability (Romero-Lankao et al. 2012, 6). Notwithstanding these valuable insights, studies in the vulnerability as impacts tradition generally ignore the social vulnerability and ecological resilience dimensions of climate change-induced hazards. The impacts tradition equates vulnerability to the magnitude of an event, not taking into account that the capacities of populations and ecosystems to withstand damage or recover are differentiated not just by proximity to events, but also by varying socio-demographic and ecological characteristics of people and places. Although analyses of individual or neighborhood socio-economic and demographic variables often identify vulnerable populations, impacts studies seldom interrogate processes within the political ecology of cities that create differential conditions of vulnerability.

In this dissertation, I explicitly integrate the explanatory potential of the risk-hazards, ecological resilience, and inherent vulnerability research traditions to gain a deeper understanding of heat-related hazards. I advance a conceptual, integrative model that combines the insights of the vulnerability traditions in relationship to each other, but also to the three key dimensions of vulnerability (Figure 2.1). In this model exposure and coping capacity emerge at the intersection of biophysical events (described by the risk-hazards tradition) with the social vulnerability of populations, but also with ecological vulnerability (renamed as the obverse of ecological resilience to indicate increasing vulnerability as resilience diminishes). Although the risk hazards tradition has usually treated biophysical events (e.g., floods, droughts) in isolation from social dimensions, exposure–and hence vulnerability–is inherently related to the presence of people. For example, the combination of populations with low socio-economic status living in urban cores where the highest urban heat island intensities are found creates high exposure to heat waves and extreme temperatures. The social and ecological vulnerability of these populations also suggests they may have diminished resources to cope with heat, which can be related to socio-economic characteristics like neighborhood trust and networks (i.e., social capital), income to run air conditioner units or to water shade-providing vegetation, or vacation in cooler climates during the summer. Similarly, sensitivity can be framed as the ensemble of the characteristics of the social and ecological systems that increase vulnerability. This is the case where low socio-economic status neighborhoods with little shading vegetation and surrounded by heat-retaining land uses like transportation corridors and industrial infrastructure become highly sensitive to heat hazards.

At the center of the model is a quantifiable measure of vulnerability to extreme heat: impacts to human wellbeing like heat-related morbidity or mortality. The implementation of the model takes place

through formal specifications of exposure, sensitivity, coping capacity, and human health outcomes, useful to unpack the causal factors that create impacts. Taking into account the inherent spatio-temporal variability of the three dimensions helps establish how inequalities in the burden of vulnerability differentially affect human livelihoods across the socio-ecological system. The strength of the model lies not only in combining the insights from the research and practices pertinent to each tradition reviewed above, but also in its integration of research venues concerned with environmental hazards, but traditionally outside the scope of vulnerability research. For example, sociology, environmental history, environmental justice, and historical geography have much to say about the historical processes that create the multiple, current differential vulnerabilities found in urban environments. In this way, I incorporate Adger's advocacy for an integrative and holistic understanding of vulnerability based on the analysis of present-day vulnerability informed by historical perspectives (2006). Another key to understanding characteristics of the biophysical environment that create present-day heat vulnerabilities is the description of air-surface energy exchanges in cities, well described by urban climatology and urban ecology, both disciplines which I draw upon in this dissertation. Finally, epidemiology, public health, and geospatial technologies research describe impacts on human wellbeing by harnessing all of these disciplines into a spatial epidemiology of human health outcomes related to extreme heat.

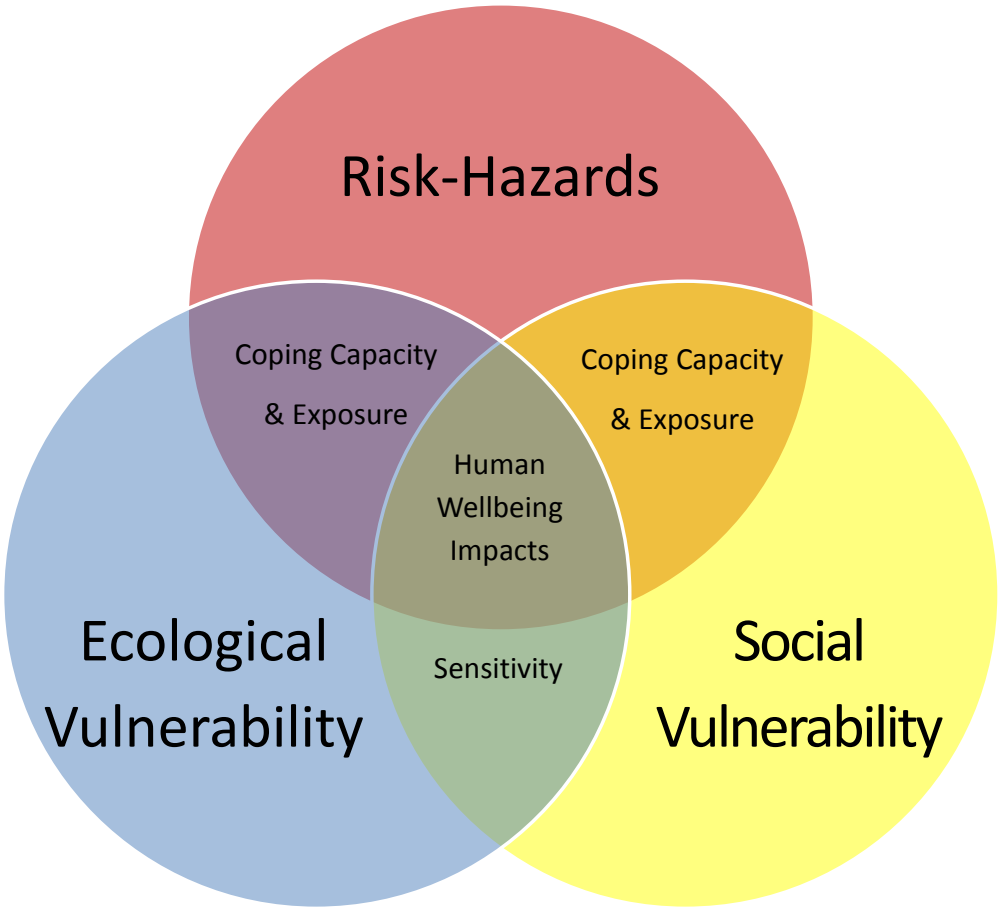

Figure 2.1: Integrative model of heat vulnerability, combining the three lineages of vulnerability research, the three key dimensions of vulnerability, and human health and wellbeing outcomes.

Chapter 3

HEAT VULNERABILITY IN MARICOPA COUNTY, ARIZONA: HEALTH OUTCOMES, SENSITIVITY, AND EXPOSURE AT THE NEIGHBORHOOD SCALE

3.1 About this chapter

In the following chapter I answer Research Question 1: *How does vulnerability to heat-related health outcomes vary according to socio-economic and ecological differences in neighborhoods in the urbanized area of Maricopa County, Arizona?* In it, I combine vulnerability theory with public health and spatial epidemiology methods to estimate rates of heat-related hospitalizations, construct an index of sensitivity to extreme heat in Phoenix, and estimate the relative risk of heat hospitalizations among neighborhoods with different sensitivity profiles.

3.2 Statement of Author's Contributions

This chapter was prepared in its entirety by me. I would like to acknowledge principally the assistance of Sharon Harlan, co-chair of my dissertation committee. Also, the help of Dr. Diana Petitti at the ASU Center for Health Information Research (CHiR), Dr. Ben Ruddell, Department of Engineering, College of Technology and Innovation, Arizona State University at the Polytechnic, and Dr. Gerardo Chowell-Puente and Mr. Shuo Yang at the ASU School of Human Evolution and Social Change (SHESC) is recognized for valuable comments and insights on model construction.

3.3 Introduction

Vulnerability to heat hazards is on the rise in cities. Heat hazards occur in seasonally hot climates and during summer heat waves, and are amplified by city-specific urban heat islands and localized climate change effects. Heat waves linked to global and regional climate change have been shown to have increased in frequency and intensity over the 20th century as high temperatures exceed normal ranges of temperature variability (Meehl and Tebaldi 2004; IPCC Working Group I 2013). Among weather-related hazards, extreme heat accounts for the majority of fatalities in the United States (CDC 2006). Extreme heat is a summertime phenomenon and prolonged events during the season are common. Additionally, intra-urban exposure varies according to ecological and built environment structure (Harlan et al. 2006; Jenerette et al. 2007). In this chapter I evaluate the socio-spatial variability of health outcomes, sensitivity, and exposure that shapes present heat-related vulnerability in urban areas in Maricopa County, Arizona. To do this, I first estimate rates of summertime heat-related hospitalizations as a function of exposure to maximum daily air temperature. Second, I construct and map a predictive heat sensitivity index from socio-economic and biophysical environment variables

identified in the climate change vulnerability and public health literature as influencing sensitivity to heat-related hazards. Third, I combine the hospitalizations data with the sensitivity and exposure components to estimate how sensitivity affects heat-related health outcomes. Fourth, I describe typical vulnerability profiles of neighborhoods to understand the factors that differentiate vulnerability in neighborhoods. I end by discussing the neighborhood-scale conditions that create vulnerability to extreme heat health outcomes in Maricopa County.

3.4 Background

The concept of vulnerability is useful to understand socio-environmental hazards and risks (O'Keefe et al. 1976; Hewitt 1983; Bankoff 2003). Vulnerability describes "states of susceptibility to harm, powerlessness, and marginality of both physical and social systems" (Adger 2006, 268) for the purpose of increasing human well-being through risk reduction. The integration of the concept into environmental hazards and risk research emerged as a progression from applied models focused on disaster events and post-event mitigation to integrative, holistic models encompassing the anthropogenic (e.g., cultural, political, economic) and biogenic (e.g., climatological, hydrologic) dimensions of human activity that create differential conditions of risk (Turner et al. 2003; Romero Lankao and Qin 2011).

Vulnerability is often measured with quantitative tools like indices, a method that increases the communicative and comparative utility of assessments. Vulnerability researchers point out, however, that the "static snapshot of a dynamic reality" (Mustafa et al. 2011, 65) presented by quantitative indicators can potentially obscure the complexity and nuance of the contexts in which vulnerability is constructed and experienced. In this regard, Adger (2006) provides a way forward by asserting that understanding vulnerability to climate change should be based on the analysis of present-day vulnerability informed by historical perspectives. In this chapter, I address these concerns by developing a quantitative assessment of current heat health-related exposure, sensitivity, and health outcomes. I then use the assessment to engage a more profound, place-based discussion of the historical and contemporary conditions that shape different outcomes of heat-related vulnerability in urban neighborhoods in Maricopa County.

A model of vulnerability to extreme heat health hazards

Vulnerability occurs within a socio-spatially differentiated spectrum of exposure, sensitivity, and adaptive (or coping) capacity that can mitigate or exacerbate the impacts of environmental hazards like extreme heat (Romero Lankao and Qin 2011; Turner et al. 2003). Exposure refers to the biophysical

environment's manifestation of hazards (e.g., extreme temperatures, flood, drought), and is usually expressed as the probability, duration, or spatial magnitude of occurrence (Cutter 1996; Luers et al. 2003; Mustafa et al. 2011). Sensitivity describes the degree to which populations are susceptible to the deleterious effects of exposure (Alwang et al. 2001; Brooks et al. 2005; Balbus and Malina 2009). Adaptive capacity–also termed resilience or coping capacity–encompasses the mechanisms through which populations cope with environmental hazards (Adger 2006; Smit and Wandel 2006), or the ability of the ecological system to recover from impacts (Klein et al. 2003; Bruneau et al. 2003; Thomalla et al. 2006).

The tri-partite framework described above is commonly used throughout the climate change vulnerability literature. For example, Cutter et al. (2003) defined exposure as the frequency of occurrence of floods, droughts, hurricanes (both winds and storm surges), earthquakes, and industrial chemical spills based on historical records in Georgetown County, South Carolina. In a study of extreme heat, Uejio et al. (2011) characterized heat exposure as nighttime surface temperature using thermal and reflection data from remote sensing platforms. Luers (2005) operationalized exposure in tandem with sensitivity to wheat crop yield fluctuations due to changes in temperature in farms in the Yaqui Valley, Sonora, México. Socio-demographic characteristics of individuals or population groups are often used to describe sensitivity. Tran et al. (2013) used age, socio-economic status, and social capital to characterize sensitivity to extreme heat in Ahmedabad, India. Eakin and Bojórquez (2008) describe sensitivity to people's livelihoods as farm income (or the capacity to generate it), but also take into account summer-winter seasonality to describe crop sensitivity to climate-change induced yield fluctuations. Adaptive capacity is often related to the institutional and political relationships of the state and people. For example, Brooks et al. (Brooks et al. 2005) have linked the capacity to reduce mortality from climate hazards to civil and political rights, government effectiveness, and literacy. A recent assessment of climate change and human health in Canada takes a similar approach, equating adaptive capacity to access to technology, information, institutional arrangements, and social networks (Health Canada 2008). Adaptive capacity also has an ecological dimension. The capacity to reduce the impacts of extreme heat is linked to shading vegetation that can mitigate urban heat island intensities (CINRHD et al. 2012, Harlan et al. 2006).

In this chapter, I present a conceptual vulnerability model that incorporates exposure, sensitivity, and adaptive capacity as three discrete, quantifiable components that influence heat-related adverse human impacts (Figure 3.1). At the center of the model are heat-related hospitalizations, a

measurable outcome of heat vulnerability. Summertime daily maximum air temperatures expose populations to heat stress that can result in hospitalization or death; socio-economic and ecological characteristics of neighborhoods like shading vegetation and poverty (a proxy for socio-economic status) mediate the sensitivity of populations to the deleterious effects of exposure. Coping capacity describes the social, material, behavioral, and biophysical environment resources that can help households to adapt to, and cope with heat-related hazards. In implementing the model, however, I focus on exposure, sensitivity, and health outcomes, explicitly omitting exploration of the adaptive capacity component. I do this in order to concentrate the analysis on refinement of the exposure and sensitivity indicators in relationship to observed heat-health outcomes, a combination of determinants of vulnerability that is not often present in current heat hazards research. Two important exceptions are Luers (2005) and Smit and Wandel (2006), who explored exposure and sensitivity in tandem in their respective vulnerability assessments. These researchers argue that exposure and sensitivity must necessarily be considered together. According to them, the challenge in this framing lies in identifying the dynamics between climate conditions (exposure) and livelihood characteristics (sensitivity) that magnify vulnerability. I explicitly engage these dynamics in this chapter in order to better understand the relationship between exposure and sensitivity.

I engage an integrative understanding of the conditions that create differential heat-related vulnerabilities across the socio-spatial fabric of cities. I estimate exposure, sensitivity, and rates of heat-related hospitalizations. This chapter is concerned with the interaction of the sensitivity and exposure components with hospitalizations. Adding the coping capacity component can potentially add another level of complexity to the study, and so will be the subject of future investigation.

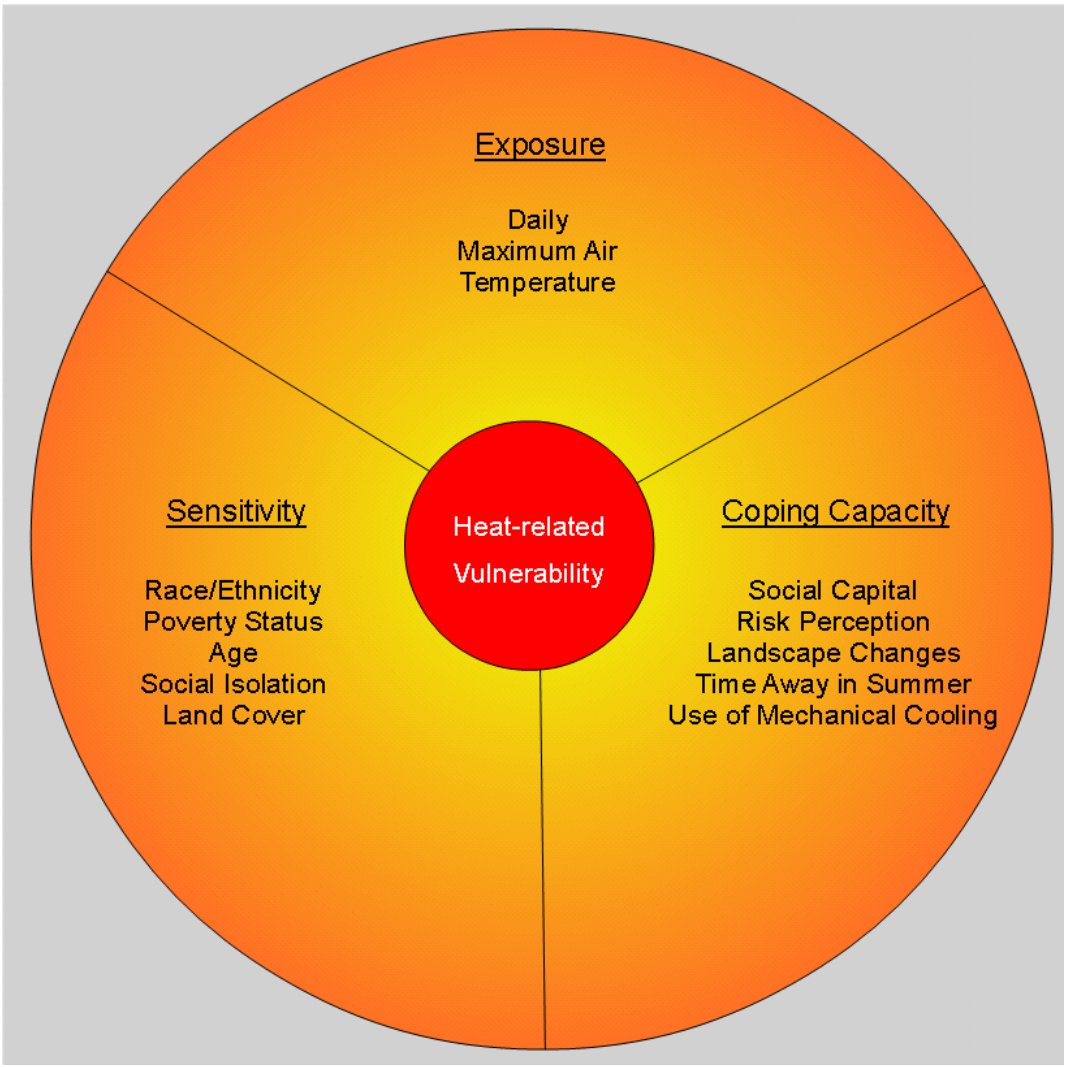

Figure 3.1: Vulnerability to extreme heat is determined by three key dimensions of exposure, sensitivity, and coping capacity. Heat-related health illnesses are a measurable outcome of vulnerability.

3.5 Vulnerability to Extreme Heat Research

Individual and neighborhood heat hazards risk factors

Research on heat-related health hazards spans many disciplines and has identified individual and neighborhood factors affecting heat health risks. Epidemiologists have found that individuals suffering from obesity, disability, pregnancy, cardiovascular, respiratory, or other underlying disease, and that are very young or very old are at elevated risk for heat-related mortality and morbidity (Reid et al. 2009; Yip et al. 2008; McMichael et al. 2006). Other individual characteristics linked to heat-related deaths include engaging in physical activity during hot weather periods, and income (Kilbourne et al. 1982; Balbus and Malina 2009; Smoyer et al. 2000; Applegate et al. 1981). Low-income, minority populations with low educational opportunities often lack access to quality employment and health care; these communities are often socially isolated, and live in zones of "concentrated disadvantage" (Sampson 2009; Wilson 2009). Air conditioning (AC) can provide immediate respite from heat exposure; however, both physical (presence of AC unit in dwelling) and socio-economic access (ability to pay for its use) are determined by socio-economic status, and have been shown to significantly affect heat health outcomes (Harlan et al. 2013; Reid et al. 2009).

Social isolation and low levels of social capital are found to contribute to poorer physical and mental health outcomes in general, and also to increased heat wave-related mortality (Lochner et al. 2003; Klinenberg 2003). At the neighborhood scale, income is also a predictor of the presence of vegetation and impervious surfaces, two important drivers of intra-urban differences in temperatures (Buyantuyev and Wu 2012). This is underscored by recent research that argues that unequal distributions of vegetated green spaces contribute to health disparities among low- and higher-income communities (Jennings et al. 2012; Wilson 2009). For example, Harlan et al. (2006) found that neighborhoods with sparse vegetation, but also with high population density and lack of open spaces are correlated with higher temperatures, and that populations there are likely to be low-income minorities. The socio-economic and demographic characteristics mentioned above shape an individual's sensitivity and exposure to extreme heat because these conditions largely determine the individual and community contexts in which people live their every day lives (Browning et al. 2006; Uejio et al. 2011; Harlan et al. 2006; Harlan et al. 2013). These contexts shape vulnerability through differences in ecological (e.g., local synoptic climate, availability of shading vegetation, urban spatial morphology) and socio-economic (e.g., social capital, population density and stability, ethnic/racial structure) conditions.

Quantitative indices in heat hazards research

Construction of indices at small geographic scales is an increasingly used methodology that combines socio-economic status and biophysical environment data in geospatial mapping and analysis platforms to predict heat vulnerability (Harlan et al. 2013; Reid et al. 2009, Reid et al. 2012). Pioneered by the Social Vulnerability Index (SoVI) approach of Cutter et al. (Cutter et al. 2003; Cutter and Finch 2008; Cutter et al. 2010), vulnerability indices are useful to policymakers for locating vulnerable populations and environmental hazards, more effectively target mitigation or prevention, or to identify areas for environmental modification. Reid et al. (2009) built a heat vulnerability index for census tracts in the United States, and found that within urban areas, inner cities have the highest predicted vulnerability. A recent update of this methodology across several cities in the U.S. finds higher predicted vulnerability is associated with increased mortality and morbidity in general, but also with significant increased rates of heat-related illnesses in some cities (Reid et al. 2012). Johnson et al. (2012) compared a heat vulnerability index to heat-related deaths during the 1995 Chicago heat wave, concluding that socio-economic risk variables, in combination with environmental variables (e.g., vegetation and land surface temperature) explained most of the variance in heat vulnerability. In Phoenix, Harlan et al. (2013) recently mapped a heat vulnerability index, compared it to heat-related fatalities, and found that socio-economic, age, and social isolation factors, coupled with surface temperature, are the most effective predictors of summertime heat-related mortality. Buscali et al. (2012) mapped a heat risk index from four equally-weighted dimensions of social vulnerability (socio-economic status, very young or very old age, population density, and residential building age) for census block groups in Rennes (France), and combined it with a hazard index (land surface temperature, LST), finding a pattern of higher LST in the city center. Another spatially-explicit heat index study focused on Phoenix suggests that Hispanics and the elderly are the most vulnerable populations there (Chow et al. 2011). Heat exposure and social deprivation indices were created and combined to describe spatial patterns of excess heat mortality in neighborhoods in France, finding that the most deprived areas in Paris experienced excess mortality rates twice as high as the least deprived areas (Rey et al. 2009).

Others have developed indices for neighborhoods or city districts without mapping their spatial distributions. For example, a human thermal comfort index (HTCI) was built for eight urban neighborhoods in Phoenix, Arizona during a heat wave, finding that minority populations with low

socio-economic status are more likely to live in hotter areas with higher HTCI scores (Harlan et al. 2006).

Other researchers have built indices that consider only biophysical environment conditions. For example, Balogun et al. (2010) constructed a thermohygrometric index (i.e., combining temperature and relative humidity) and found higher heat stress conditions in the city center than in the rural areas in a tropical, developing country. Semenza (1999) built a highest hourly heat index from apparent temperature (also combining temperature and relative humidity) during the 1995 Chicago heat wave, concluding that pre-existing medical conditions accounted for most of the excess hospitalizations. Basu et al. (2008) estimated and mapped daily mean apparent temperature for nine California counties, taking into account bias in weather station observations due to concentrations of ambient air criteria pollutants.

Many index-based heat risks studies predict vulnerability using social and environmental factors identified in the heat risk literature, but do not evaluate the explanatory power of indices against actual health outcomes. This is an important validation step for spatially explicit, quantitative predictors of heat vulnerability. For example, Harlan et al. (2013) conducted a binary regression of their vulnerability index against the presence/absence of heat-related deaths in census block groups. They test for spatial clustering of heat-related deaths, finding that 25 percent of decedents lived in areas of high predicted vulnerability. Johnson et al. (2012) compared observed heat mortality rates to expected rates based on their heat index. Both of these studies have found that the combination of socio-economic and environmental variables is the best predictor of heat-related deaths.

Assessing human vulnerability to extreme heat presents methodological challenges. Although the conditions that make people vulnerable to extreme heat vary greatly among individuals, the biophysical environment, socio-economic, and demographic data that describe places and people are often available only at the neighborhood or larger scales, or are temporally mismatched, making individual-scale assessments of vulnerability impractical. For example, quantifying exposure to extreme heat is often a compromise between either spatially or temporally explicit data. Weather station networks in urban areas often provide hourly or daily air temperature, wind speed, and relative humidity measurements, but lack the spatial coverage to account for microclimate variations created by land use/land cover differences in cities. Remotely-sensed data can provide the spatial coverage to describe land surface temperature of an urban region, but are often limited to a snapshot at a particular point in

time. Similarly, census data provide neighborhood-aggregated descriptions of households and neighborhoods, but do not account for the variability in socio-economic conditions within neighborhoods that make some individuals more sensitive than others to extreme heat. Similarly, variability in the adaptive capacity of individuals is not adequately captured by national censuses.

3.6 Methods

Study Area

In this research, I explore heat-related vulnerability in urban areas of Maricopa County, Arizona. Maricopa County contains 3.9 million people spread across 25 self-governing municipalities. The county seat and state capital, Phoenix, developed in the late 19th century as an isolated farming community, becoming one of the fastest-growing metropolitan regions in the United States by the mid 20th century. Given the relatively recent history of sustained modern human occupation, intense large-scale land-use/land cover modifications brought on by urban development, and extreme summertime temperatures, urban Maricopa County is an ideal place to study heat-related vulnerability. The region has a well-documented–and extremely intense–urban heat island (UHI) effect originating in the Phoenix central business district (CBD) and diminishing in intensity as distance from there increases (Balling and Brazel 1987; Grossman-Clarke et al. 2005). Surface cover modifications in the metropolitan region have dramatically altered the urban landscape since the early 20th century. Heat-trapping horizontal and vertical surfaces are correlated with predicted extremely high summertime air temperatures (Grossman-Clarke et al. 2010). In addition, the historical and geographical legacies of racist segregation and marginalization of minorities in the CBD point to the role of race, class, and socio-economic status in shaping heat-related and other forms of hazards vulnerability in the county (Bolin et al. 2002).

Geospatially-referenced census block group (CBG) boundaries from the 2010 Census were overlaid in GIS with the 2010 Urban Areas boundaries for Maricopa County (United States Census Bureau 2010c). The U.S. Census Bureau defines urban areas based on population density, count, and size thresholds (DOC 2011). CBGs with centroids outside the urban area boundaries were excluded from the analysis. In addition, four CBGs within the urban areas boundary identified as wholly housing populations in institutional or transitory quarters were eliminated (i.e., college dormitories, state prison, and state hospital). Out of a total of 2,505 CBGs in Maricopa County, 2,383 (95.1%) were selected for the analysis. Figure 3.2 shows the study area and weather stations included in the study. Some

weather stations outside the urban areas polygon were included in the study because they were closest to some CBGs in the urban fringe.

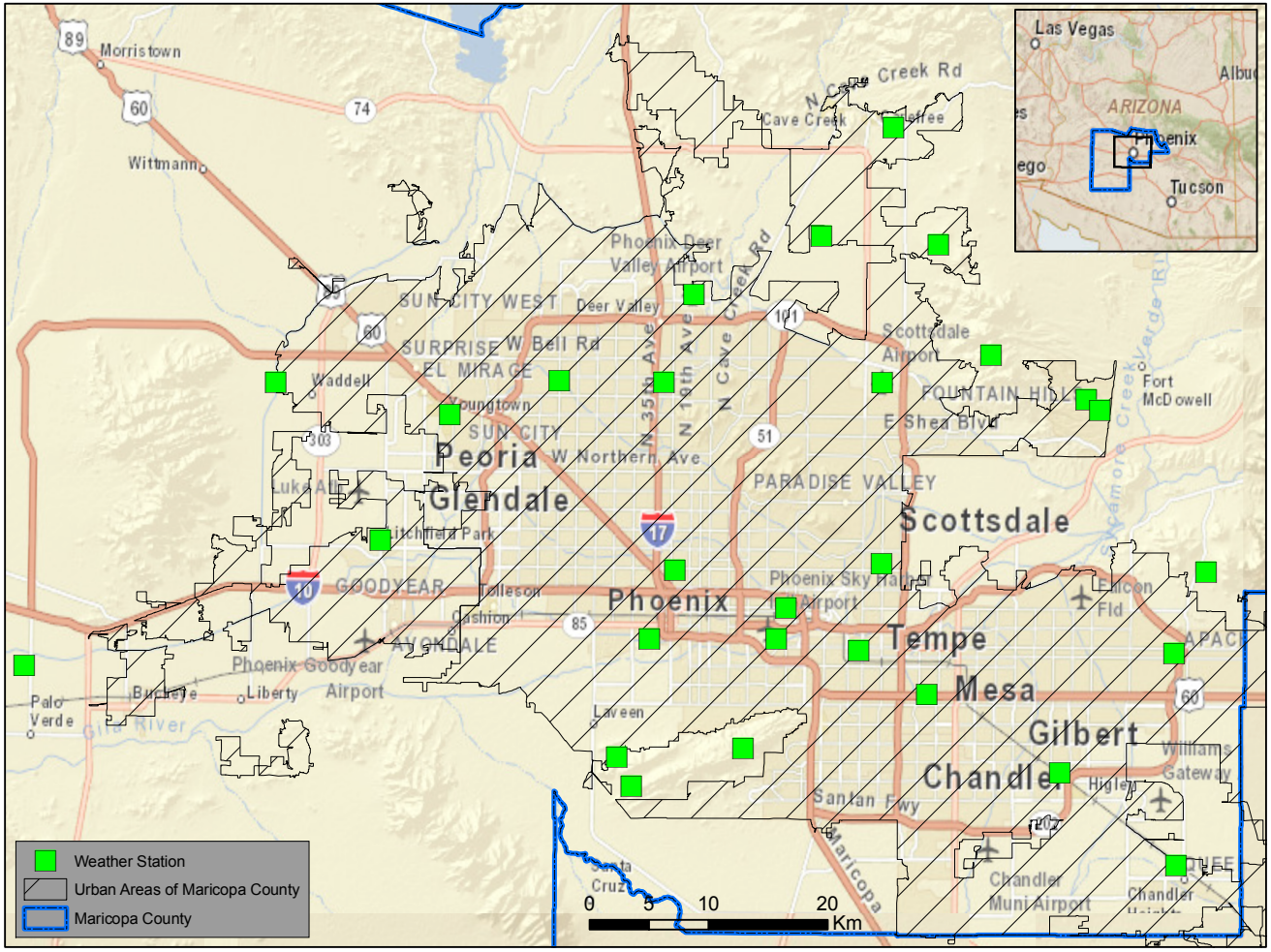

Figure 3.2: Study Area: Urban areas of Maricopa County and weather stations included in study

Heat-related hospitalizations

Heat-related health outcomes data were extracted from a database containing inpatient (i.e., hospitalizations) visits to Maricopa County hospitals from 2005 to 2009. The database does not include hospitalizations in Veteran's Administration, Indian Health Service, or military hospitals. The dataset used in this study was assembled by Arizona State University's Center for Health Information and Research (CHiR) from data provided by the Arizona Department of Health Services (ADHS). CHiR epidemiologists queried ADHS hospital visits that matched International Classification of Diseases (ICD-9-CM) codes for illnesses directly related to heat exposure or illnesses that may be indirectly related to heat because they are potentially aggravated by high temperatures. The illnesses directly related to heat exposure included 1) exposure to high environmental heat; 2) dehydration, hypovolemia, or volume depletion; and 3) conditions that are a consequence of heat and/or dehydration, hypovolemia, or volume depletion. Conditions that are potentially aggravated by high temperatures included: 4) cardiovascular diseases; 5) chronic renal failure; 6) heart failure; 7) diabetes; 8) respiratory diseases; 9) nephritis and nephrosis. In total, the data contain nine categories (three directly-related to heat exposure and six indirectly-related) represented by ICD-9 discharge diagnoses and external cause of injury codes (E-codes). In this study, I used only cases diagnosed with direct exposure to high environmental heat because every case in this category is likely to be a heat-caused illness.

The dataset used for analysis is a merger of two inpatient datasets for 2005-2007 and 2008-2009, which were provided separately because the number of captured codes increased in 2008 from 9 to 25 discharge codes and from 4 to 9 E-codes. In an epidemiological or longitudinal research design, merging the two datasets would be incorrect because estimated changes in inpatient hospitalizations rates could reflect reporting changes in the number of captured codes and not changes in real rates of heat-related illnesses. However, in this research I am treating the data as a cross-section and aggregating hospitalizations using the same ICD-9 coding system across all years (2005-2009). In comparing hospitalization rates across urban space, the change in number of captured codes is less of a concern because all locations are treated the same in any given year.

Dates of hospital admission and discharge, individual demographic information, and latitude and longitude from the geocoded address of a patient's place of residence were also included in the dataset. Cases were extracted based on criteria related to heat-related health outcomes. First, to account for visits related to summertime temperatures, hospitalizations that occurred between May and

October of 2005 and 2009 were selected. These months correspond to the Maricopa County surveillance period for heat-related deaths (MCDPH 2011). Second, cases with an ICD-9 code in the exposure to environmental heat category were included in this study regardless of the position of the code in the discharge or E-code lists. I focus on these because they are caused by extremely high outdoor environment temperature. Looking only at heat exposure cases may give a conservative estimate of heat effects because heat may be implicated in other illnesses–but not coded–in the data. However, focusing on these cases allows for the identification of a clear heat exposure signal.

To locate hospitalizations in the neighborhood of a patient's residence, cases with a residential address geocode precision of at least the CBG of residence were selected. Cases were also filtered spatially in GIS by selecting those within urban areas of Maricopa County. Lastly, cases in CBGs within the urban area identified as containing sub-populations not represented in the health outcomes data were eliminated (i.e., CBGs made up mostly or wholly of college dormitories, prisons, Native American reservations or state hospitals). Out of a total of 1,569 hospitalizations directly related to heat exposure, 415 were eliminated from the analysis because they did not have a date of admission within the surveillance period or the patient's residence was outside of Maricopa County. From the remaining 1,154 eligible cases, 148 cases had a geocoding precision of zip code, census tract, or county and were also deemed unfit for analysis at the CBG scale. In the end, 1,006 cases (64.1% of all cases directly related to heat) were selected for the analysis.

Exposure

Exposure was characterized as maximum daily air temperature (*tmax*, °C). Increases in air temperature are the best documented and understood effect of UHIs (Roth 2002). Air temperatures are strongly correlated to thermal comfort and heat-related mortality and morbidity (Harlan et al. 2006; Hondula et al. 2012). *tmax* data were obtained from 29 weather stations across three monitoring networks operated throughout Maricopa County (AZMET 2013; MCFCD 2013; NOAA 2013) with valid *tmax* observations for May through October of each year between 2005-2009, inclusive. Where necessary, observations were converted to °C and rounded to the nearest integer. Figure 1 shows weather stations selected for the analysis. Although some stations are outside the urban areas boundary, these were included in the study because they were the closest stations to many of the geocoded hospitalization cases in the urban fringe. Table 3.1 summarizes *tmax* recorded in the 29 weather stations from May through October of 2006-2009. The lowest absolute *tmax* value was observed in October, while the

highest *tmax* value occurred in July. July also was the month with the highest 5-year mean *tmax* value during the study period.

Table 3.1: Descriptive statistics for daily *tmax* (°C) in weather stations in May-October 2005-2009 (31,783 observations from 29 stations)

Month	Min	Max	Mean	StdDev
May	12.8	46.1	34.4	4.6
June	25.0	48.9	39.0	3.8
July	26.1	50.0	40.8	3.3
August	26.7	47.2	39.3	3.1
September	23.3	47.8	36.8	3.2
October	11.1	41.1	30.5	4.2

Daily *tmax* values were assigned to all 1,006 geocoded hospitalizations. First, the weather station with the shortest straight-line distance to each CBG was assigned to that CBG using a "near" GIS operation. Based on this assignment, a hospitalization case was given the *tmax* value of the weather station assigned to that case's CBG by matching the date of admission to the same date on the weather station record. This method assumes that the station closest to a CBG accurately represents the daily maximum air temperature in that CBG. Although there are other methods like interpolation to create continuous surfaces of temperature based on observed data, the method used here is a compromise between spatial and temporal resolution, especially because it is of interest to assign temperature values to the day of a hospital admission. Spatially-continuous data commonly used to interpolate temperature in unsampled locations (e.g., land surface temperature from spaceborne sensors, downscaled simulations of regional predictive models) are not currently available at a daily temporal resolution to match the date of hospitalization admissions in the health outcomes data. Appendix A explains procedures that were explored, then discarded, for estimating *tmax* for unsampled locations.

Sensitivity

A heat sensitivity index was constructed in order to predict sensitivity of the population to heat-related health outcomes. Building on recent research on heat vulnerability (Harlan et al. 2006; Reid et al. 2009, 2012; Johnson et al. 2012), a sensitivity index for CBGs in Maricopa County incorporating population socioeconomic indicators and biophysical environment variables consistently identified in the heat vulnerability literature as determining heat health risks was built and mapped. Previous research terms the indicator a "vulnerability index". In the model presented in the present research (Figure 3.1),

vulnerability is framed as an adverse human health outcome, in which the variables in previous research make up the sensitivity component. I thus refer to it as a sensitivity index in order to differentiate it from exposure and adaptive capacity, the other two discrete components of the vulnerability model. Table 3.2 summarizes data sources included in the sensitivity index.

Table 3.2: Data sources used in heat vulnerability assessment

Indicator	Source	Date	Geographic scale
Exposure and Health Outcomes			
Heat-related Inpatient Admissions	CHiR [1]	2005-2009	Point
Daily Air Maximum Temperature	AZMET, MCFCD, NOAA [2]	May-Oct 2005-2009	Point
Sensitivity			
Percent Minority	U.S. Census	2010	Census Block Group
Percent without Air Conditioning	County Assessor	2010	Parcel
Percent without High School Diploma	U.S. Census	2010	Census Block Group
Percent in Poverty	U.S. Census	2006-2010	Census Block Group
Unvegetated Surface in Residential Area (Mean)	Landsat	2010	30 meters/pixel
Unvegetated Surface in Residential Area (StdDev)	Landsat	2010	30 meters/pixel
Unvegetated Surface in Non-Residential Area (Mean)	Landsat	2010	30 meters/pixel
Unvegetated Surface in Non-Residential Area (StdDev)	Landsat	2010	30 meters/pixel
Percent Developed Imperviousness	NLCD[3]	2006	30 meters/pixel
Age 65 or Older	U.S. Census	2010	Census Block Group
Living Alone	U.S. Census	2010	Census Block Group
Age 65 or Older Living Alone	U.S. Census	2010	Census Block Group

1: Center for Health Information and Research
2: Weather station networks: Arizona Meteorological Network, Maricopa County Flood Control District, and National Oceanic and Atmospheric Administration
3: National Land Cover Dataset

Socioeconomic variables identified in the literature as strong correlates of individual sensitivity to heat-related health outcomes were aggregated to the neighborhood scale to characterize the residential population. Variables were selected from the 2010 U.S. Census and American Community Survey 5-Year Estimates for 2006-2010 (U.S. Census Bureau 2010a; U.S. Census Bureau 2010b). Individual parcel data from the Maricopa County Assessor's Office (2010) cadastral registry were used to calculate an air conditioner (AC) deprivation indicator for census block groups that represents percentages of single family homes with evaporation cooling (swamp cooler) or no mechanical cooling availability. Swamp coolers are present in some homes in older and low income neighborhoods, and are largely ineffective after the drier early summer air transitions to the higher humidity conditions characteristic of the August monsoon season in central Arizona (Kalkstein and Kalkstein 2004). The presence of AC units is positively correlated with decreasing heat-related mortality (O'Neill et al. 2005).

Lack of vegetation is correlated to higher land surface and air temperatures, and consequently, heat stress (Harlan et al. 2006; Jenerette et al. 2007; Jenerette et al. 2011). Impervious surfaces and lack of tree canopy are associated with ethnic/racial minority residential segregation, suggesting that heat-retaining land covers are more prevalent in African-American, Hispanic, and Asian neighborhoods that in White areas (Jesdale et al. 2013). Two indicators of unvegetated surfaces were calculated separately for residential and non-residential areas of neighborhoods. Similar to Johnson et al. (2012), residential areas were considered separately from non-residential to accurately characterize abundance or lack of vegetation in areas where people live. I also considered areas dominated by non-residential land uses to account for local or regional open spaces where vegetation may be a factor in regulating temperatures. To do this, I first extracted residential and non-residential areas in each neighborhood from a geospatially referenced land-use file for Maricopa County (MAG 2009). The Normalized Difference Vegetation Index (NDVI, Tucker 1979), an indicator of photosynthetically-active vegetation, was calculated for residential and non-residential areas of neighborhoods based on a Landsat scene (Row 37/Path 37, spatial resolution 30 meters/pixel; acquired on 13 August 2010, NASA 2010). NDVI range is $\pm$1.0, with positive values indicating more vegetation. Mean and standard deviation for all pixels in neighborhoods within each of the two areas were calculated and the means were multiplied by minus one to rescale the indicator in increasing order of sensitivity (i.e., the higher the NDVI value, the lower the vegetation density, and thus less capacity for temperature regulation). Finally, an indicator of the density of the built environment was extracted from the 2006 National Land Cover Database Percent Developed Imperviousness database (NLCD, Fry et al. 2011). Values for each

pixel in the NLCD data represent the percentage of land that is developed (i.e., part of the built environment). Values for individual pixels in neighborhoods within each of the residential and non-residential areas were averaged for each neighborhood and included separately as residential and non-residential indicators in the sensitivity index creation. The variables selected for this analysis differ from a similar index calculated previously for year 2000 Census data in Harlan et al. (2013) in two important ways. First, the previous study included a Hispanic immigrant variable consisting of linguistic isolation in Spanish and the foreign born population, a variable representing the undocumented population of Hispanic origin in Maricopa County. Unavailability of the two component Census items at the CBG enumeration unit prevented the inclusion of the variable in this study's index calculation. Second, Percent Developed Imperviousness was not included in the previous sensitivity index.

3.7 Analysis

Heat-related hospitalization rates

Heat-related health outcomes and exposure data were combined to estimate rates of hospitalizations directly due to heat. A rate of hospitalizations per person-days was constructed as the ratio between the number of hospitalizations on days at each observed temperature over the number of person-days at risk, i.e., the population considered to be at risk during the number of days that each temperature value was recorded. This was done for two reasons. First, the hospitalizations data represent individual visits, not persons, presenting the possibility that an individual who was hospitalized more than once during the study period is represented more than once in the data. Second, the database assembled by CHiR does not include all-cause hospitalizations in Maricopa County. These two characteristics of the data precluded a cohort study design of exposed vs. non-exposed populations because no absolute population denominator could be constructed for the hospitalization cases. Instead, I consider the number of person-days at risk to be the base population potentially exposed to heat hazards at a specific daily *tmax* value. The rate of hospitalizations by person-days at risk for each observed *tmax* value was calculated as

$$E_x\left(tmax\right) = \frac{1}{P_x} \times \frac{H_x\left(tmax\right)}{D_x\left(tmax\right)} \tag{3.1}$$

where E_x is the rate of hospitalizations per person-day at temperature *tmax* for population group *x*,

P is the total population for population group *x*,

H_x is the total number of heat-related hospitalizations on days with temperature *tmax*, and

D_x is the total number of days with temperature *tmax*.

Construction of heat sensitivity index

The socioeconomic and biophysical environment variables selected for the heat sensitivity index (Table 3.2) were entered into a Principal Components Analysis (PCA). The first three principal components (PC) were selected as factors and combined to estimate a cumulative heat sensitivity index for each census block group in the study area. Z-scores for each factor were recoded based on six equal increments of $\pm$1.0 standard deviations (SD) from the mean, and assigned integer values of 1 (2 or more SD below mean) through 6 (2 or more SD above mean). The cumulative sensitivity for each block group was calculated by adding the three factor recoded scores. The resulting distribution was the basis to classify neighborhoods as having low (less than 1 SD below mean), medium (between 1 SD above and 1 SD below mean), or high (more than 1 SD above mean) sensitivity for each individual factor and the cumulative sensitivity index.

Calculation of relative risk of hospitalization

Estimation of hospitalization rates (Eq. 3.1) only considers the effect of the exposure component (temperature) on heat-related hospitalizations and ignores the role of sensitivity variables in shaping health outcomes. To evaluate how sensitivity affects the exposure-hospitalization relationship, exposure and sensitivity data were combined to generate temperature-hospitalization curves and estimate relative risk of hospitalizations for neighborhoods in the low, medium, and high cumulative sensitivity groups.

For each of the three sensitivity groups, total population was defined as the sum of the 2010 Census population in all CBGs in each sensitivity group (the P term in Eq. 3.1). The number of heat-related hospitalizations (H_x) and the frequency of each observed *tmax* value (D_x) were calculated for each sensitivity group. Exponential growth models were fitted to each of the temperature-hospitalization curves.

In order to estimate the risk of hospitalization, a Poisson regression was performed and relative risk was estimated. Poisson regression is often used in morbidity studies to estimate relationships for count data, and is especially useful for relatively rare events like hospitalizations directly related to heat (Cromley and McLafferty 2012). The number of hospitalizations was regressed as a dependent variable on temperature, with the natural log of person-days at risk (H_x / D_x) as an offset variable. To account

for the effects of sensitivity (i.e., the sensitivity profile of an inpatient's neighborhood) a categorical dummy variable representing sensitivity group membership was included in the regression. Relative risk was calculated as e^{β}, where β represents the parameter estimate for the dummy variable. To facilitate interpretation of relative risk, the low sensitivity group was selected as the reference category.

3.8 Results

Heat-related health outcomes and exposure

Summertime heat-related hospitalization rates across Maricopa County increase exponentially with temperature (Figure 3.3). The small rates on the y-axis show that hospitalizations directly related to heat are a rare occurrence. Visually, rates appear to be unstable for *tmax* <= 30, raising the possibility that the hospitalization-temperature relationship may only grow exponentially past some *tmax* threshold. I attempted to find the *tmax* threshold beyond which the hospitalization-temperature relationship increases exponentially by conducting multiple log-linear regressions on subsets of consecutive data points sorted in order of increasing *tmax* (made up of 3, 4, 5...24 observations) from Figure 3.3. I then plotted the r^2 values against the *tmax* value of the observation added in each subsequent regression. For example, Figure 3.4 shows that a regression conducted using the first three observations (again, sorted in increasing *tmax* order) has a r^2 value of 1.0, and the *tmax* value of the third observation is 26. As the next observation is added to the regression–and with the corresponding *tmax* increase–, explanatory power of adding more *tmax*-ordered observations decreases for *tmax* < 32, suggesting that, below this threshold, the hospitalizations-temperature relationship in Figure 3.3 is not exponential. For observations with *tmax* => 32, the relationship is consistently exponential. This indicates that *tmax*=32 is the threshold temperature beyond which heat exposure triggers hospital visits.

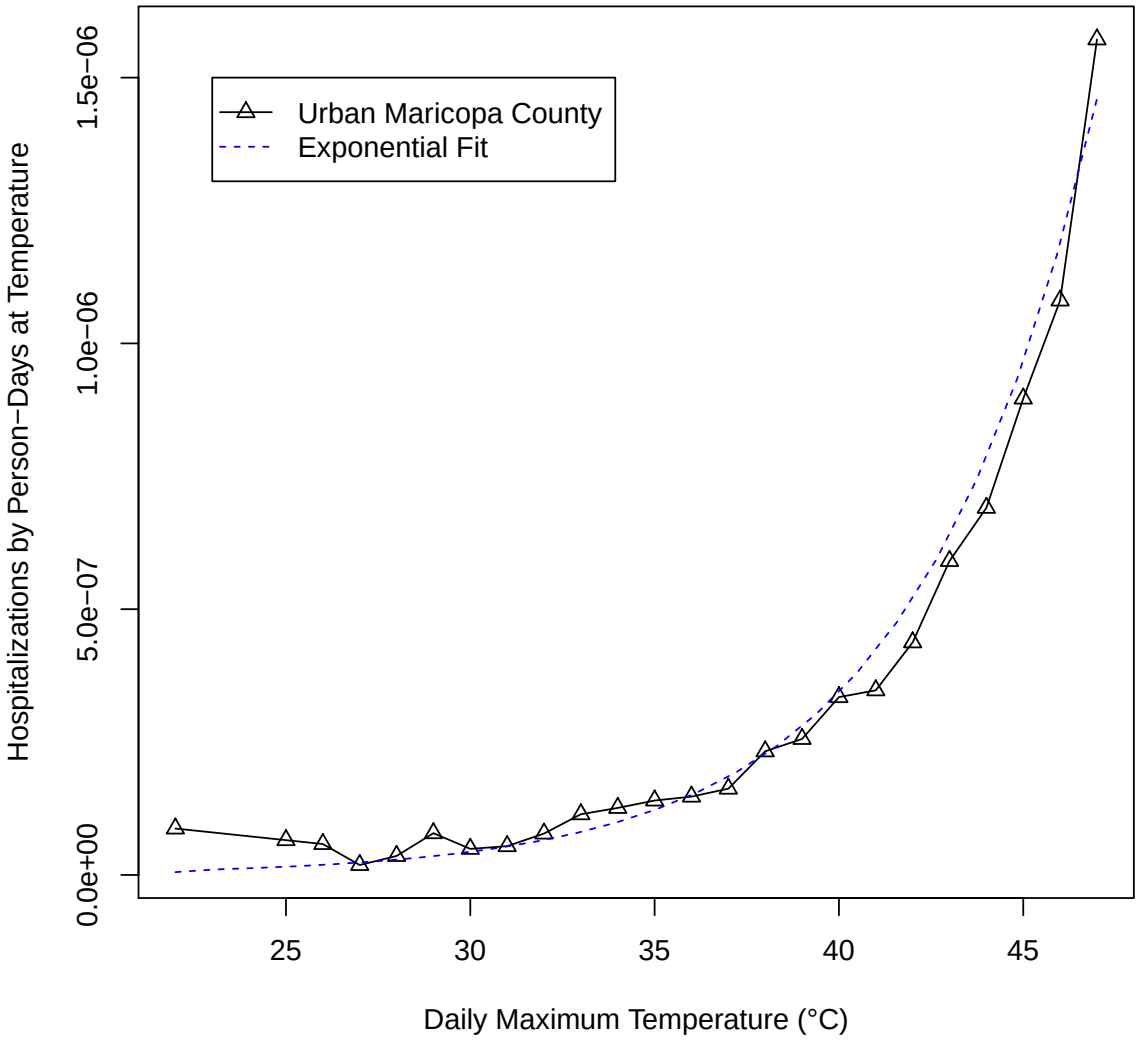

Figure 3.3: Heat-related hospitalization-temperature rates for May-October (2005-2009) surveillance period in urban areas in Maricopa County

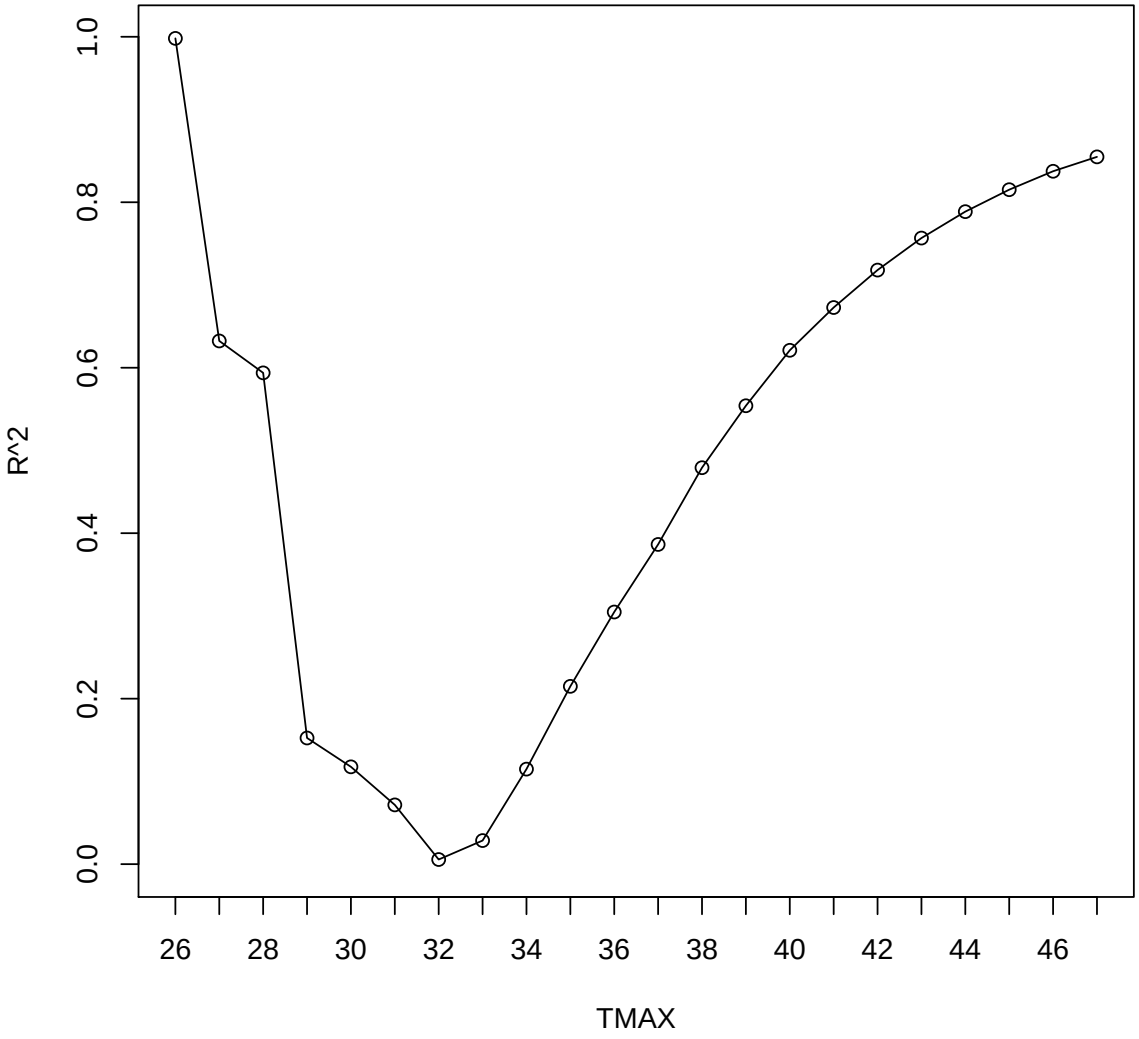

Figure 3.4: r^2 vs *tmax* for subsets of consecutive data points sorted in order of increasing *tmax*

Sensitivity

Statistical correlations and descriptive statistics for the socio-economic and biophysical environment variables selected for the sensitivity index are reported in Table 3.3. Three principal components (PC) explained 71.8% of the common variance (varimax rotation, eigenvalues>1.5). The PC structure of the variables is shown in Table 3.4. Similar to the year 2000 index in Harlan et al. (2013), variables correlated to socio-economic vulnerability make up the first factor, here labeled "Socio-economic Sensitivity": ethnic minority, no AC, no high school diploma, and poverty. The developed imperviousness and NDVI variables load together into the second factor, termed "Vegetation and Built Environment Sensitivity". Finally, the elderly and isolation variables load into the third factor, called "Age and Social Isolation Sensitivity".

Table 3.3: Spearman's correlations, means, and standard deviations of sensitivity index variables in Census Block Groups in urban areas of Maricopa County, Arizona

	Ethnic Minority	No AC	No H.S. Diploma	Below Poverty	Age 65 or Older	Living Alone
Mean	0.40	0.10	0.15	0.14	0.14	0.25
SD	0.26	0.19	0.16	0.15	0.17	0.14
Ethnic Minority	1.00					
No AC	0.49^{***}	1.00				
No H.S. Diploma	0.69^{***}	0.52^{***}	1.00			
Below Poverty	0.60^{***}	0.46^{***}	0.58^{***}	1.00		
Age 65 or Older	-0.64^{***}	-0.07^{***}	-0.26^{***}	-0.27^{***}	1.00	
Living Alone	-0.18^{***}	0.03	-0.04^{*}	0.17^{***}	0.38^{***}	1.00
Age 65 x Alone	-0.40^{***}	0.09^{***}	-0.04^{*}	-0.02	0.85^{***}	0.62^{***}
Developed Impv.	0.24^{***}	0.28^{***}	0.34^{***}	0.40^{***}	0.07^{***}	0.43^{***}
Unv. Surface - Res. (Mean)	0.38^{***}	0.20^{***}	0.46^{***}	0.43^{***}	-0.12^{***}	0.21^{***}
Unv. Surface - Res. (SD)	-0.10^{***}	-0.17^{***}	-0.16^{***}	-0.13^{***}	-0.07^{***}	0.09^{***}
Unv. Surface - Non-Res. (Mean)	0.42^{***}	0.28^{***}	0.44^{***}	0.47^{***}	-0.15^{***}	0.26^{***}
Unv. Surface - Non-Res. (SD)	-0.10^{***}	-0.14^{***}	-0.13^{***}	-0.09^{***}	0.05^{**}	0.12^{***}

	Age 65 x Alone	Developed Impv.	Unv. Surface - Res. (Mean)	Unv. Surface - Res. (SD)	Unv. Surface - Non-Res. (Mean)	Unv. Surface - Non-Res. (SD)
Mean	0.08	41.28	0.16	0.06	0.16	0.09
SD	0.09	16.05	0.04	0.02	0.05	0.03
Age 65 x Alone	1.00					
Developed Impv.	0.31^{***}	1.00				
Unv. Surface - Res. (Mean)	0.10^{***}	0.55^{***}	1.00			
Unv. Surface - Res. (SD)	-0.07^{***}	-0.28^{***}	-0.45^{***}	1.00		
Unv. Surface - Non-Res. (Mean)	0.08^{***}	0.70^{***}	0.79^{***}	-0.42^{***}	1.00	
Unv. Surface - Non-Res. (SD)	0.04^{*}	-0.27^{***}	-0.31^{***}	0.59^{***}	-0.46^{***}	1.00

Table 3.4: Principal Components Analysis of cumulative heat sensitivity in census block groups in urban areas of Maricopa County

	Heat sensitivity factor loadings [1,2]		
	Factor 1: Socio-economic Sensitivity	Factor 2: Vegetation and Built Environment Sensitivity	Factor 3: Age and Social Isolation Sensitivity
Ethnic Minority	**0.86**	0.09	-0.33
No AC	**0.78**	0.11	-0.03
No H.S. Diploma	**0.85**	0.14	-0.09
Below Poverty	**0.83**	0.13	0.03
Age 65 or Older	-0.29	-0.07	**0.81**
Living Alone	0.06	0.06	**0.81**
Age 65 x Alone	-0.13	-0.01	**0.92**
Developed Imperviousness	0.36	**0.54**	0.41
Unvegetated Surface - Residential (Mean)	0.39	**0.65**	0.30
Unvegetated Surface - Residential (StdDev)	-0.01	**-0.79**	0.10
Unvegetated Surface - Non-Residential (Mean)	0.42	**0.77**	0.19
Unvegetated Surface - Non-Residential (StdDev)	0.06	**-0.80**	0.25

1: Factor extraction performed using varimax rotation
2: Scores in bold indicate similar factor loadings

The highest sensitivity clusters are found in the metropolitan urban industrial core of Phoenix, along the historical corridors of second-tier East Valley cities, and in the elderly retirement communities in the northwest and east urban fringes (Figure 3.5). The high sensitivity cluster in the central city contains Phoenix's sparsely-vegetated, low income, minority neighborhoods, and consequently, the highest socio-economic and vegetation and built environment sensitivity. The historical corridors along the US-60 in the suburban communities of Tempe and Mesa contain smaller pockets of high sensitivity. Finally, the age-restricted retirement communities of Sun City and Youngtown in the northwest edge of the metro area, along with other retiree neighborhoods like LeisureWorld in the eastern edge of the county, have high rates of vulnerability, largely due to age and social isolation.

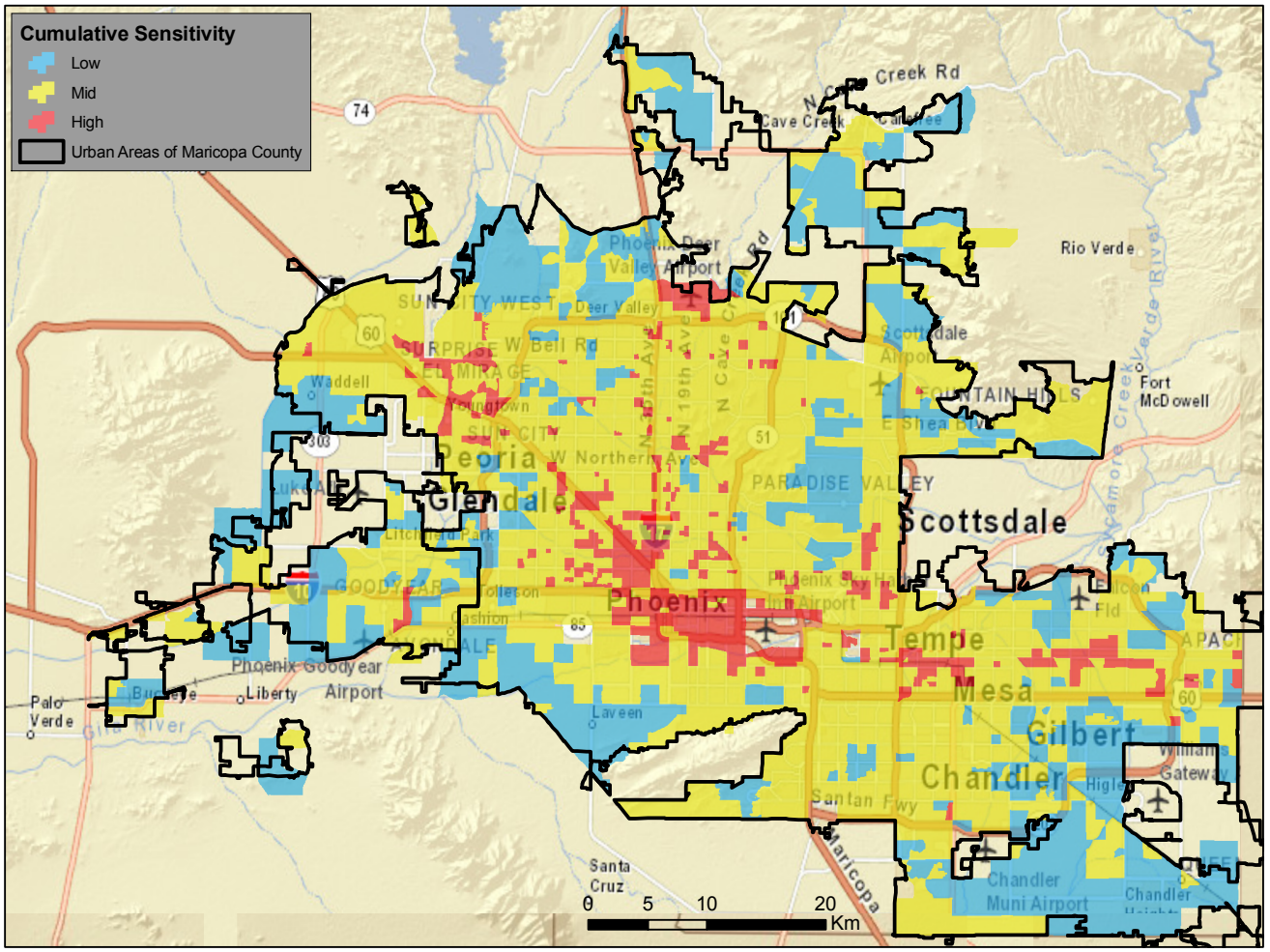

Figure 3.5: Cumulative heat sensitivity index in census block groups in urban areas of Maricopa County

How does sensitivity affect exposure and heat-related health outcomes?

Sensitivity factors affect exposure and heat-related health outcomes in significant ways. Hospitalization rates for the low, mid, and high sensitivity groups are shown in blue, yellow, and red, respectively, in Figure 3.6. The county curve from Figure 3.3 is also reproduced in black for reference. The mid sensitivity curve appears to track the county curve; the low sensitivity curve observes hospitalizations rates below both the mid sensitivity and county curves, while the high curve is above the mid and county curves. Exponential model fits for each of the curves describe each distribution well (r^2 of 0.710, 0.822, and 0.860 for low, mid, and high sensitivity), implying that hospitalization rates increase exponentially with temperature increase, and that rates are higher for higher predicted sensitivity groups.

The Poisson regression results indicate that the relative risk of hospitalization for the three sensitivity groups is significantly different. Parameter estimates, relative risk, and statistical significance are displayed in Table 3.5. Goodness of fit is strong (Pearson's χ/df = 0.978), indicating little overdispersion in the model. The intercept β parameter included in the regression can be used to estimate the baseline risk for the reference category (low sensitivity group, -23.105). The baseline risk of 9.2 X 10^{-11} hospitalizations/person-days (calculated as e^{β}), when evaluated against relative risk calculated from parameter estimates suggests that individuals in neighborhoods in the medium sensitivity group present a risk of a heat related hospitalization almost twice as high (84.8 percent) as those in low sensitivity neighborhoods, while individuals in high sensitivity neighborhoods are almost three times as likely (272.5 percent) to suffer a heat-related hospitalization than those in the low group (Table 3.5). The β estimate for *tmax* (0.192) indicates there is a 21.2 percent increase (i.e. relative risk) in hospitalization rates for each °C increase in *tmax* for all three sensitivity groups. Inclusion of an interaction term (sensitivity group * *tmax*) to determine if different *tmax* β parameters could be established for each sensitivity group rendered both individual (sensitivity group, *tmax*), and interaction (sensitivity group * *tmax*) model effects statistically non-significant, indicating that temperature thresholds for sensitivity groups are not significantly different.

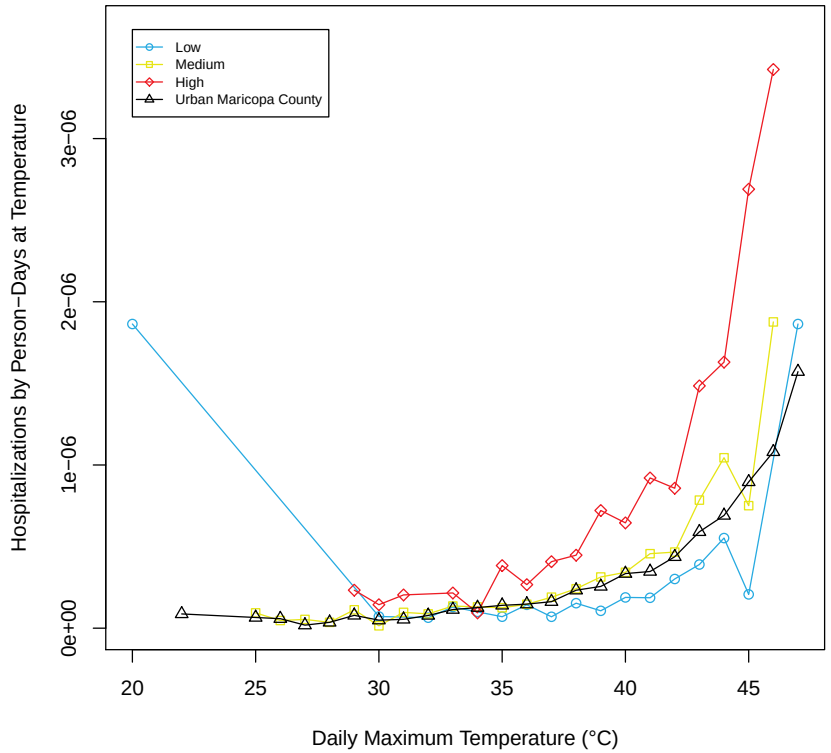

Figure 3.6: Heat-related hospitalization-temperature rates for May-October (2005-2009) surveillance period in heat sensitivity groups in urban areas in Maricopa County

Table 3.5: Poisson regression coefficients and relative risk with Low sensitivity group as reference category

Sensitivity Group	β	Relative Risk (e^{β})	Sig.
Low	–	–	0.000
Mid	0.614	1.848	0.000
High	1.315	3.725	0.000
tmax	0.192	1.212	0.000
Intercept	-23.105	9.2E-11	0.000

What makes neighborhoods more sensitive to heat-related hazards?

The sensitivity index map on Figure 3.5 shows that the most sensitive neighborhoods are those with the highest cumulative score aggregate of the Socio-economic, Vegetation and Built Environment, and Age and Social Isolation factor components. The design of the index, however, allows neighborhoods with different combinations of the component factor scores to group together in the same sensitivity group. To better understand why neighborhoods are highly sensitive, I now focus on neighborhoods in the high cumulative sensitivity category.

Table 3.6 shows a cross-tabulation of the low, medium and high individual factor scores for the 309 neighborhoods in the high cumulative sensitivity group. The most frequently observed category is high SES sensitivity with medium Built Environment and Isolation factors, found in 110 neighborhoods. These neighborhoods are located in the Phoenix downtown core and along historical east-west core corridors of the east Valley communities of Tempe and Mesa. The second most commonly found interaction of sensitivity factors is high SES sensitivity and Built Environment and medium Isolation (58), comprised mostly of neighborhoods along Grand Avenue, extending northwest of the intersection with 7th Avenue and Van Buren Street, historically the Phoenix-Wickenburg Highway. Additionally, 50 communities characterized by mid SES sensitivity and Built Environment factors–but with high Isolation–are found in the retirement subdivisions of Sun City in the northwest urban areas of the county. Finally, 48 communities mostly in age-restricted subdivisions in the east Valley have medium SES sensitivity and high scores in the Built Environment and Isolation factors. These combinations of high cumulative sensitivity point towards two broad patterns of sensitivity. First, sensitivity to heat hazards in Maricopa County urban cores is driven by SES and Built Environment factors, while high cumulative sensitivity areas in the suburban fringe is determined, for the most part, by Age and Social Isolation factors.

Table 3.6: Cross-tabulation of low, medium, and high heat sensitivity factors in neighborhoods with high cumulative heat sensitivity

	Low Age/Social Isolation			Mid Age/Social Isolation			High Age/Social Isolation		
	Built Environment			Built Environment			Built Environment		
Socio-economic	Low	Mid	High	Low	Mid	High	Low	Mid	High
Low	0	0	0	0	0	0	0	0	2
Mid	0	0	0	0	0	22	0	**50**	**48**
High	0	0	0	0	**110**	**58**	2	13	4

What do high sensitivity neighborhoods look like?

As shown in the previous section, high sensitivity neighborhoods have similar cumulative sensitivity scores, but due to different combinations of individual factor scores, reflecting very different socio-economic, vegetation and built environment, and age and social isolation conditions. To illustrate what these neighborhoods look like, I present land cover maps of two neighborhoods in the high cumulative sensitivity category. Figure 3.7 shows the Northwest Valley Age-Restricted neighborhood, a retirement community in Maricopa County's northwest suburban fringe. This neighborhood has medium socio-economic sensitivity and high scores in the vegetation and built environment and age and social isolation sensitivity factors. As indicated by the individual factor composition, heat sensitivity in this neighborhood is driven by high concentrations of elderly residents, little vegetation, and abundant heat-retaining impervious surfaces. The Central City South neighborhood (Figure 3.8) shows a different pattern: medium sensitivity in the vegetation and built environment and age and social isolation factors, but a high score in socio-economic sensitivity, reflecting a social geography of low-income, minority residents with reduced AC saturation in these neighborhoods.

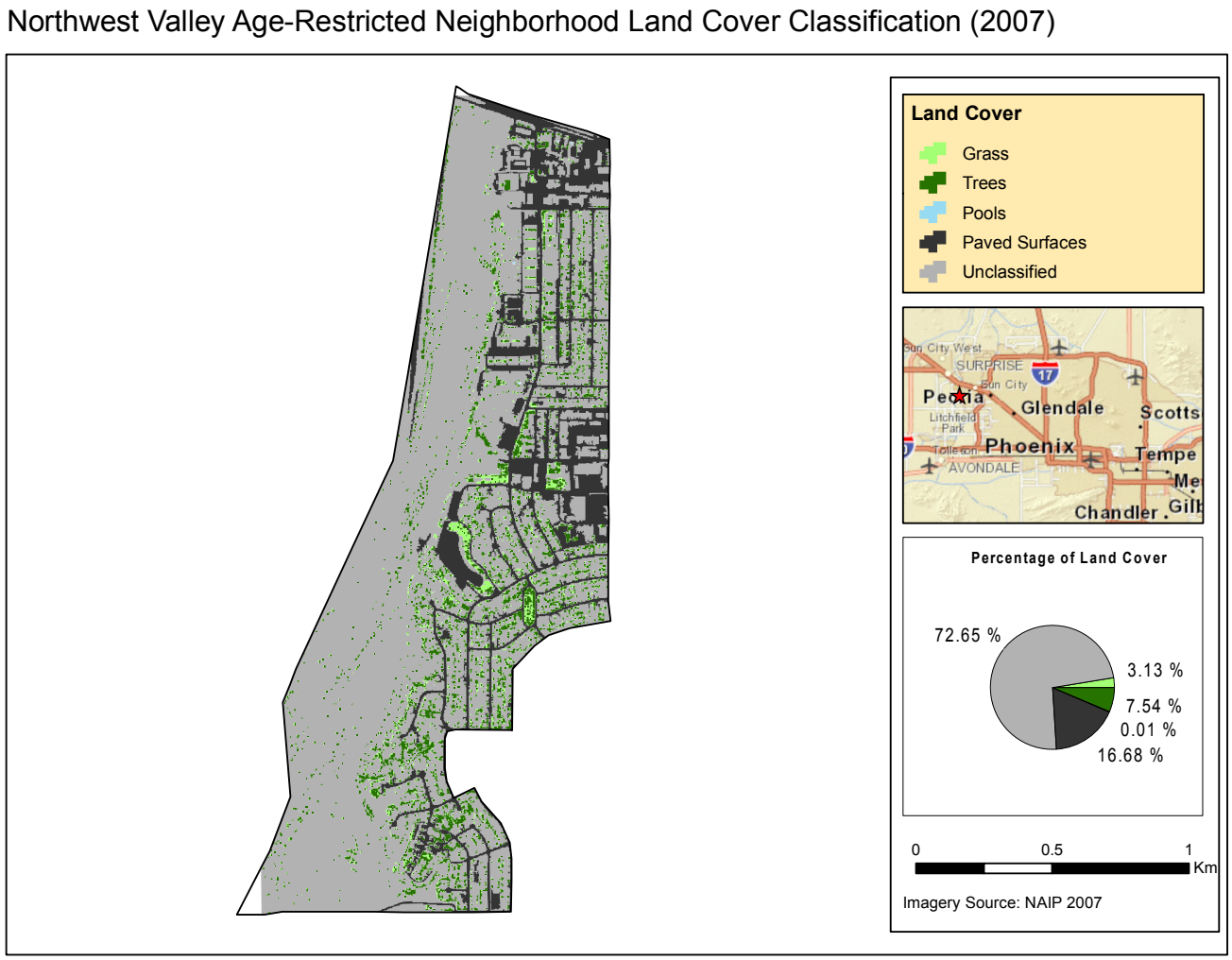

Figure 3.7: High cumulative sensitivity due to age and social isolation and vegetation and built environment factors: Northwest Valley Age-Restricted Neighborhood

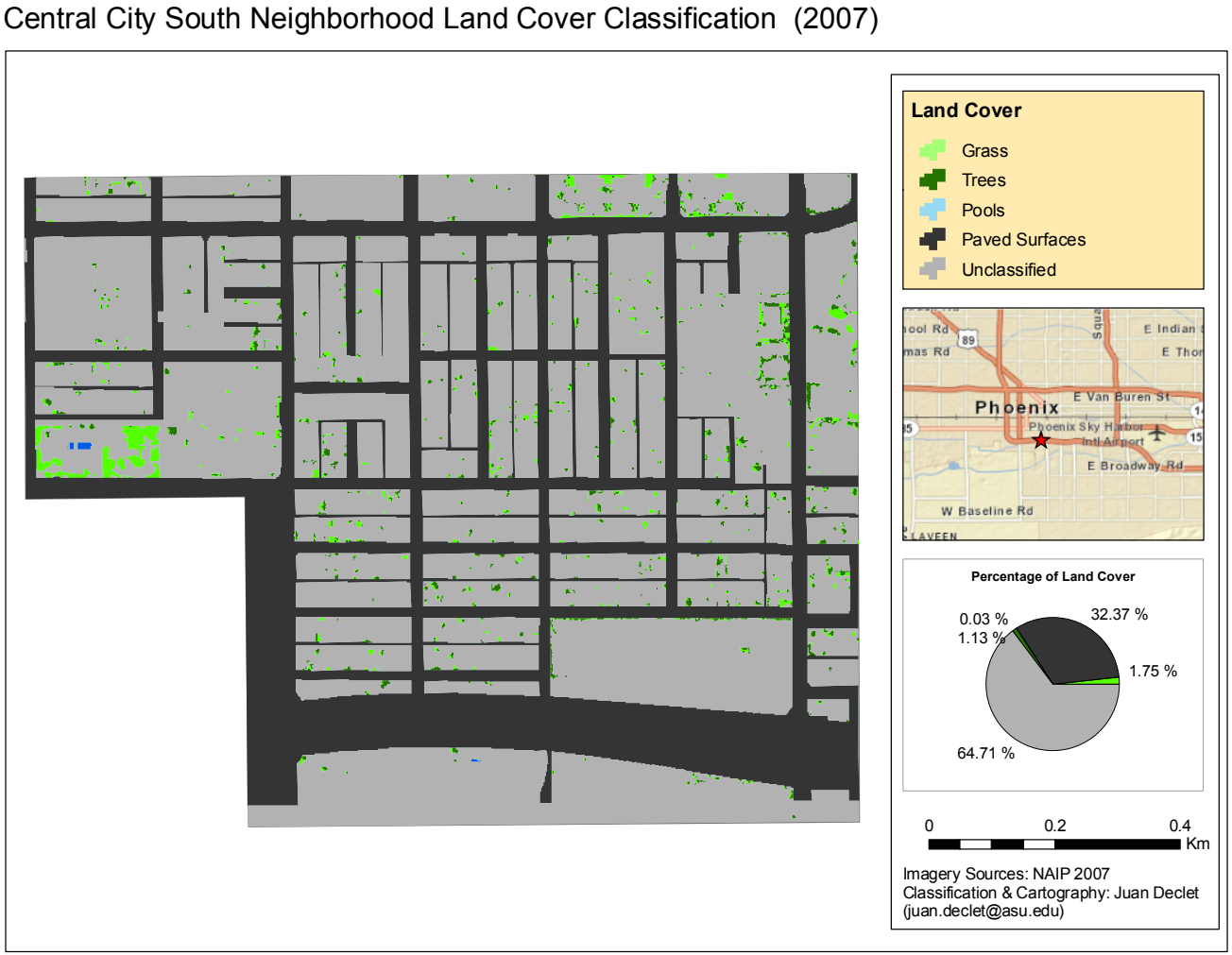

Figure 3.8: High cumulative sensitivity due to socio-economics and vegetation and built environment factors: Central City South Neighborhood

3.9 Discussions and Conclusions

Main findings

The primary finding of analysis of exposure and heat health outcomes for urban Maricopa County is that heat-related hospitalizations increase exponentially with daily maximum air temperature. The relationship appears to be unstable for temperatures lower than 32 °C, and demonstrably exponential beyond this value. This indicates that 32 °C is the threshold temperature beyond which the heat exposure signal is strong enough to result in an exponential increase in heat-related hospitalizations. Combination with the sensitivity index shows that neighborhood-scale heat risk factors mediate exposure and health outcomes in a manner consistent with the assumptions built into the index: lower sensitivity neighborhoods have reduced hospitalization rates compared to neighborhoods with higher sensitivity, as evidenced by the higher estimated relative risk for each sensitivity group. As the analysis shows, individuals in neighborhoods in the medium sensitivity group are almost twice as likely (85 percent) to be hospitalized, and individuals in neighborhoods in the high group are almost three times as likely (272 percent) to be hospitalized than those in the low group.

A second finding is the identification of three discrete socio-ecological factors that make neighborhoods differentially sensitive to extreme heat: socio-economic, vegetation and built environment, and age and social isolation characteristics. The cumulative sensitivity index built from these components varies widely throughout urban areas, but in general, is highest in the Phoenix city urban core, decreases in the expanding suburbs, and is lowest near the suburban fringes. However, a more nuanced pattern of heat risk emerges when cumulative sensitivity is disaggregated into its factor components. The pattern is now one of high socio-economic sensitivity in the urban core due to income and minority status, and high sensitivity due to old age and social isolation in the suburban fringe. These two regions of similarly-high sensitivity–one made up of urban cores with impoverished immigrants, the other suburban white, and elderly–suggests a dual pattern of urban vulnerability. Populations at risk in urban vulnerability studies are typically minority, low income, live in urban cores, and bear the largest burdens of exposure to not only climate-related, but also to technological and industrial hazards. This social and spatial pattern is more typically found in older cities with traditional central business districts and post-industrial legacies, but has also been demonstrated to be the case in Phoenix (see Bolin et al. 2002; Bolin et al. 2005). As I have shown in the analysis, this is found in urban Maricopa County, but a pattern that has not received much attention is also evident. Due to the sustained, large scale postwar expansion of the urban footprint and the increased magnitudes and

duration of heat waves posed by local UHIs and global climate change, age- and social isolation-based vulnerabilities are now evident at the suburban fringes, and also in second-tier urban cores, which are replicating the pattern of poor minorities occupying central city neighborhoods and becoming more exposed to extreme heat. The index presented here also validates the results of the 2000 heat vulnerability index in Harlan et al.(2013). The indices are similar in construction methodology, diverge in evaluation against health outcomes, and have similar findings. Comparison of the indices against mortality (2000) and morbidity (the present work) reveal that prediction of adverse health impacts spatially coincide with actual outcomes, pointing out urban core, low-income minorities and elderly suburban fringe populations as the most burdened with heat-related death or hospitalization. Both of these studies used variables similar to the index developed by Reid et al. (2009) for U.S. counties (with the exception of diabetes morbidity among the elderly). That research was later validated against heat health outcomes, finding strong associations between the index and mortality/morbidity (Reid et al. 2012). Another index recently created for Phoenix includes only four socio-economic variables (median income, old age, nativity, and residential mobility) and three biophysical (maximum and minimum temperature and NDVI) (Chow et al. 2011). This index also identifies urban core minorities and suburban elderly populations as at-risk for adverse heat-related outcomes, but the small number of variables used do not allow for the nuanced explanation of socio-ecological characteristics of minority and elderly neighborhoods that contribute to higher heat risks, which I engaged in the present research.

The final main findings are that in urban Maricopa County, there is a 32 °C threshold beyond which summertime hospitalization rates increase exponentially, and that, across the county, the estimated relative risk for temperature indicates there is a 21.2 percent increase in the hospitalization rate for each °C increase in temperature. An attempt to find sensitivity group-specific temperature thresholds did not yield statistically-significant results. Possible explanations are that there are not enough cases in the health outcomes data to establish temperature thresholds for the sensitivity groups, or that temperatures were homogenized due to the procedure used to assign *tmax* values to hospitalizations.

The historical-geographical context of present heat vulnerabilities

To understand the heat-related vulnerabilities described here, it is necessary to frame the present conditions within the historical trajectory of urban development of the region. Since the founding of Phoenix in the late 19th century, growth in Maricopa County has been characterized by an aggressive pattern of space-consuming conversion of natural land covers into urban land forms, fueled by

successive speculative waves of agricultural, industrial, and suburban growth-led development. Pervasive discrimination and marginalization of mostly African American and Mexican American minorities–but also Chinese and American Indians–combined with concentrated industrial expansion have relegated these groups to the Phoenix urban core areas, creating a persistent "geography of despair" (Bolin et al. 2005) where industrial, hazardous, and transportation-related land uses surround high density, impoverished residential areas. Concentration of heat-retaining surfaces and removal of surface water and shading vegetation contributed to the urban heat island signature that is most intense in central Phoenix, making the urban core populations the most highly exposed to extreme heat. This process occurred in tandem with "white flight" (Pulido 2000), the self-removal of the white and affluent to the expanding suburbs north of the Phoenix municipality following severe flooding in the early 20th century. The sustained postwar population and economic expansion boom of the whole region–including rapidly-changing suburban communities like Tempe and Mesa–underscores the polycentric nature of the urban agglomeration, helping to explain the pockets of high socio-economic sensitivity in the historical downtown and transportation cores of second-order cities in Maricopa County. An important consequence for heat exposure of sustained industrial and transportation infrastructure growth in the Phoenix core (but also in the expanding industrial corridor along Grand Avenue) is the absence of canopied vegetation and green spaces in general, which, combined with persistent poverty and high population density, reinforces exposure to the heat health consequences of the summertime urban heat island. More recently, other areas of concern for heat-related risk have emerged along the suburban fringe in urban Maricopa County. Flourishing since the 1960s, retirees were attracted here by a combination of climate, scenic natural landscapes, cost of living, and an amenities-oriented planned community lifestyle (McHugh et al. 2002). By the 1990s, Maricopa County was the leading retirement community in the United States (Longino and Manheimer 2006), attracting large numbers of the active elderly to communities like Sun City in the northwest and Leisure World in the east. The elderly in these communities are at increased risk to heat risks due to their advanced age and physiological characteristics, but also due to the isolation many find themselves in. These population groups are likely to experience higher vulnerability in the future. Recent climate change assessments predict that mortality and morbidity among urban dwellers–but especially the elderly, young children, and those with pre-existing medical conditions–will increase as heat waves in cities increase in magnitude and duration (Rosenzweig et al. 2011).

Contributions to understanding heat vulnerability

In this study, I have presented a sophisticated model of climate change-induced heat risks framed within the vulnerability tradition in hazards geography. Exposure and sensitivity have been described and quantified, coping capacity has been identified as an important component–but left out for future research–, and heat-related hospitalizations have been described an linked as measurable outcomes of vulnerability. The research presented here complements traditional, non-spatial public health assessments of individual risk factors for heat illness by linking socio-demographics to the characteristics of neighborhoods. This research is useful to identify neighborhoods in which to target prevention and mitigation interventions.

The implementation of the vulnerability model presented here encountered limitations related to available data which forced compromises between the spatial and temporal accuracy of the constructed indicators. These limitations have some bearing on the conclusions that can be made about heat vulnerability. First, the hospitalizations data–a unique dataset often not available for heat risk research due to patient privacy concerns and data availability limitations–provided a high degree of both spatial (census block group) and temporal (date of admission) precision of the occurrence of health outcomes. Admittedly, matching of hospitalizations to the recorded maximum daily air temperatures in the temperature monitor closest to a hospitalization's geocode does not account for microclimate differences known to be created by the heterogeneity of land uses like horizontal and vertical impervious surfaces, urban canyons, open spaces, and agricultural fields that characterize spatial form in cities. In this regard, the magnitude of under- and overestimation of the local temperatures in the vicinity of a geocoded hospitalization based on arbitrarily distant observations with potentially distinct land use mixes is unknown in the present study. One way in which this may be resolved is through the application of spatial interpolation techniques. In my research, some techniques were explored and later discarded due both to their complexity and the realization that adequate resolutions are beyond the scope of this chapter. Notwithstanding these reasons, I explored and then discarded some techniques for estimating air temperatures at unsampled locations, the details of which can be found in Appendix A. Although the method for temperature assignment described in this chapter can potentially understate the microscale variability of air temperatures known to be highly regulated by urban form in arid environments (Oke 1982), it is deemed an adequate compromise in order to incorporate the spatial and temporal detail of the air temperature and hospitalizations datasets. Another

way of improving estimates of localized temperatures is by incorporating downscaled simulations of regional climate models in heat vulnerability assessments. This emerging area of computational modeling research is linking the localized impacts of anthropogenic land use changes (e.g., UHIs) to global climate change effects (e.g. greenhouse gases, atmospheric boundary conditions, see Cooney 2012). These models consider the outputs of global climate models as boundary conditions affecting urban warming at the regional scale, providing more realistic predictions of the spatio-temporal variability of temperatures. Downscaling has been recently applied to extreme heat research. For example, Georgescu et al. (2012) recently modeled the warming impacts of future urban growth along Arizona's Sun Corridor, the area of projected growth between metro Phoenix and the Tucson, Arizona metro region. Their model predicts that urban warming will depend on urban expansion scenarios, but also on global greenhouse gas emissions. Weather forecasting models coupled to land surface models like the High-Resolution Land Data Assimilation System (HRLDAS, Chen et al. 2007) can also help refine estimates of temperature at a fine scale (e.g., <10 km). Observations from weather stations like the ones used in the present research can be used to validate predictions of models like HRLDAS. This is a promising area of research that can improve the estimation of temperatures with a good deal of spatio-temporal detail and increase the understanding of temperature, heat hospitalization, and land cover dynamics at the urban microscale.

Another compromise made in this analysis related to the weather data was the use of maximum air temperature instead of apparent temperature, a calculated indicator more closely related to heat stress. Only 11 out of the 29 weather stations used in this study (38 %) belong to a weather observation network that collects relative humidity, preventing comparison of apparent temperature against heat-related hospital visits. The strong statistical relationship found between maximum air temperature and heat hospitalizations indicates this is a minor issue. The hospitalization data were also limited in that there is no indication that a hospitalized person was present in their neighborhood of residence at the time of being overcome by heat. This means that an unknown number of hospitalizations could have been due to environmental factors in other areas of the County than the neighborhood of residence. First-responder report data for hospitalizations (which contain time and place of intervention) were not available for the hospitalization cases used, so assessing this potential issue is beyond the reach of this chapter.

The hospitalization records also have characteristics that limit their applicability to the analysis presented. First, the data do not include hospitalizations in Veteran Affairs, Indian Health Service, or

military hospitals since these institutions do not report to CHiR or the Arizona Department of Health Services. Second, an important distinction must be made that the data represent visits to hospitals, not individuals. This means that any one individual who was hospitalized multiple times during the study time period can potentially show up more than once in the data. Because of this, the data effectively represent the utilization of hospital services rather than an accurate count of hospitalized persons. This also prevented the study from creating a cohort design of exposed/non exposed populations typical of traditional public health studies. Third, the severe real estate and mortgage crisis and subsequent employment downturn in Maricopa County around and beyond 2007 very likely affected hospital service utilization, conceivably biasing the estimates of hospitalization rates. The main reason for this is that in the United States, access to affordable health care services is largely attached to employment. Research shows that during economic downturns and concomitant loss of health care coverage, individuals often respond by using emergency rooms as primary care physicians, a behavior not explicitly accounted for in the analysis, and that could signal adaptation to a different kind of socio-economic vulnerability. In spite of this, the consistency in the exponential shape of the County aggregate and sensitivity group hospitalization rate curves–as well as the goodness-of-fit metric in the Poisson regression–suggest that the hospitalization-temperature relationship is adequately modeled, even when allowing for the possibility that the magnitude of the real heat morbidity rates is overestimated. The choice of using only direct heat exposure cases is another limitation of this study because heat may be implicated in admissions for any of the eight categories of indirect heat-related illnesses–but it was deemed adequate because it provides the strongest directly heat-related hospitalization signal. Finally, because this study is primarily concerned with heat risk determinants at the neighborhood scale, I used hospitalization records that had a geocoding precision of at least the census block group, which represented 64.1% of all directly heat-related hospitalizations in the summertime study period. This suggests that hospitalization rates in this research are underestimated, but the distribution of place of residence among the three sensitivity groups is unknown. This is a data limitation that could not be overcome because hospitalization records provided by CHiR were provided with a latitude/longitude value, and specific address data were removed from the dataset due to patient privacy concerns.

Future Research

The next step to fully explore all three dimensions of the vulnerability model presented in this research is estimation of coping capacity. Although the coping capacity component of vulnerability is presented

in the conceptual model, I did not describe it in this chapter. Coping capacity is arguably the least understood of the components of climate change vulnerability. Vulnerability research largely agrees that the biophysical characteristics of exposure and the socio-economic dimensions of sensitivity are well understood mainly because remotely-sensed, atmospheric models, or census data are often available at local, regional or global scales. Assessing coping capacity is often hampered by scarcity of data on resources available at the community, household, or individual scales, important because these are the geographic scales at which climate change and vulnerability scholars argue adaptation strategies unfold. Design and implementation of place-specific survey instruments are often necessary to gather data on household and community resources, ethnographies, environmental histories, and life experiences that potentially enable affected communities to adapt to or fend off the deleterious impacts of climate change vulnerabilities. A future direction in my research agenda is to fill in this final component of the vulnerability model presented here with social survey data. The 2011 Phoenix Area Social Survey (PASS, Harlan et al. 2003; Harlan et al. 2007) shows promise in this direction. PASS is a social survey of 45 neighborhoods designed to explore relationships between social and biophysical environments in urban Maricopa County. Preliminary exploration shows that several questions related to social capital, neighborhood networks, climate risk perceptions, household landscape changes, self-reported heat-related health outcomes, and summer activities and time away can help elucidate some of the ways in which people deal with heat risk hazards.

Finally, the link between ambient air pollution and heat illness was not explored here. This is an important step in considering atmospheric interactions among temperature and air pollutants on heat health outcomes, which have been found to be significant. For example, concentrations of criteria air pollutants like ozone and particulates have been empirically linked to elevated heat-related mortality and morbidity (Jackson et al. 2010; Knowlton et al. 2008; see Harlan and Ruddell 2011 for a review on this literature). Adequate characterization of these phenomena require integration of atmospheric dispersion modeling of pollutants and temperature characterizations like urban heat island simulations. Linking these predictive, spatio-temporally explicit models with heat health outcomes can provide valuable information for heat warning systems and other mitigation and prevention efforts during the extreme heat season that metropolitan areas like urban Maricopa County experience.

Chapter 4

THE HISTORICAL-GEOGRAPHICAL PRODUCTION OF THE URBAN RISKSCAPE OF PHOENIX, ARIZONA

4.1 About this chapter

In this chapter, I answer Research Question 2: *How has urban development in Maricopa County shaped the uneven landscape of socio-ecological heat hazards vulnerability during the 20th century?* Urban development creates landscapes of differential vulnerability to environmental risks. Understanding the historical-geographical trajectories of urban development in both their biophysical and social dimensions can help explain present socio-ecological disparities and vulnerabilities. In this chapter, I trace how urban development in Maricopa County has created an uneven landscape of environmental risk, or *riskscape*, through two simultaneous socio-spatial processes: anthropogenic land use/land cover change, and segregation and marginalization of minorities. These conditions have historically produced an unevenly-distributed riskscape of environmental vulnerability characterized by exposure to air pollution, industrial toxics, extreme heat, amid poverty and race-based segregation in the central city core. I use historical photos and archival material, in addition to longitudinal land use, population, and climatological records to document the environmental history and historical geography of urban development in Maricopa County. In doing so, I argue that urban, suburban and industrial development in the metropolitan region have shaped inequitable geographies of technological and weather-related environmental hazards exposure for low-income and minority groups in the urban core.

4.2 Statement of Author's Contributions

This chapter was prepared in its entirety by me. I would like to acknowledge the help of Christine Marín and Rebekah Tabah, historical materials archivists at Arizona State University. They provided valuable help in locating historical documents to help piece together the past of Maricopa County's landscapes of heat vulnerability.

4.3 Introduction

The transformation of the Salt River Valley into the Maricopa County metropolitan region has entailed the creation of complex socio-ecological landscapes of unequal vulnerability to industrial, technological, and weather-related hazards. In this chapter I trace the history and geography of urban development in Maricopa County and its role in creating differential exposure to extreme heat, a human health and livelihoods hazard brought on by urban development and anthropogenic land use and land cover change.

Historically, exposure to heat in Maricopa County has been driven by gradual temperature increases brought on by urban development and the concomitant population growth of a naturally hot and arid, subtropical region (Brazel et al. 2000; Brazel et al. 2007). The central core of the city of Phoenix is the epicenter of the Maricopa County metro region's urban heat island, also the site of historical, concentrated poverty and social marginalization of low-income minorities. Economic and racial marginalization, in tandem with temperature-increasing land use/land cover changes and the self-removal of wealthy elites to the expanding suburbs of the region shape the *riskscape* of extreme heat in the region. I refer to heat vulnerability as existing within a *riskscape* in order to emphasize the unequal distribution of environmental hazards and risks across the urban landscape of Phoenix. The term is not my own; urban ecology researchers have used the term to describe the spatio-temporal heterogeneity of social and ecological conditions in the Phoenix urban landscape that shape differential sensitivity, exposure, and coping capacities related to extreme heat exposure (Jenerette et al. 2011; Ruddell et al. 2010). Environmental justice scholars have used it to describe the racial and spatial character of industrial toxics exposure in Southern California (Morello-Frosch et al. 2001) and Phoenix (Bolin et al. 2002), while Cutter et al. use it to describe the "mosaic of risks and hazards that affect people and the places they inhabit" (Cutter et al. 2000, 716). I concur with these definitions, but expand upon them to also consider the structural factors in Phoenix's regional political economy and trajectory of urban development that created inequalities in the spatial distribution of land uses, land covers, populations, and consequently, temperatures. In this chapter, I conceptualize the riskscape as a particular form of the more general process of geographically uneven development (Smith 1990). The concept of uneven development provides the key structural entry point critical to engage the multiple socio-spatial inequities present today in the Phoenix metropolitan region. I then describe how the Phoenix urban landscape of risk came to be, and how it has been sustained over time. I present the history and geography of uneven development in metro Phoenix, engaging its discursive and material transformations as the urban development process unfolded since the late 19th century to the present. I intertwine the insights of urban political ecology and environmental history to uncover how trajectories of urban development produce and reproduce inequitable geographies of environmental hazards vulnerability.

4.4 The production of environmental hazards in urban space

Marxist geography and urbanism

Understanding the production of environmental hazards inequities in cities requires recognizing that urban space is socially produced as a historically and geographically specific process in the search for exchange values (Lefebvre 1991). Social space is "subsumed under the domain of capital, since... [capital's]... command of property, money power, technology and mass media enable it to dominate and appropriate the space of global capitalism" (Merrifield 2002, 521). Capital is a structural determinant in producing space because it continuously seeks to incorporate the world in the creation of exchange values while marginalizing social values (Smith 1990). The search for exchange values creates urban space through the operation of the contradictory tendencies of capital: first, that it must move around to find new spaces for creating exchange value, and second, that it must remain in place for a while until it extinguishes its capacity to generate value. It is the profit-seeking logic of capital that creates geographical difference as a spatio-temporally specific pattern of uneven development (Smith 1990). Smith's assertion that "[c]apitalism inscribes itself in the landscape as the extant pattern of uneven development" (Smith 1990, 133) emphasizes the role of capital in producing space.

In creating exchange values, urban development creates spatio-temporal configurations that are contingent on the material and discursive deployments of political actors, in turn tied to conceptions of society, nature, and ideology (Harvey 1973) that provide the economic and political empowerment to shape the material and social world (Pelling 2003). This approach to urban space moves away from the traditional, apolitical question of "what is space?", towards a process-oriented line of inquiry that seeks to uncover how specific socio-spatial human praxes conceptualize, create, and use space, and more importantly for addressing uneven development, for whose benefit, and at whose expense. The structural treatment posits that space must be understood as a historico-geographically contingent process where the socio-spatial contradictions of "value-in-motion" (i.e., fixed vs. mobile capital), are expressed. The abstract contradictions expressed here take concrete form by shaping urban space and creating the spaces of uneven development, more often than not through explicit discursive and physical violence deployed to creating space for the generation of exchange values (Lefebvre 1991).

Urban political ecologists and other critical geographers have built on these perspectives to conceptualize the city as a socio-ecological process that actively produces urban natures through complex arrangements of socio-spatial relations that include the biophysical/ecological and social

realms (Heynen et al. 2006). The socio-ecological transformations brought about by the urban require the reproduction of such socio-spatial relations to sustain themselves (Harvey 1996). The production of particular urban natures is shaped by political struggle among different actors according to socio-political power and filtered through key differentiations like class, race/ethnicity, and gender.

The view from landscape geography

Materialist accounts in landscape geography complement the production of space and uneven development theories, also privileging the process of production of inequalities in urban space. Mitchell, for example, calls for a geography of landscape that is "able to respond... and intervene in the destruction of landscape and livelihood that is everyday life" for marginalized groups (Mitchell 2003a, 791). Mitchell reinforces the central role of capital in socio-spatial differentiation by declaring that such a landscape geography must necessarily be committedly progressive, grounded in theories of uneven development, "deeply social-historical" by willing to penetrate the history of particular places (Mitchell 2003a, 791), and reliant on empirical evidence from historical, archival, documentary, and ethnographic sources.

The environmental history perspective

Environmental history scholarship by Donald Worster (1988) offers three critical focal points useful to map the material and discursive deployments that create socio-ecological changes like environmental hazards. These foci provide a way forward to explain, both historically and geographically, the creation of environmental hazards and urban natures. For Worster, there is a human intellectual realm made up of ideologies of nature, ethics, laws, and myths. Ideological ensembles compel elite political actors to deploy cultural and racial hegemony against ethnic minorities through socio-spatial practices like race- and class-based residential segregation. Complementing this is the socio-economic realm of modes of production, which include the specific material practices that transform the biophysical environment like hydraulic resources development or conversion of natural land covers into the built environment. A third cluster encompasses the processes that involve the realms of human intellectual and modes of production that transform biophysical "nature" into urban natures.

Towards a holistic understanding of the production of the heat riskscape

The theoretical frameworks of socio-ecological change in Marxist and landscape geography, urban political ecology, and environmental history allow us to ask the critical questions related to present inequities in urban environmental hazards vulnerability: How are urban spaces produced, for whose

benefit, and at whose expense? I use these insights to excavate the history and geography of urban development in Phoenix by focusing on two specific questions: First, how has urban development historically shaped the geography of differential vulnerability to socio-ecological hazards in Phoenix? Second, what has been the role of the socio-spatial practices of land use/land cover change and racial marginalization in shaping the riskscape? To do this, I identify three key transitions in the Phoenix political economy that I argue identify socio-ecological changes in relation to shifts in capital accumulation strategies. I will use these historical-geographical inflection points to show how the material and discursive practices associated with each moment help understand the production of contemporary environmental hazards vulnerability.

4.5 A model of production of the urban riskscape

The urban riskscape is produced as the process of urban development unfolds. A set of distinct, but intertwined socio-spatial practices shape both the biophysical/built environments and the cultural landscape (Figure 4.1). In metro Phoenix, anthropogenic alterations have affected hydrology and surface-atmosphere heat exchanges as desert surface covers were substituted for impervious surfaces like highways, roadways, farms, and commercial, residential, and industrial buildings, and the development of hydraulic resources through irrigation canal reconstruction, channelization, and surface water removal. In tandem, the cultural landscape has been shaped through race-based and hegemonic marginalization of minorities, creating a subordinate class of ethnic minorities through economic dispossession and residential segregation in the central business district.

These socio-spatial practices have created a geography of differential vulnerability across the metropolitan region. Differences in exposure to environmental hazards like extreme heat and the urban heat island, air pollution, and industrial toxics are shaped by socio-spatial inequalities in both the sensitivity of populations to the effects of hazards (largely determined by class, race, and socio-economic status), and their capacity to cope with health and livelihoods effects, often consisting of social or ecological resources at the household and neighborhood scales.

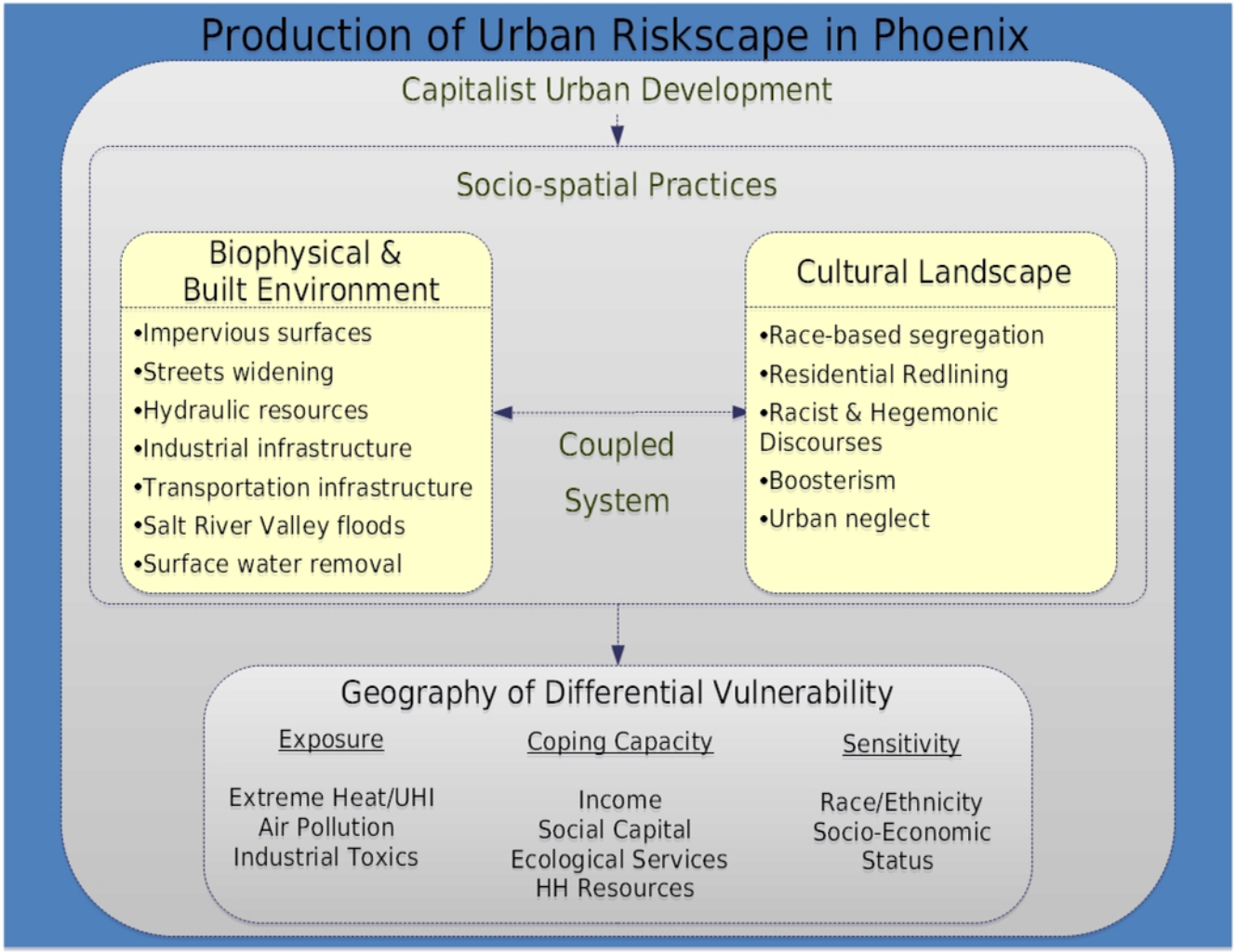

Figure 4.1: Conceptual model of the production of the Phoenix urban riskscape

4.6 Extreme heat and the Urban Heat Island

In this chapter, I focus on a specific environmental hazard produced by anthropogenic transformations: extreme heat. The most intensely studied effect of anthropogenic climate change and urban expansion in cities is the Urban Heat Island (UHI), defined as "the phenomenon of warmer temperatures at the core of the built-up urban area compared with the surrounding rural countryside" (Brazel et al. 2007). The increasingly large UHI footprint in Phoenix is typical of microclimates of heavily built-up urban areas, and largely driven by conversion of natural land covers (e.g., trees, grass, river channels, floodplains, open desert) to impervious horizontal and vertical surfaces (e.g., offices, residences, pavement, freeways, see Balling and Brazel 1987; Brazel et al. 2007; Grossman-Clarke et al. 2010; Guhathakurta and Gober 2010). The spatial configuration of the city–or "urban geometry"–alters wind flows, radiative flows, air and surface temperatures, and rain patterns, effectively creating a microclimate characteristic of the city (Golden 2004, 324; Oke 1981).

Research has shown that UHI intensities and temperatures vary greatly within urban areas: warmer temperatures are correlated with high population densities, low income, absence of irrigated and shading vegetation, and minority neighborhoods, all of which are evidence of demographic and land configurations characteristic of the Phoenix urban core (Harlan et al. 2006; Ruddell et al. 2010; Jenerette et al. 2011; Harlan et al. 2013). Urban core, low-income and minority populations are more exposed to warmer temperatures because the highest UHI intensities are found there. Elevated heat exposure is magnified by limited adaptive capacity to defend against extreme heat. For example, poverty and unemployment among low-income populations may preclude access to preventative health care, potentially increasing the impacts of preexisting disease such as hypertension on heat-related illnesses. Other factors that narrow the spectrum of adaptive mechanisms available to the poor are reliance on swamp coolers in older sections of the city (largely ineffective in Phoenix during the humid summer monsoon season, see Kalkstein and Kalkstein 2004), and lack of available income to pay for air conditioner and shading vegetation irrigation.

4.7 Towards a geographical and historical understanding of the heat riskscape

Urban climatology documents the atmospheric and surface energy balance processes of UHI formation and extreme heat in Phoenix, and links it to expansive, low-density urban growth and natural land cover transformations into impervious surfaces. Social science research reveals that socio-spatial inequities in the distribution of extreme heat exposure render low-income and minority groups markedly exposed

and vulnerable to UHIs and extreme heat. Notwithstanding these valuable insights, a historical and geographical perspective that recognizes social and spatial inequalities in the socio-ecological production of extreme heat is presented here. By conceptualizing the socio-spatial configuration of the extreme heat landscape of risk as the outcome of a historico-geographical project of capital accumulation, I can situate the social and biophysical dimensions of the UHI within the production of urban space.

Scholars and scientists have outlined the socio-spatial processes that can help understand the production of heat-related geographic difference in Phoenix. As the urban climatology literature reviewed above has demonstrated, the substitution of 'natural' land covers like open desert, rivers and streams, riparian areas, and trees and shrubs into heat-absorbing surfaces shapes a landscape of extreme heat that is demonstrably most intense in the Phoenix urban core. As urban development converts more land and industrial, commercial, residential, and transportation activities increase, both the magnitude and spatial footprint of the UHI intensify and radiate most intensely from the urban core. Industrial infrastructure development has been historically concentrated in the central core, where the bulk of unwanted land uses like railroads and service railyards, manufacturing, highways, degraded housing stock, toxic emissions, and warehousing, have been located (Luckingham 1989; Bolin et al. 2002, 2005; Grineski et al. 2007). On the cultural landscape front, race and class-based marginalization have relegated the city's ethnic minorities (predominantly African Americans and Mexicans, but also Chinese and Native Americans) to the slums south and west of the central business district, an area known as "South Phoenix".

These broad processes of socio-spatial concentration of minorities in and around heat-retaining land uses in the urban core have continuously shaped the urban riskscape through land use/land cover and social geography transitions in the regional political economy. Successive waves focused on agricultural, industrial, and suburban development are identifiable. The first land use transition began with the late 19th century Anglo-European settlement of the Salt River Valley through the reclamation of hydraulic resources, providing the means to develop a profitable export-oriented agricultural economy and the emergence of the urban infrastructure to support it. The second transition emerged during the Great Depression years, and ramped up as production for the Second World War increased, shifting use of land and hydraulic resources towards high technology, aerospace, and military industrial production in the urban core. The third transition signals the current, sustained suburban expansion since the postwar period (1960s on), the coalescence of the previously isolated

communities around Phoenix into a metropolitan region, and the simultaneous diminishing of agricultural and industrial production. I consider now in detail the history and geography of these three transitions in Maricopa County, and what each has meant for the development of the landscape of heat risk.

4.8 First transition: Agricultural resurgence in the Salt River Valley

> *"Aside from the ready market of hungry soldiers, ranchers, and miners, the Salt River Valley showed ample evidence of the agricultural potential of the region."* (Dean and Reynolds 2006, 10)

The modern production of the urban riskscape in Phoenix began, as the urban political ecology scholar Erik Swyngedouw has said of a similar process elsewhere, "within [the] already constructed historical socionatural conditions" of the ancient and abandoned Hohokam irrigation canals (Swyngedouw 1999, 449). First as small-scale irrigation ditches in the late 1800s, and later as federal water reclamation projects brought on by the New Deal, the reclaimed hydraulic resource shaped Phoenix's early agricultural and urban geographies. The reconstructed irrigation canals, coupled with the existing "ready market of hungry soldiers, ranchers, and miners" in the mining and military outposts surrounding the Salt River Valley helped materialize the agricultural potential of the region and provided the basis for commercial agriculture. Lacking a feudal history as well as private enterprise restrictions, the development of agricultural capitalism in Phoenix advanced unhindered, a pattern typical of the Western region's development at large (Robbins 1994). But unlike Southwestern cities such as Los Angeles, Santa Fe, Tucson, or San Diego, Phoenix was not originally a Spanish *presidio* (military garrison), *pueblo* (agricultural village), or *misión* (Jesuit outpost) that transitioned into an American town. Mexican and African-American farmers, laborers and businessmen, along with Anglo-European land and trade speculators hoping to profit from commerce with the nearby mining and military outposts of Wickenburg and Fort McDowell initiated the speculative settlement of the Salt River Valley (Mawn 1977; Whitaker 2000; Larsen and Alameddin 2007). Spurred by the Homestead (1862), Desert Land (1877), and Carey (1894) Acts, canal irrigation made possible the development of an industrial agriculture system that became "the base of the urban economy" (Kotlanger 1983, 5) in Phoenix from the turn of the 19th century through the interwar years. As agricultural production of citrus, dairy, cattle, olives, dates, alfalfa, cotton, cantaloupes, and other cash crops in the region increased, the urban infrastructure to process, warehouse, and distribute commodities also grew. Railroads, railyards, stockyards, meatpacking plants, warehouses, ice plants, bakeries, and flour mills were built in the burgeoning Phoenix townsite, replacing the natural desert land covers with wooden or adobe buildings.

In 1911, Roosevelt Dam was completed as the first federally-funded water reclamation project under the Newlands Reclamation Act of 1902 (U.S. Bureau of Reclamation 2013). The availability of water under the stewardship of the Salt River Project (SRP) further stimulated agricultural and urban expansion in Phoenix (Autobee 2013).

In addition to land use/land cover transformations in support of the agricultural economy, natural desert land covers were also altered for heat mitigation purposes during the early period of growth. As far back as 1872, property owners were placing cottonwoods and *acequias* (water ditches) along principal streets, "giving a dense and welcome shade to pedestrians passing along the city streets" (Farish 1918, 178). Trees and surface water provided shading and transpirational cooling, valuable ecological services before mechanized cooling became commonplace in Phoenix (Figure 4.2). Trees along canals provided "almost continuous shade over the waterways and created cool, attractive and welcoming places to escape the desert heat" (Simon 2002, 27).

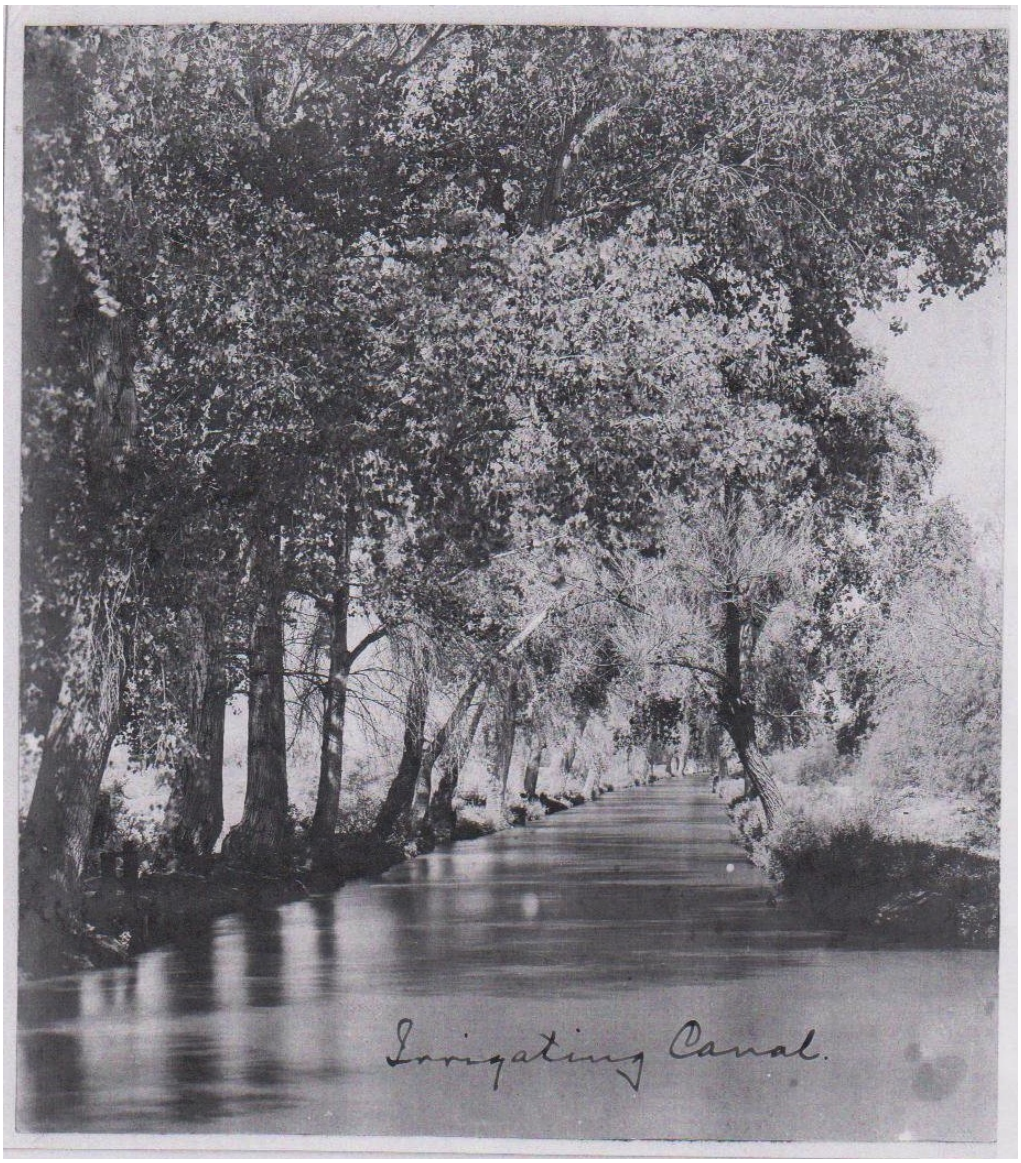

Figure 4.2: Irrigation canals in the early Phoenix settlement provided surface water and made possible the growth of shade trees. Barry M. Goldwater Historic Photograph Collection (FP FPC 1, Box 8, Folder 1. Historic Photographs, Places: Canals and Irrigation. 1890-1901. Arizona Collection, Arizona State University Libraries.

Along with urban and agricultural expansion came practices that increased the economic standing of Anglo-Europeans in Phoenix and decreased that of Mexicans, establishing the first marginalization conditions for the latter. Mexican laborers, subsistence farmers and ranchers had come to Phoenix since the 1860s and 1870s from the border state of Sonora and other towns in Arizona (Dean and Reynolds 2006). Various land grab schemes were devised by Anglos, often at the expense of the Mexican population. For example, between 1873 and 1896, Michael Wormser, a European

businessman, succeeded in dispossessing the incipient Mexican landowner farmer class of at least 9,000 acres of lands between the Salt River and the Phoenix townsite. The underhanded subterfuge is described by Goldberg (1973):

> *"He* [Wormser] *advanced the poverty-stricken Mexicans along the San Francisco Ditch the seed and supplies necessary to sow and harvest a grain crop, and he held a mortgage on the crop. At harvest time the farmer was obligated to deliver to Wormser the first threshed wheat or barley from a particular acreage. If the farmer failed to deliver the crop, Wormser had the right to seize the grain, or if the wheat or barley had been neglected, he would sue for his money plus interest. Michael, however, disliked the insecurity of relying upon the Mexicans to deliver grain from the land, and he settled into a new role, that of land baron. As the San Francisco Ditch crumbled and the farmers fell in debt to him for seed and merchandise, Wormser took advantage of the situation. He insisted that the Mexicans get legal title to their farms. When they did so, he acquired almost all of their land as well as the Ditch itself in return for wiping out their indebtedness. Approximately 9,000 acres of agricultural property adjoining the San Francisco Canal passed directly into Wormser's ownership or fell under his control. The canal, which he broadened, deepened, and expanded in order to bring water to his agricultural domain, became popularly known as Wormser's Ditch."* (Goldberg 1973, 185)

In parallel to the dispossession directed against Mexican farmers, Anglo settlers engaged in a systematic, fraudulent land and water rights grab by exploiting loopholes in the Desert Lands Act of 1877. A "desert land scheme" staged by New York businessman William Murphy, and his absentee family members–on whose names thousands of acres were filed claims to–and lasting around 35 years, resulted in the transfer to the Murphy family of more than 24,000 acres of land in the Salt River Valley in the late 19th century (Zarbin 2001). Similarly, Dr. A.J. Chandler–founder of the eponymous community in Maricopa County–accumulated for himself land and water rights by procuring "financing, people willing to make dummy entries under the Desert Land Act and mortgage the unpatented government land to Chandler, and a one-time source of water" (Zarbin 1995, 175). By 1895, Chandler had amassed more than 10,000 acres of land under a water rights fraud scheme later investigated and uncovered by a congressional subcommittee, but that resulted in no legal action against him. Practices of dispossession and land fraud contributed to the formation of a landed economic Anglo elite class in Phoenix. These practices helped set the stage for the augmentation of elites' economic and political power, while simultaneously diminishing that of minorities, preceding the spatialization of pernicious forms of marginalization that had lasting consequences for the urban riskscape.

Origins of land use differentiation and socio-spatial segregation in Phoenix

Climate events at the turn of the 19th century heralded marginalization against Mexicans and other minorities. An early spring flood in 1891 pushed the Salt River more than eighteen feet above its normal

level and widened its channel to eight miles before it receded (Honker 2002). In the aftermath of the flood, wealthy Anglos dispersed to higher elevation areas north of the town, marking the beginning of a north-south geography of segregation between whites and minorities (Kotlanger 1983; Bolin et al. 2005). The floods, in conjunction with the arrival of the Southern Pacific (1879) and Santa Fe (1895) railroads–linking the Valley to distant populations, markets, and capital–reinforced the displacement of the Mexican population. Before this time, Mexicans and Anglos could be found in the city in more or less equal numbers (Dean and Reynolds 2006). Mexicans were on par with Anglos in political, social, religious, and economic activities, as newspaper, business and property owners, landed farmers, civil servants, merchants, teachers, and registered voters. The arrival of the railroads linking eastern markets and the naming of Phoenix as territorial capital in 1889 brought large numbers of Midwestern and East Coast Anglos to the town, along with a "booster" campaign to promote White population influx to Phoenix, precipitated a demographic shift in their favor. Agriculture and commerce expanded, largely because the railroads increased access to both outside capital and markets. Demand for Mexican goods and services, and also the "[m]ixed marriages and inter-ethnic business partnerships" between Anglos and Mexicans–common inter-ethnic alliances during the two previous decades–began to disappear, rapidly relegating the Hispanic community to a "second-class status" (Dean and Reynolds 2006, 26). By 1890, the Mexican population was reduced from 45 percent in 1880 to a mere 14 percent (Dean and Reynolds 2006). The arrival of small numbers of African Americans and Chinese immigrants coincided with this period. Newcomer minorities lived in mixed neighborhoods with Mexicans during this time, when the lineaments of the South Phoenix district began to emerge as wealthy Anglos removed themselves away towards the north and non-whites were segregated in the central business district.

Residential segregation of Chinese, Mexicans, Native Americans, and African Americans to the industrial and warehouse district of South Phoenix was one of many socio-spatial practices aimed at maintaining a subordinate source of cheap labor while simultaneously marginalizing the cultural and economic contributions of minorities to Phoenix's development. For example, Mexican wage laborers and property owners shaped the early Phoenix landscape through commerce and farming, civil service and the construction of adobe houses and *acequia* water ditches, but were quickly relegated to the central business district's industrial and warehouse areas during the decade following the floods (Gober 2005; Oberle and Arreola 2008). Mexicans and Native Americans became sources of cheap labor in the agricultural and urban domestic economies: the first group was by 1920, "the principal work force in the entire region" (Kotlanger 1983, 425), and the second group was integrated into the capitalist

economy as domestic servants educated in the federally-funded Indian School. Mexican farmers had already been dispossessed of their fertile agricultural lands between 1873 and 1896. In combination with the land grab and dispossession schemes, previous Mexican land owners became destitute farm workers, forcing them and their families into the South Phoenix hovels that their low wages could afford them (Figure 4.3). The Chinese were also segregated. By 1920, a Chinatown in South Phoenix had emerged, where Chinese merchants, businesspeople and residents developed their own social and cultural institutions in part because they were excluded from those created by Anglos (Kotlanger 1983). African Americans, besides being also relegated to the disamenity zone south of the railroad tracks known as South Phoenix, were perniciously segregated in the use of public facilities, education, employment, health care, and membership in social organizations in the Jim Crow tradition experienced in the South (Whitaker 2000).

By the first years of the 20th century, inequities between Whites and minorities in housing and heat-mitigating vegetation were evident. Mexican farmhands were relegated to slums adjacent to the irrigation canals (Figure 4.3), or the segregated areas within the town labeled "Mexican Tenements" (Oberle and Arreola 2008). White neighborhoods, in contrast, were made up of standard housing and had irrigated shading vegetation (Figure 4.4).

Figure 4.3: Mexican laborers and their families lived in slum, makeshift housing nearby the Salt River irrigation canals. Barry M. Goldwater Historic Photograph Collection (FP FPC 1, Box 8, Folder 1. Historic Photographs, Places: Canals and Irrigation. 1890-1901. Arizona Collection, Arizona State University Libraries.

Figure 4.4: Water from *acequias* fed shading vegetation in wealthy neighborhoods in central Phoenix. Barry M. Goldwater Historic Photograph Collection (FP FPC 1, Box 8, Folder 1. Historic Photographs, Places: Canals and Irrigation. 1890-1901. Arizona Collection, Arizona State University Libraries.

Intensification of segregation in South Phoenix

Changes in the broader political economy brought on by the First World War intensified the concentration of minorities in the industrial area of Phoenix and exacerbated the conditions of uneven development between South Phoenix and the expanding northern part of the city. The outbreak of hostilities in Europe increased domestic cotton demand for producing textiles and rubber, but the previously steady supply of the Egyptian variety was interrupted by the conflagration (Sheridan 1995). Salt River Valley farmers responded by converting almost all agricultural lands to cotton production, a drastic turn towards monoculture in the previously diversified farming economy. Increased cotton production brought thousands of Mexicans as farm hands, who were largely left homeless and stranded in the valley after the cotton market crashed in 1920 when cotton imports resumed following armistice. Hundreds of homeless Mexicans "moved into the barrio or encamped alongside the canals, roads, and railroad tracks leading into the city" (Kotlanger 1983, 426).

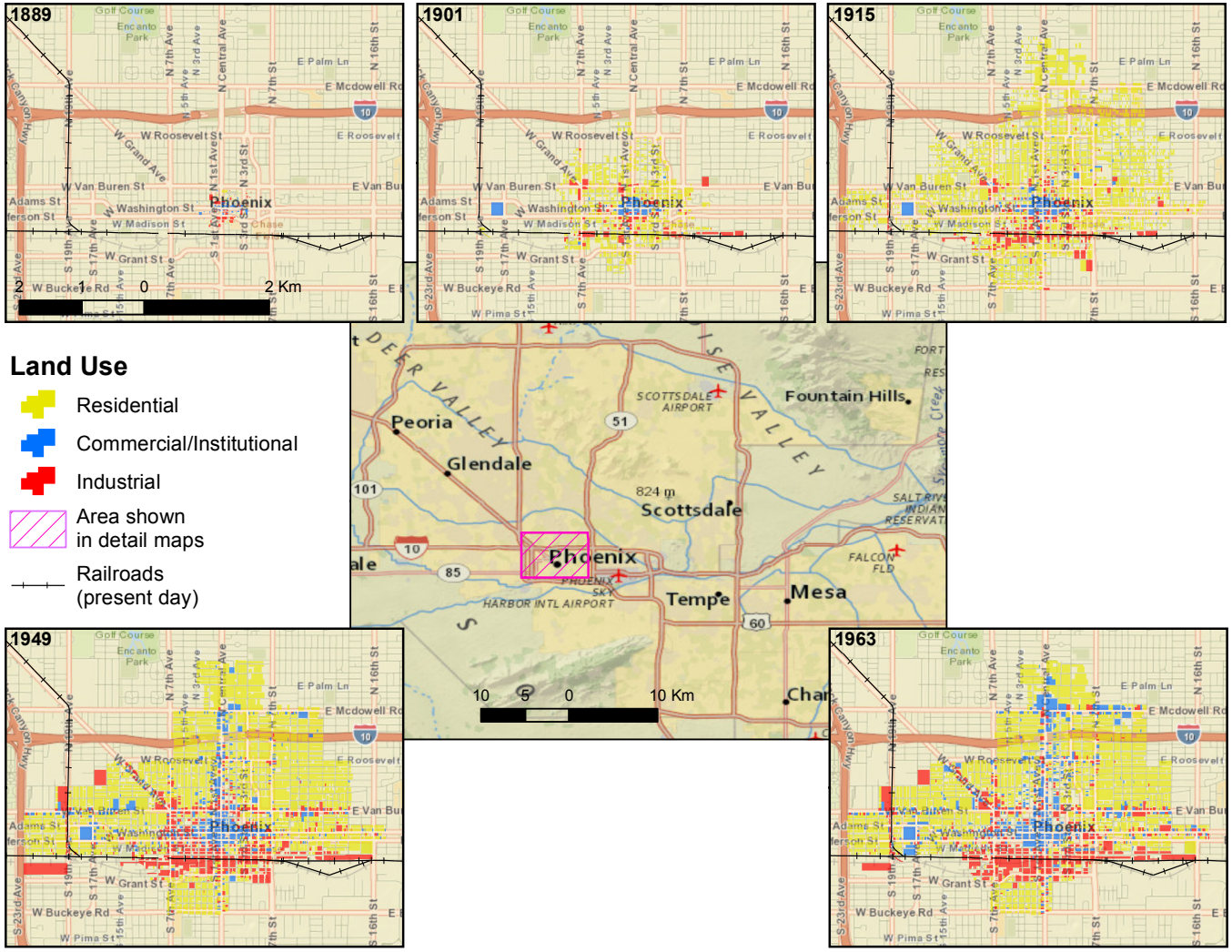

Figure 4.5: Industrial land uses agglomerated south of the railroad tracks in Phoenix. Source: Author's reconstruction from Sanborn Fire Insurance maps (1889) and Tuccillo 2011 (1901, 1915, 1949, and 1963).

The spatial segregation of minorities in South Phoenix proceeded apace with the discursive construction of Mexicans and other groups as devious, boisterous, dirty, uncivilized and mentally or culturally unfit to enjoy the social and economic benefits of Phoenix's growth. The Anglo-dominated press routinely described minorities with denigrating epithets such as "wily Mongolians" or "noisy Chinamen" (Chinese), "child-like and ignorant" (Native Americans) or "lawless niggers" (African Americans) (Whitaker 2000, 198). It was common to refer to any issues related to these ethnic groups as an Indian, Mexican, or Negro "problem" (e.g., Horton 1941). Racist banking and redlining practices rendered minorities and South Phoenix neighborhoods ineligible for mortgage loans and lacking in well paying jobs (Bolin et al. 2005). One particular effect was that land values remained low, further attracting industries to the railroad and warehousing infrastructure already in place. These socio-spatial practices allowed Anglos to maintain non-whites as a subordinate class of cheap laborers, and justified the dumping of unwanted land uses like industry, railroads, and open sewage in the South Phoenix district, in addition to limiting expenditures on urban services like quality vegetation and parks, schools, and housing. The growth of the urban and agricultural economies of Phoenix throughout the interwar years, characterized by the concentration of industrial activity south of the railroad tracks (see 1889, 1901, and 1915 maps in Figure 4.5), set the conditions for intensifying the degraded ecology of the district during the next transition in the urban landscape, brought by the New Deal and wartime production. By 1921, the familiar UHI gradient of higher temperatures in urban areas and lower temperatures in rural parts had been documented (Gordon 1921).

4.9 Second transition: Industrialization during the Great Depression and Second World War years

> *"The development of an agriculture-related industrial infrastructure made Phoenix like other Sunbelt cities, which were capable of serving a variety of economic sectors. The city gained a position by 1940 to capture a share of the nation's industrial and tertiary activity when they grew in prominence during the war. The agricultural development in the hinterland surrounding Phoenix prepared the city for a new era of growth and prosperity."* (Kotlanger 1983, 86)

New Deal-era land use transformations in Phoenix

The transformation of Phoenix's urban infrastructure into an industrial agriculture-oriented one during the Great Depression prepared the region for a land use transition towards industrial development during the Second World War. The relatively late onset of the Great Depression in Phoenix provided the opportunity for Phoenix to modernize its urban infrastructure. One of the reasons for the lag in the effects of the Depression was that the stock market crash of 1929 did not immediately impact the city, mainly because the Phoenician economy was not fully integrated into the global finance economy.

Consequently, the Great Depression's effects in Phoenix were delayed until 1931, when a severe reduction in copper demand resulted in state-wide mine closures and job losses in Phoenix (Niebur 1967). As demand for all commodities dropped nationwide, the federal government intervened by propping up sectors like agriculture throughout the country. In Phoenix, for example, the citrus sector not only held fast, but grew as production surpluses were purchased by the Federal Surplus Commodities Corporation, stimulating the creation of box manufacturing, produce packing, distribution, and juice extraction facilities in the city (Kotlanger 1983).

During the 1930s decade, other national government interventions in Phoenix came as New Deal funds for unemployment relief. New Deal infrastructure projects accelerated conversions of natural land covers into heat-retaining impervious surfaces and also the removal of surface water throughout Phoenix. Street widening and paving, and bridge building were made possible by highway funds allocated to the city in 1935 (Niebur 1967). New Deal money carried the local economy through the Depression, also providing the fiscal and technical resources for the city to modernize its hydraulic infrastructure. By 1934, many canals built in the previous decades and criss-crossing the townsite had been piped, covered with dirt, or otherwise dismantled (see maps for 1914 and 1934 in Figure 4.6). In 1937, three major canals were fitted with concrete pipes, and feeder streetside ditches like those in Figure 4.4 were covered with dirt, which allowed the city to widen and pave roads (Kotlanger 1983). Lining and piping of canals and the burial of acequias eliminated water seepage through the soil, a technical efficiency aggressively sought by the Salt River Project (SRP). A careful accounting of water was a requisite for the increasingly high demands of industry for water, but also for electrical power, a by-product of the SRP that became a critical resource for Second World War-related industrial development. The removal of free flowing surface water and the trees fed by it, and the paving of city roads signaled a structural change in the Phoenix economy as agriculture began diminishing in importance and industrial activity increasingly took its place.

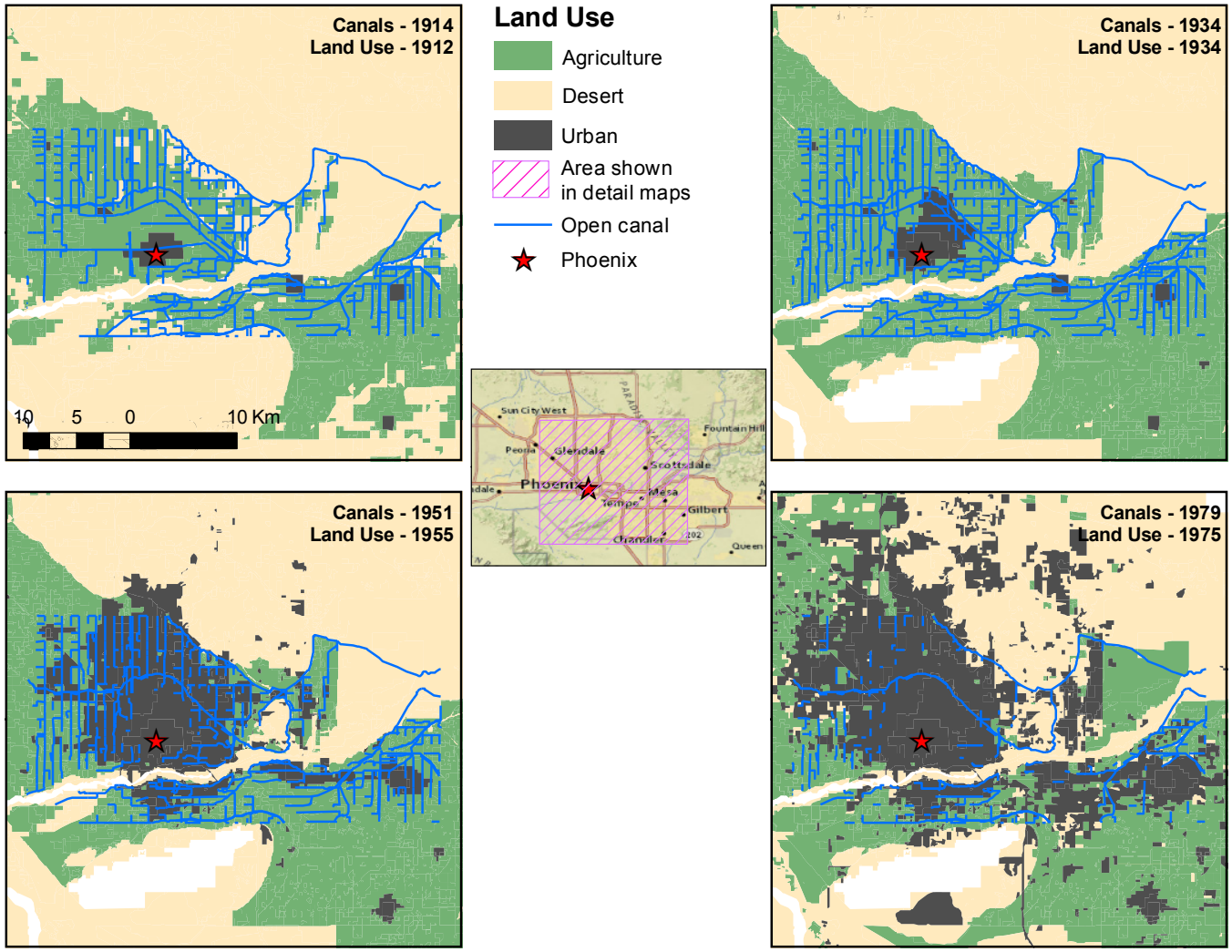

Figure 4.6: Irrigation canals built during the early period were dismantled, piped, or covered with dirt as the Phoenix urban footprint expanded. Source: Author's map based on CAP LTER 2003 and (REF).

The transition in the use of land for industrial activities in Phoenix responded to the increase in demand for Second World War arms and supplies. The Phoenix region's dry and sunny year-round climate, inland location that afforded safety from Axis incursions, and low unionization rates attracted manufacturing of electronics, airplane parts, and other components for military aircraft (Konig 1982; McCoy 2000). Phoenix thus modernized its previously resource-based economy into an industrial manufacturing regional hub. White-collar workers were attracted to Phoenix during this time as war production stepped up and flagship industries like AiResearch, the Aluminum Company of America (Alcoa), and Goodyear Aircraft established in the area.

Reinforcement of the industrial character of South Phoenix

The transition from a resource extraction and export-based economy into an industrial manufacturing regional hub stimulated explosive postwar population growth in Phoenix, accelerating land use and land cover changes that intensified the urban riskscape. However, the "era of prosperity" alluded to by Kotlanger (1983, 86) did not materialize for the people of South Phoenix. The role of South Phoenix as the manufacturing and transportation hub of the region was cemented; minority populations were largely excluded from the economic benefits of urban and industrial growth, but their neighborhoods were burdened with industrial land uses largely unseen in the northern, more affluent areas of the city (see the 1949 map in Figure 4.5). Indeed, a clear geography of difference between South Phoenix (south of the railroad tracks), and the suburbs in the north had emerged during this period. A passage in a state guide compiled by the Writer's Program of the Work Projects Administration (WPA) describes the socio-spatial segregation and pattern of uneven development in the urban landscape:

> *The better residential sections of Phoenix–Encanto, Palmcroft, Country Club Manor, Biltmore, and Arcadia–have green lawns and flowers throughout the year.* ***The many cottonwood trees that shade the lawns and walks are never completely bare, for new leaf buds are formed before all of the winter-killed leaves have fallen. Palm, tamarisk, eucalyptus, olive, and citrus trees also provide shade****. On spring nights the sweet heavy perfume from the outlying orange groves floats over the city, and in late spring oleander hedges burst into white and pink bloom. The majority of Mexicans and Negroes live south of the railroad tracks. At Jackson and South 16th Streets and at Grant and 5th Streets, are the homes of many of the more well-to-do Negroes. Here dwellings are neat and attractive with lawns, shade trees, and flowers. The Negroes have their own churches, hospitals, newspapers, and social activities. Farther east is the "shack-town" of the poorer Mexicans, and "7-Up Camp", a block of shacks along the north side of the railroad tracks housing hundreds of Mexican families.* ***The houses are nondescript in materials and appearance with bare unshaded yards****. The more prosperous Mexicans live between Second and Fourth Avenues south of Madison Street, in rows of well-kept homes with landscaped lawns. From Seventh Avenue west is the poorer Negro section with living conditions similar to that of the poorer Mexican sections*(emphasis added) (WPA 1940, 218).

The passage provides a vivid description of vegetation differences between the "better residential sections" with "cottonwood trees" and lawns that "are never completely bare", and the "shack-towns" with "bare unshaded yards", where poor Mexicans lived. Housing for most Mexicans in South Phoenix was described in one social survey as having "no running water and no electricity" (Kotlanger 1983, 426). The WPA narrative also provides an indication of class differentiation among both Mexicans and African Americans. Middle class Mexican American neighborhoods were scattered throughout the area, as were African American ones in a similar fashion. Historic property surveys document two distinct middle-class African American neighborhoods, emerging through what Phoenix historian Whitaker has termed the "black professional tradition" that Blacks fleeing the Jim Crow South brought to the U.S. Southwest (Whitaker 2005). So although a certain amount of affluence was enjoyed by some Mexicans and Blacks, these groups were largely segregated from the white population, and even the affluent ones were segregated from Anglo neighborhoods.

The process of industrialization and minority segregation and the conversion of desert land covers into impervious surfaces created a distinct pattern of difference between South Phoenix and the expanding, affluent suburbs. For Phoenix, the end of the Second World War would signify an unprecedented population boom, when returning service personnel attracted by land availability and white-collar defense jobs–reintroduced by the private sector under the demands of the Cold War–settled in the region. The postwar influx of people into the Sunbelt region changed the character of Phoenix from an isolated agricultural outpost to a suburban destination (Redman and Kinzig 2008), and helped trigger the third large-scale transformation of the region into its current form: that of an expansive, sprawling Southwestern metropolis.

4.10 Third transition: Expansive suburbanization of a Southwest Metropolis in the postwar and beyond

The immediate postwar period

The postwar period in the Salt River Valley signaled the coalescing of the relatively isolated communities in and around Phoenix into a metropolitan conurbation. As service personnel returning home after 1945 found employment in defense-related industries, the availability of jobs, land, power, and water for urban development drove the westward migration of population not only in Phoenix, but in the Sunbelt in general. The spatial pattern of wide streets and automobile-oriented development begun in the earlier decades continued, while aggressive annexation policies promoted both outward expansion to unincorporated areas and leapfrog development due to availability of incorporated land within municipal boundaries (Heim 2001). The dismantlement of the streetcar system in downtown

further cemented the city boosters' vision of Phoenix as an automobile city, promoting street widening, paving, and highway construction (Konig 1982). By 1960, the city was crisscrossed by four federal highways concentrated in the central business district and South Phoenix, adding vehicular air pollution to the degraded environmental conditions there.

A reliable water supply also contributed to the growth of industrial and residential dwelling manufacturing. Improvements to the water delivery system increased the water capacity through more dams, spillways, wells, and the more salubrious water from the Verde River to the northeast. The availability of water for urban use also aided the spatial expansion of the city, as residential unincorporated areas outside of the Phoenix municipal boundaries were enticed towards annexation in order to secure a connection to the water grid (Kupel 2006). Recognizing an increase in the demand for urban services, the role of SRP as a provider of water almost exclusively for agricultural use changed markedly after the Second World War. In 1950, the SRP dedicated 86.2 percent of its water production for agriculture and 13.8 to municipal (including commercial and residential) and industrial users. In the next decade Phoenix's population increased by more than 300 percent, and the share of SRP water for farming had decreased to 74.1 percent. The remaining quarter was dedicated to industry and municipal customers (Famisa 1977).

As Wenum has argued (1968), the availability of unincorporated, mostly agricultural areas adjacent to the municipal fringe provided the land base for expansion. The growth of the industrial and urban economies in the previous transitions–made possible through irrigated agriculture–increased the potential rent value of lands for residential and commercial uses, and motivated farmers to sell their lands to developers. To promote and accommodate population influx, city elites created the bureaucratic and political preconditions necessary for effective annexation in Phoenix. For example, an Arizona statute allowing legal annexations of land was codified into law. Lastly, the reformation of the Phoenix city administration into a professionalized charter government during 1948-50 increased the trust that residents of unincorporated areas placed on the municipal government, long derided as corrupt and fraught with nepotism (Heim 2001). The move towards charter government also increased the reputation of Phoenix's administrators as efficient and business-friendly, boosting both the local and national profile of city elites, heralding the rise of conservative, business-oriented city development and politics not only in Arizona, but also in the Sunbelt region (Luckingham 1989). These social and legal conditions were produced by city administrators and business elites to promote the city of Phoenix as the dominant municipality in the region and increase tax revenues that would bankroll further growth.

Their efforts were critical in securing the dominance of Phoenix because the city faced a choice between annexing land and increasing its tax base and status as dominant municipality, or remaining a small city surrounded by satellite communities that benefitted from nearby urban facilities, but did not contribute tax dollars to its maintenance (Luckingham 1989).

The expansion of suburban Phoenix through agricultural land conversions and annexations of developed areas proceeded swiftly, but at the expense of the central business district where minority populations were concentrated. From the 1950s decade on, the urban core infrastructure was neglected as amenities and development focused on the expanding suburbs. Luckingham illustrates the definitive postwar shift towards an automobile-oriented suburban city:

> *While the Phoenix suburbs developed rapidly during the 1950s, the city's central business district (CBD) went into...decline. As residential dispersal progressed, business decentralization, especially of retail outlets, increased. During World War II, retail business in downtown Phoenix recorded spectacular growth, but following the war the increasing population began to spread out. Streetcars stopped operating in 1948, and automobile drivers increasingly declined to deal with the severe lack of downtown parking. During the 1950s shopping centers outside of downtown appeared to serve affluent, automobile-oriented suburban customers.* (Luckingham 1989, 162)

The lack of retail and residential amenities in the downtown core served to keep land values low and attract industry to the already depressed area. By 1963, industrial facilities were concentrated in the CBD and South Phoenix (Figure 4.7). Although a great deal of middle class affluence was achieved by industrial worker transplants from other parts of the country, most of Phoenix's minorities did not share in the postwar bonanza. Mexicans and Mexican-Americans had little upward mobility, remaining in substandard housing or racially-segregated projects and schools. In 1960, the overwhelming majority of Black Phoenicians lived in seven census tracts south of the Southern Pacific railroad tracks, in some of the worst slums in the city. Similarly, opportunities for Native Americans were restricted to vocational training in the Indian School, effectively boxing them into low wage employment. One notable exception to limited upward mobility was the Chinese population, who by 1960 had abandoned the small downtown Chinatown and dispersed to the suburbs. Associations that served as investment sources for family enterprises and the pursuit of college degrees were some ways that the Chinese population increased their socio-economic standing to escape the downtown district.

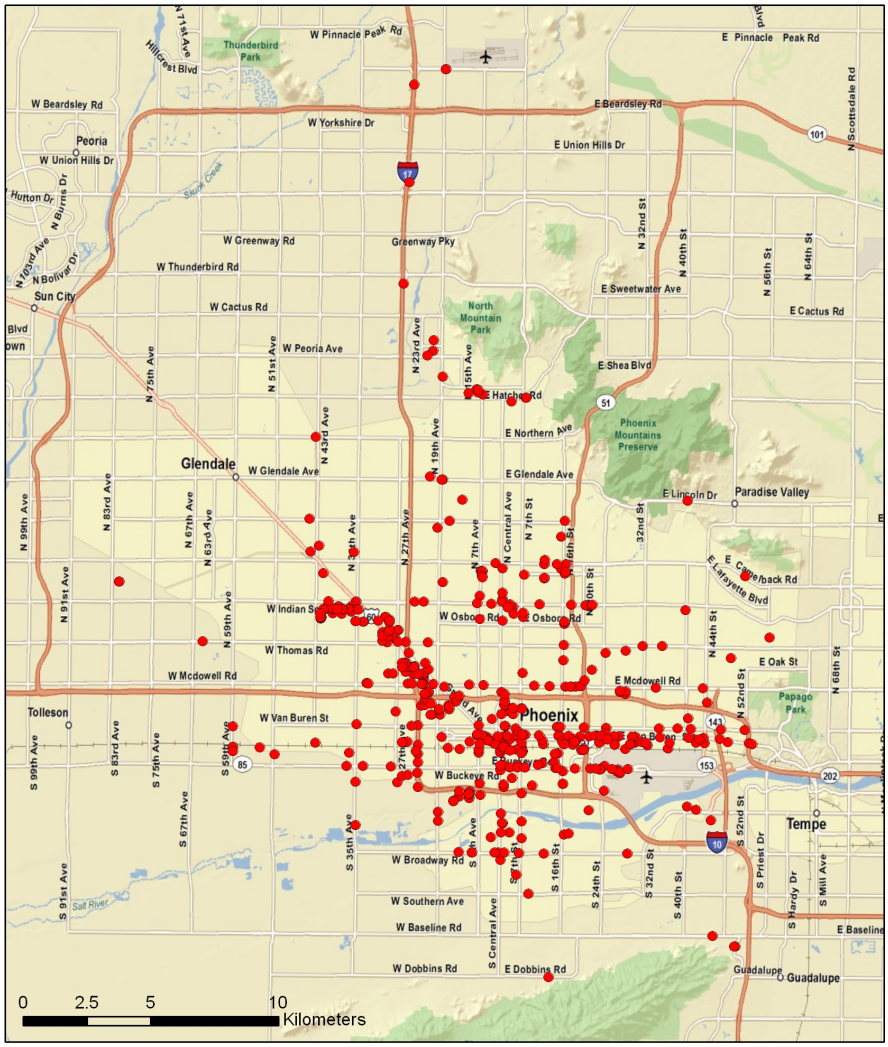

Figure 4.7: By the 1960s decade, industrial facilities had concentrated in South Phoenix. Source: Author's elaboration based on Directory of Manufacturers in the Phoenix Area. Phoenix Chamber of Commerce.

Expansion of the Urban Heat Island

The rapid development of Phoenix in the postwar period had a clear impact on the expansion of the urban heat island. Maximum air temperatures in the Sky Harbor airport location increased by about 0.21 °F per year from 1949 to 1985. Underscoring the uneven distribution of the landscape of heat risk, the gradient of minimum temperature increase north of the CBD for the same period attenuated to the point of showing yearly average reductions of 0.05 °F in the northern areas of the city; downtown

Phoenix areas were not only the hottest area, but also experienced the most warming (Balling and Brazel 1987). As the annexation of land progressed north and west towards the agricultural districts, more and more land became available for urban development, changing natural land covers into roadways, buildings, and other impervious surfaces. Computational simulations for the period 1973-2005 have estimated temperature increases of 2–4 °C in former agricultural lands converted to built up areas (Grossman-Clarke et al. 2010). Urban canyons formed by buildings and other vertical surfaces also contributed to increased temperatures in the built up area by reducing advection-based air cooling.

4.11 Conclusions

The Phoenix urban landscape has been shaped by successive transitions in agricultural, industrial, and suburban development. Following the logic of capitalist development, various socio-spatial practices of land use/land cover change and marginalization of minorities were deployed to shape biophysical and cultural landscapes with differential distributions of socio-environmental risks. Historically, environmental risks in general, heat risks in particular–and the populations most affected by them–have been concentrated in the South Phoenix district south of the CBD.

The first transition of modern settlement in Phoenix began in the late 19th century through the development of an agricultural economy that in turn drove land use/land cover changes through economic expansion. Biophysical conditions in the natural environment like a long growing season, ample sunshine, water availability, fertile soil, and a flat, low topography were harnessed to produce agricultural and urban landscapes in early Phoenix. The development of railroad connections and hydraulic works for irrigation also spurred the growth of the urban infrastructure to put agricultural commodities in circulation towards regional and national markets. land use/land cover changes in the early urban environment set the historical and geographical trajectory of a riskscape of environmental hazards centered around the central city core and South Phoenix. Contributing to the intensification of the landscape of extreme heat was the industrial, low-rent character of the central business district, further cemented after the 1891 floods. In their aftermath the railroad became "both the physical and symbolic boundary between two developing urban worlds" (Bolin et al. 2005, 158), reinforcing a pattern of race and class segregation that persists to this day. The riskscape continued to grow in magnitude and spatial extent as Phoenix's urban economy and footprint expanded through New Deal infrastructure investments, signaling the second transition towards industrial development. The modernization of the city's automobile-centric transportation and hydraulic infrastructure brought intensified land use/land

cover changes like streets widening and paving, lining of canals, burial of irrigation ditches and removal of trees along streets, reducing the potential for transpirational cooling and shading, and increasing the heat-storage capacity of surfaces in the growing city. Although land use/land cover changes related to infrastructure modernization occurred across the city, residents of South Phoenix became more exposed to extreme heat and to the degraded ecology of the district. Their subordinate status as sources of cheap labor relegated them to the slum areas, where bare yards with no shade and sub-standard dwellings afforded them little protection from extreme heat, a situation that contrasted with standard housing and canopied vegetation typical of the affluent residential sectors north of South Phoenix and the central business district. Postwar industrial proliferation concentrated in and around South Phoenix fostered employment and suburban population growth, which the city absorbed through an aggressive land annexation policy. Annexation provided abundant, incorporated developed and vacant land for urban expansion, promoting the replacement of previously agricultural land into residential and commercial subdivisions. The space-consuming pattern characteristic of the immediate postwar period has continued unabated into the early decades of the 21st century, along with increasing temperatures in the urbanized areas, especially high in the central city.

The historical and geographical analysis of the landscape of risk in Phoenix posits the production of urban space as a process of capital accumulation directed at maximizing exchange value. The concentration of industrial and agricultural capital in the original townsite and the central business district created an uneven distribution of socio-ecological conditions, in general of degraded environmental conditions, and in particular of extreme heat. The townsite-cum-industrial core became a zone of acute heat exposure as minorities were relegated there by socially constructing them as a low-income, subordinate laborer class unfit for full participation in the Phoenician society. In the process of seeking exchange values, elites actively sought to concentrate industrial development, transportation infrastructure, and low land rents in South Phoenix, while reaping the benefits of suburban living away from that district. Simultaneously, social values like temperature-reducing ecological services (e.g., water ditches and irrigated shade trees) were marginalized, creating a riskscape of heat that is most intense in South Phoenix. The landscape of risk thus emerged as a decidedly historical and geographical project of capital accumulation through transitions in Phoenix's agricultural, industrial, and suburban dominant modes of accumulation. By unpacking the configuration of the landscape of heat risk as an inequitable urban geography of environmental hazards exposure, it

is revealed how the process of capital circulation for profit generation actively creates uneven geographies that affect social groups differently.

Chapter 5

CREATING THE PARK COOL ISLAND IN AN INNER-CITY NEIGHBORHOOD: HEAT MITIGATION STRATEGY FOR PHOENIX, ARIZONA

5.1 About this chapter

In the last case study chapter in this dissertation, I address Research Question 3: *What is the potential impact of increased vegetation in mitigating extreme heat in an urban core neighborhood in Phoenix?* The case study presented in this chapter is a co-authored peer-reviewed research paper published in the journal Urban Ecosytems. The paper's citation is the following:

> Declet-Barreto J, AJ Brazel, CA Martin, WTL Chow, SL Harlan (2013). Creating the park cool island in an inner-city neighborhood: heat mitigation strategy for Phoenix, AZ. Urban Ecosystems 16(3):617-635. doi:10.1007/s11252-012-0278-8.

This chapter explores the impact of vegetation in lowering temperatures during an extreme heat event in an urban core neighborhood park in Phoenix, Arizona. Air and surface temperature predictions were simulated under two different vegetation regimes: existing conditions representative of Phoenix urban core neighborhoods, and a proposed scenario informed by principles of landscape design and architecture and Urban Heat Island mitigation strategies.

5.2 Statement of Author's Contributions

I declare that my contribution to developing the theoretical framework, research design, analysis, results, and conclusions in this paper was substantial, and the bulk of the work my own. AJ Brazel contributed his extensive urban microclimate research expertise; CA Martin provided vegetation survey data as well as guidance on ecosystem services; WTL Chow contributed his ENVI-Met 3.1 expertise, while SL Harlan provided guidance on the general direction of the work and its significance to the broader question of heat-related vulnerability.

5.3 Introduction

Urban climate research has empirically established spatio-temporal relationships between land cover and heat fluxes in cities, and is especially attentive to Urban Heat Islands (UHIs) in cities (Roth 2002; Voogt and Oke 2003; Mills 2006). The climatic consequences of anthropogenic surface cover changes at the regional scale are well understood. The replacement of natural covers with the urban fabric results in significantly higher nighttime temperatures in built-up areas compared to the surrounding rural environment (Lowry 1967; Balling and Brazel 1987; Oke 1997). Reintroducing urban green spaces with canopied vegetation can alter surface and near-surface energy flows and act as wind tunnels or barriers, potentially reducing the intensity of UHIs (Oke 1989; Grimmond et al. 1996; Barradas et al. 1999). There are two principal ways in which vegetation influences surface energy flows that in turn affect surface and near-surface temperatures. Larger plants such as trees attenuate radiant energy flows through absorption and reflection. Less radiant energy contacting the ground surface reduces surface and near-surface temperatures. This microclimate ecosystem service is known as shading. The second mechanism is related to plant consumption of energy during transpiration. As water is evaporated from a liquid to a gas at the surface of cellular structures inside leaves, temperature reductions occur in the immediate environment surrounding a leaf. We refer to this microclimate ecosystem service as transpirational cooling.

One way to study these ecosystem services is by examining the Park Cool Island (PCI). The PCI is an irregular pattern of cooler areas nested within generally warmer urban areas, created by shading and transpirational cooling and extended to the air above non-vegetated areas through advective cooling (Chow et al. 2011). Creating the PCI by increasing vegetation is an increasingly studied strategy for mitigating the effects of the UHI. Numerical modeling of the PCI at the microscale is a valuable tool to explore vegetation modification and its effects on microclimate cooling, especially in areas where energy flux interactions among canopied vegetation and impervious surfaces at a fine scale are not well documented. The purpose of our study was to evaluate the role of vegetation in creating the PCI in a sparsely-vegetated, low-income, ethnic minority community in inner-city Phoenix, Arizona. We modeled air and surface temperatures to better understand the role of vegetation in providing shading and transpirational cooling as a strategy for moderating the UHI. We conducted microclimate simulations in ENVI-Met, a three-dimensional prognostic simulation of surface-plant-air energy interactions (Bruse and Fleer 1998). The modeling system solves a series of differential

equations to simulate processes of surface heat, vapor and vegetation exchange, vertical surface air flows, particle dispersion, turbulence, and bioclimatology. We used ENVI-Met to simulate the PCI during an extreme heat event (EHE). EHEs are characterized by sustained periods of high temperatures above the range of normal variability (Meehl and Tebaldi 2004; Pachauri and Reisinger 2007). For the duration of the EHE, we predicted air and surface temperatures within the park at the microscale (modeling cell size 3.59 meters x 1.00 meters). We first modeled the 24-hour profile of predicted surface and air temperatures by surface cover type for representative existing park vegetation conditions compared to an alternative proposed park landscape design with more vegetation. Second, we examined the spatial distribution of temperature differences between the representative existing and proposed vegetation conditions, and estimated the extent of the potential PCI. We contribute to urban ecology research by evaluating the relationships among vegetation, ecosystem services, and the PCI with microclimate modeling and by applying a spatial analysis technique to mapping the PCI.

5.4 Literature Review

Vegetation and extreme heat mitigation in Phoenix

Mitigating high temperatures in desert cities like Phoenix, where the weather is chronically hot for half of the year and EHEs occur frequently in the summer, is an important policy goal. Mesoscale climate modeling and analyses of historical temperature data in metropolitan Phoenix have shown that both the severity and extent of UHIs continue to increase, especially in the urban core (Grossman-Clarke et al. 2005; Ruddell et al. 2010). Indeed, Maricopa County (where metropolitan Phoenix is located) experienced an increase in average temperature of more than 3°C during the 20th century, while temperatures in Arizona's urban areas increased at three times the rate of regional temperature increase (Brazel et al. 2000) . Heavily built-up urban areas like Phoenix are expected to experience more—and more severe—extreme heat events and longer warm seasons throughout the 21st century (Diffenbaugh et al. 2005). Extreme heat is a threat to human health, increases atmospheric pollutants and energy and water use, alters regional hydrology, and impacts interactions between humans and ecological processes (Brazel et al. 2007; Jenerette et al. 2007; Wolf et al. 2010; Anderson and Bell 2011).

Recent research in metropolitan Phoenix stresses the critical role of vegetation in mitigating high temperatures in desert cities. Ruddell et al. (2010), for example, found that Phoenix neighborhoods with higher vegetative densities had significantly lower temperatures during an EHE than those with xeric or sparse vegetation. Stabler et al. (2005) studied relationships of vegetated land

cover (expressed as NDVI) with land use, air temperature, and humidity, and found that microclimates in Phoenix are caused by heat flux interactions between vegetation and non-vegetated surfaces. Similarly, Jenerette et al. (2007) combined remotely-sensed surface temperature and vegetated land cover (NDVI) at the scale of U.S. census tracts and found a statistically significant correlation between sparse vegetation and high temperatures. Desert cities like Mexicali (Baja California, México) also show significant intra-urban land cover-dependent variability in the composition and intensity of the UHI (Garcia-Cueto et al. 2007). A study in Cairo, Egypt found a distinct nocturnal heat island effect during the warm season, associated with land cover: urban areas had drier and warmer atmospheric conditions compared to rural or suburban parts of the city (Robaa 2003).

Social dimensions of green spaces (parks) in urban areas

The association of temperature and vegetation with ethnicity and socioeconomic status is also well documented in urban ecology and social science research in Phoenix. Some research has been especially attentive to weather conditions that expose humans to the effects of heat stress. Heat stress, which is a threat to human health and can cause severe illness or death (EPA 2011), is triggered when temperature thresholds of human tolerance are exceeded. Harlan et al. (2006) found that low-income, minority neighborhoods in Phoenix were warmer and more sparsely vegetated than higher-income, predominantly white neighborhoods and consequently residents were more exposed to temperatures that cause heat stress. Multivariate modeling of the entire metropolitan area by Jenerette et al. (2007) found a positive statistical relationship between neighborhood affluence and more vegetated land cover. In Phoenix, economic stratification in access to vegetation-based ecosystem services is a relatively recent phenomenon, which was not present in the 1970s, but clearly increased each decade through 2000 (Jenerette et al. 2011). Buyantuyev and Wu (2012) found that although surface temperatures in Phoenix are driven largely by vegetation and impervious surface distributions, median family income mediates this relationship. Together, these studies suggest that green spaces have desirable ecological outcomes in Phoenix but low-income communities are receiving fewer benefits and the gap between higher- and lower-income neighborhoods is increasing over time.

In addition to the demonstrated impacts of vegetation on UHI mitigation, green spaces provide other ecosystem services, such as reduction of airborne contaminants, absorption of rainfall, buffering against flooding, and habitats for wildlife (Boone et al. 2009; Currie and Bass 2008; de Groot et al. 2010; Payne-Sturges et al. 2006). These ecosystem services play a role in creating "salutogenic" urban environments that can help mitigate human health problems, such as asthma, allergies, obesity, and

increased stress. It has been shown that lack of green spaces in cities contributes to health disparities among people in lower- and higher-income neighborhoods (Jennings et al. 2012; Wilson 2009). Public outdoor heat mitigation strategies in parks and other public spaces are especially needed in socially and ecologically vulnerable areas of cities because residents in these areas have fewer household social and economic resources to adapt their microscale outdoor and indoor environments to extreme heat (Harlan et al. 2006; Martin et al. 2004).

Studies focused on environmental equity find that both the quantity and quality of parks are unevenly distributed within cities, and that low-income and minority communities sometimes have less access to such amenities (Boone et al. 2009; Byrne et al. 2009). Research in this field combines urban socio-ecological and historical perspectives to argue that intra-city disparities in the location of quality parks are the outcome of complex interactions between cultural, ecological, and political processes that continuously reshape urban environments and differentially benefit socio-economically advantaged populations at the expense of poor or low-income communities (Brownlow 2006; Dooling et al. 2006). The provision of ecologically adequate—and adequately maintained—vegetation is important for equitable outcomes, especially since neglected parks often create “ecologies of fear” that emphasize legacies of race-based social control and criminalization of environments and their occupants (Brownlow 2006, 235; see also Davis 1998).

Increasingly, minority communities argue that the dearth of adequate park facilities is an environmental injustice that demands redress by authorities and city planners. Inequities in park access and ecological conditions can be framed according to intra-city differences in fiscal expenditures for parks infrastructure. In inner-city Phoenix, inadequate parks infrastructure is most evident in lack of grass and tree irrigation, paucity of regular park maintenance by city staff, particulate matter pollution from dirt lots on park grounds, and unbuffered industrial land uses and freeways sited near parks–conditions that prevail in the poorer areas of the city. Therefore, the environmental justice issues related to urban green spaces suggest that vegetation-based UHI mitigation strategies may help address not only extreme heat, but also contribute to achieving a more equitable distribution of ecological services in the city.

5.5 Methods

Study Area

Our study area is the Latino Urban Core (LUC) neighborhood, a sparsely-vegetated, low-income, ethnic minority neighborhood in the urban core of downtown Phoenix. It is bounded by industrial land uses to

the north, south, and east, and by an interstate freeway to the west. As shown in Figure 5.1, the portion of the neighborhood in the modeling domain (3.59 hectares in area) currently has little vegetation. A central feature of the neighborhood, as seen in the aerial photo, is an electric utility company easement currently used as a linear park space almost entirely devoid of vegetation. The sparse vegetation in the neighborhood is located mostly in the front and backyards of residences, and is comprised of both desert and non-native plant species (Table 5.1). Abundant patches of exposed soil are found throughout the neighborhood in vacant lots, front and backyards, and in the park grounds.

Figure 5.1: The Latino Urban Core (LUC) study area is characterized by a linear park with little vegetation and residential areas unbuffered from industrial land uses.

Figure 5.2: Sparse vegetation, exposed soil, and high-capacity electrical towers typical of the LUC study area. Image source: Google Street View.

Table 5.1: Taxa in LUC study area

Symbol	Taxonomic name	Common name
BG	*Cynodon dactylon*	Bermuda Grass
SA	*Fraxinus uhdei*	Shamel Ash
WM	*Morus alba*	White Mulberry
OG	*Muhlenbergia capillaries*	Pink muhly
OG	*Muhlenbergia rigens*	Deer grass
OG	*Stipa tenuissima*	Mexican thread grass
EO	*Olea europaea*	European Olive
PV	*Parkinsonia culeata*	Palo Verde
MP	*Pinus eldarica*	Afghan Pine
TM	*Prosopis hybrid*	Thornless Mesquite
AS	*Rhus lancea*	African Sumac
CE	*Ulmus parvifolia*	Chinese Elm
FP	*Washingtonia filifera*	Desert Fan Palm
MP	*Washingtonia robusta*	Mexican Fan Palm

This neighborhood was deemed suitable for modeling the relationship between vegetation and energy fluxes based on previous research in Phoenix that found similar low-income and minority communities were associated with higher temperatures, sparse vegetation, and increased heat stress (Harlan et al. 2006; Jenerette et al. 2007). We focused our analysis on the park and on the industrial and residential blocks immediately north and south of it.

Microclimate Modeling in ENVI-Met 3.1

ENVI-Met is useful for analyzing small-scale impacts of vegetation and rooftops on local microclimates because spatially-explicit thermal data from remote sensing platforms are too coarse for studying intra-urban environments. The highest spatial resolution (pixel size) of available remotely-sensed thermal data ranges from 30-90 m (ASTER Science Project 2006). Such coarse resolutions render thermal sensor data unsuitable for microclimate investigations, where the influence of individual land covers, trees or other plants, on atmospheric and surface energy fluxes is of interest. We compared the modeled results of air (*Ta*) and surface (*Ts*) temperature for two vegetation scenarios to gauge how differences in vegetation cover would change the intensity of a major heat wave's effect on the park. We also mapped a local indicator of spatial autocorrelation to estimate the magnitude and spatial extent of the potential PCI created by differences in air temperature between the scenarios. We relied on validation of simulated temperatures in Chow et al. (2011), which included ENVI-Met modeling and a temperature data collection campaign conducted in a site in metropolitan Phoenix with similar vegetation and microclimate conditions.

The ENVI-Met system divides a study area into equal-sized cells, for which surface and air temperature, air flow, and other indicators are predicted based on user-provided initial atmospheric conditions and urban spatial structure. Microscale models (typically 0.5-10.0 meters horizontal resolution) can describe intra-urban variability in microclimatic signatures that are not captured by the coarser resolution (˜5-30 km) of mesoscale simulations. ENVI-Met has been applied in European cities to evaluate strategies for UHI mitigation (Huttner et al. 2008), to estimate the cooling effects of green spaces (Lahme and Bruse 2003), and to simulate the localized effects of global warming (Huttner et al. 2008). In studies within metropolitan Phoenix, Ozkeresteci et al. (2003) modeled scenarios to inform urban design and planning strategies and Rosheidat et al. (2008) evaluated strategies to increase pedestrian thermal comfort. Chow et al. (2011) used ENVI-Met to model the role of vegetation in creating the PCI, and Hedquist et al. (2009) modeled an urban canyon near the Phoenix city center. The latter two studies compared their respective simulation results with field-collected surface and atmospheric data, and the models compared well to field observations. Chow et al. (2011) used several difference measure indices (e.g. Root Mean Square Error and Mean Absolute Error) to evaluate ENVI-Met simulations against observed temperatures and reported reasonable model accuracy of both spatial distribution and time-series of simulated temperature data. Hedquist et al. (2009) found that simulation temperatures compared best to observations during the hours of maximum UHI intensity, typically 3-5 hours after sunset.

Air and Surface Temperatures

Increases in *Ta* and *Ts* are the best understood and most frequently observed indicators of the effects of urbanization in UHIs (Roth 2002). *Ta* can describe UHIs at the urban canopy layer (i.e., beneath the general height of buildings or trees, whichever is greater), and is obtained from data 2 meters above surface level (a.s.l.) from the ENVI-Met model. *Ts* is an important UHI indicator because the properties of surface materials and processes associated with them greatly influence the radiative, thermal, and emissions properties of both surfaces and the atmosphere (Roth 2002). In ENVI-Met, *Ts* is obtained from surface output data.

Model Specification

We modeled temperatures under two distinct vegetation regimes, for which we specified two 200 X 50 X 25 cell modeling grids at spatial resolutions of 3.59, 1.00, and 2.00 meters for the x-, y-, and z-axes, respectively. The locations of rooftops in the study area are identical in both scenarios, and were specified by overlaying aerial imagery in the ENVI-Met editor software interface and assigning a height

of 4 meters to residential structures and 8 meters to industrial or commercial rooftops. To model vegetation, ENVI-Met 3.1 requires structural characteristics such as stomatal resistance, leaf area density (LAD), and carbon fixation type. Default vegetation types included in ENVI-Met, however, are typical of European temperate forests, and do not adequately characterize vegetation in desert cities like Phoenix. To address this limitation, we conducted a vegetation survey in the study area to generate an ENVI-Met ready plants database that is representative of vegetation in the study area (Table 5.2). Leaf area indices (LAI) of vegetation found in the study area were measured with a Li-Cor LAI-2000 plant canopy analyzer (http://www.licor.com/). Vertical LAD distributions were estimated for each vegetation species based on the method proposed by Lalic and Mihailovic (2004). As part of the survey, we also obtained GPS coordinates of plants and trees in the park portion of the study area. Taxa of non-grass vegetation on private property or in otherwise inaccessible areas were identified using a combination of fieldwork and Google Maps Street View. We relied on the Virtual Library of Phoenix Landscape Plants (Martin 2009) for visual matching of vegetation species in our fieldwork.

Table 5.2: Field-derived plant modeling parameters for ENVI-Met

Plant	CO_2 fixation	Plant type	min stomatal resis-tance	short-wave albedo	height (m)	root zone depth (m)	LAD1[1]	LAD2	LAD3	LAD4	LAD5	LAD6	LAD7
BG	C4	grass	200	0.20	0.10	0.50	0.30	0.30	0.30	0.30	0.30	0.30	0.30
OG	C4	grass	100	0.20	0.75	0.75	0.30	0.30	0.30	0.30	0.30	0.30	0.30
WM	C3	dec. tree	400	0.20	9.00	2.00	3.13	3.56	3.77	3.75	3.66	3.44	2.97
PV	C3	dec. tree	400	0.20	9.25	2.00	2.41	2.79	3.01	3.01	2.95	2.78	2.42
AS	C3	dec. tree	400	0.20	8.25	2.00	3.87	4.28	4.39	4.35	4.22	3.93	3.35
EO	C3	dec. tree	400	0.20	8.25	2.00	2.99	3.30	3.39	3.36	3.26	3.04	2.59
MP	C3	dec. tree	400	0.20	4.75	2.00	1.62	2.02	2.42	2.67	2.67	2.58	2.34
CE	C3	dec. tree	400	0.20	8.50	2.00	1.34	1.55	1.67	1.67	1.64	1.55	1.35
FP	C3	dec. tree	400	0.20	10.00	2.00	0.00	0.01	0.01	0.03	0.07	0.17	0.52
TM	C3	dec. tree	400	0.20	9.00	2.00	2.55	2.83	2.92	2.89	2.81	2.62	2.24
MP	C3	dec. tree	400	0.20	20.00	2.00	0.00	0.00	0.00	0.00	0.01	0.02	0.07
SA	C3	dec .tree	400	0.20	12.00	2.00	2.24	2.43	2.46	2.43	2.35	2.18	1.84

Plant	LAD8	LAD9	LAD10	RAD1[2]	RAD2	RAD3	RAD4	RAD5	RAD6	RAD7	RAD8	RAD9	RAD10
BG	0.30	0.30	0.30	0.10	0.10	0.10	0.10	0.10	0.10	0.10	0.10	0.10	0.10
OG	0.30	0.30	0.30	0.10	0.10	0.10	0.10	0.10	0.10	0.10	0.10	0.10	0.10
WM	2.04	0.51	0.00	0.10	0.10	0.10	0.10	0.10	0.10	0.10	0.10	0.10	0.10
PV	1.69	0.44	0.00	0.10	0.10	0.10	0.10	0.10	0.10	0.10	0.10	0.10	0.10
AS	2.24	0.51	0.00	0.10	0.10	0.10	0.10	0.10	0.10	0.10	0.10	0.10	0.10
EO	1.73	0.40	0.00	0.10	0.10	0.10	0.10	0.10	0.10	0.10	0.10	0.10	0.10
MP	1.77	0.59	0.00	0.10	0.10	0.10	0.10	0.10	0.10	0.10	0.10	0.10	0.10
CE	0.94	0.25	0.00	0.10	0.10	0.10	0.10	0.10	0.10	0.10	0.10	0.10	0.10
FP	1.70	2.96	3.00	0.10	0.10	0.10	0.10	0.10	0.10	0.10	0.10	0.10	0.10
TM	1.50	0.35	0.00	0.10	0.10	0.10	0.10	0.10	0.10	0.10	0.10	0.10	0.10
MP	0.36	2.39	3.00	0.10	0.10	0.10	0.10	0.10	0.10	0.10	0.10	0.10	0.10
SA	1.20	0.26	0.00	0.10	0.10	0.10	0.10	0.10	0.10	0.10	0.10	0.10	0.10

1: Leaf-area Density; 2: Root-area Density

In addition to land surface characterization, the model requires wind speed and direction, relative humidity of the air (RH), and surface roughness (Z_0) parameters to initiate the model. We obtained these from the 16 July 2005 (0500 hrs) record for a nearby PRISM network station ("Kay" site, 33.421°N, 112.151°W, 1032 feet a.s.l.), approximately 4.85 kilometers SW from the study area. Table 5.3 shows the initial atmospheric, soil, rooftop, and human comfort conditions specified for our 26-hour modeling run beginning 16 July 2005 at 0500 hours. Summer 2005 was an extremely hot season in Phoenix. There were 16 instances of record high temperatures and, furthermore, the five-day period 15-19 July of that year constituted the most acute EHE of the season according to Ruddell et al. (2010), using Meehl and Tebaldi's (2004) methodology to identify EHEs. We conducted our modeling run from 16 July 2005 0500 hours to 17 July 2005 0700 hours. Although we report results for the 24-hour simulation period, we concentrate on the results for 16 July 2005 1700 hours and 17 July 2005 0500 hours to allow adequate time for model spin-up and stability.

Table 5.3: Initial parameters for ENVI-Met simulation runs

Atmosphere	
Wind speed 10 m a.s.l. (m/s)	3.58
Wind direction (degrees)	246
Roughness Length (Z_0)	0.3
Initial Atmospheric Temperature (K)	305.2
Specific Humidity at 2,500 m a.s.l. (g H_2O/kg air)	6
Relative Humidity at 2 m a.s.l. (%)	25
Building	
Inside Temperature [K]	305.2
Heat Transmission Walls (W/m^2K)	3.0
Heat Transmission Roofs (W/m^2K)	9.0
Albedo (Walls)	0.2
Albedo (Roofs)	0.3
Soil	
Initial Temperature Upper Layer (0-20 cm) (K)	300.0
Initial Temperature Middle Layer (20-50 cm) (K)	300.0
Initial Temperature Deep Layer (below 50 cm) (K)	300.0
Relative Humidity Upper Layer (0-20 cm) (%)	50
Relative Humidity Middle Layer (20-50 cm) (%)	60
Relative Humidity Deep Layer (below 50 cm) (%)	60

Two scenarios were developed to evaluate the impact of vegetation on mitigating extreme temperatures during a documented EHE in Phoenix during 15-19 July 2005. Area input files from the ENVI-Met 3.1 interface are shown in Figure 5.3. Table 5.4 details the distribution of surface covers in each of the modeling scenarios.

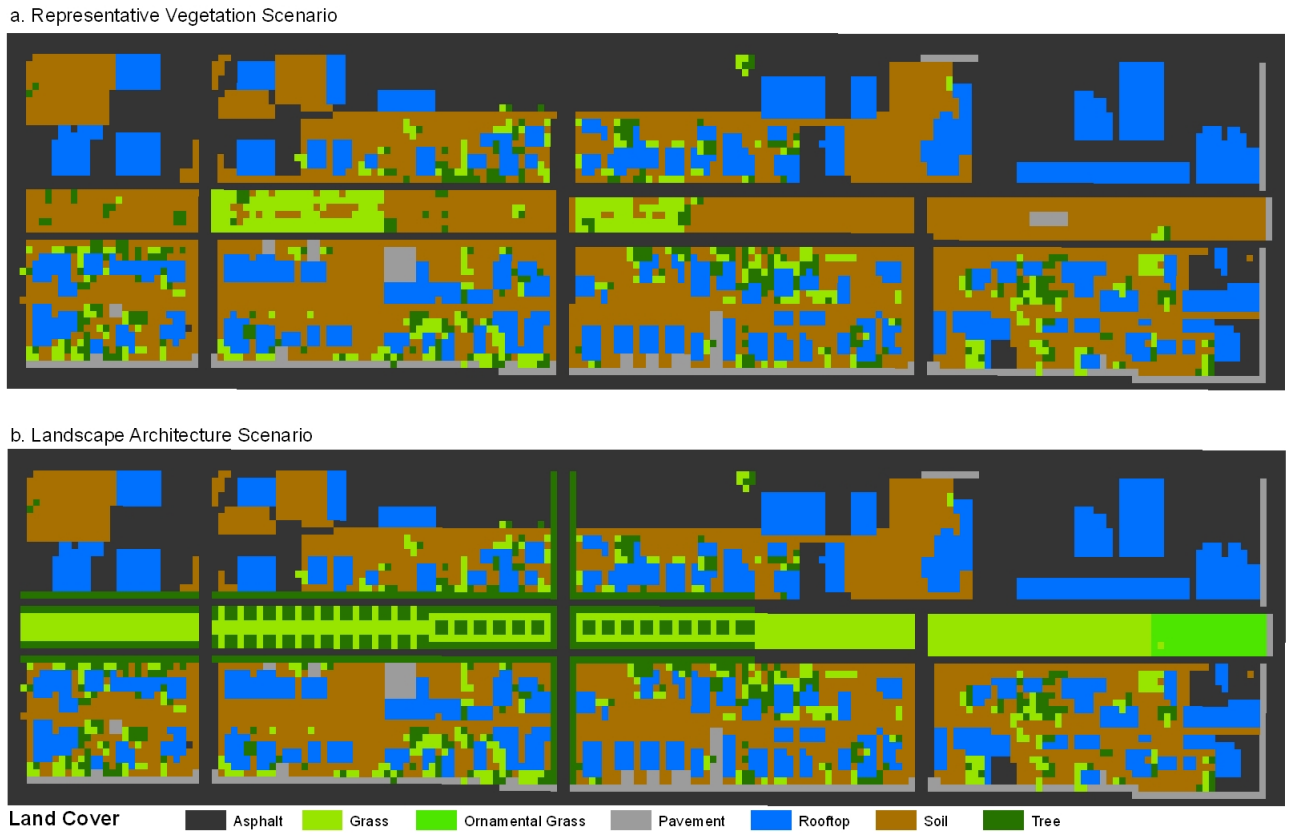

Figure 5.3: ENVI-Met input area files for (a) Representative Vegetation (RV), and (b) Landscape Architecture (LA) modeling scenarios.

Table 5.4: Number of modeling cells by surface cover class by scenario

Surface Cover	RV Scenario *n*	RV Scenario Percent of Total Area	LA Scenario *n*	LA Scenario Percent of Total Area
Vegetated Covers				
Bermuda Grass	521	5.21	992	9.92
Ornamental Grass	0	0.00	107	1.07
African Sumac	15	0.15	0	0.00
Afghan Pine	13	0.13	12	0.12
Palo Verde	30	0.30	15	0.15
Shamel Ash	5	0.05	289	2.89
Thornless Mesquite	271	2.71	565	5.65
Non-Vegetated Covers				
Asphalt	3,740	37.40	3,604	36.04
Loamy Soil	3,359	33.59	2,387	23.87
Pavement	328	3.28	311	3.11
Rooftop	1,718	17.18	1,718	17.18
Total	**10,000**	**100.00**	**10,000**	**100.00**

Scenario 1 — Representative Vegetation (RV)

For our first scenario, we generated a geospatially-referenced dataset representing the 2007 vegetation distribution from a simplified land cover classification dataset created using Object-Based Image Analysis (OBIA), a methodology increasingly used to generate land use/land cover datasets from high-resolution imagery (Hill and Polsky 2007; Walker and Blaschke 2008). We obtained scenes from the 2007 National Agriculture Imagery Program (NAIP, USDA 2007) image catalog for Arizona. The generated dataset represents land cover conditions during July 2007, the latest year for which multispectral (RGB plus NIR), high spatial resolution (1 m/pixel) aerial imagery were publicly available. Our land cover classification distinguished trees, grass, and paved roads. It was loaded into the ENVI-Met interface as a raster image and used to assign vegetation and impervious covers to modeling grid cells. Individual species were assigned to modeling cells in ENVI-Met based on the fieldwork and Google Street View method explained above. This scenario was intended to be representative of vegetation typically found in urban core neighborhoods in metropolitan Phoenix.

Scenario 2 — Landscape Architecture (LA)

Our second scenario was designed specifically to address UHI mitigation, aesthetic values, and ecological considerations. It also conformed to regulations specific to the land in which the park is located. In consultation with a local landscape architect, we designed a modeling scenario that

incorporated both desert and non-native grass and tree species (see Table 5.1). The park land is a local power company easement with four electrical towers interspersed along the length of the park. Electric utility regulations prohibit the planting of tree species with canopies that could come in contact with overhanging cables and cause electrocution injuries or death. The main danger is that power lines regularly warp under high electrical load conditions. To overcome this limitation, we designed a scenario that placed Arizona mesquite (*Prosopis velutina*) trees within the park (the narrow east-west central band in Figure 5.3). Shamel ash (*Fraxinus uhdei*) trees were placed along the residential sidewalks north and south of the park, where there are no limitations related to the electrical transmission towers. Finally, we added ornamental grasses to the eastern end of the park, which is currently dominated by disturbed soil that becomes airborne under windy conditions. The ornamental grass land cover category (see Table 5.1) generalized three grassy taxa commonly planted in Phoenix: pink muhly (*Muhlenbergia capillaries*), deer grass (*Muhlenbergia rigens*) and Mexican thread grass (*Stipa tenuissima*).

Integration of GIS and ENVI-Met 3.1

Our ENVI-Met simulation runs generated a large amount of data. In order to visualize and analyze these data spatially and temporally, we programmed a series of Python-language tools within the geoprocessing framework of ArcMap 9.3 GIS software. These tools allowed us to correlate observations in each grid cell to the surface covers specified in the ENVI-Met area input files. We first programmatically parsed the ENVI-Met area input files for each scenario to generate a GIS polygon vector file (shapefile) with features that corresponded to each of the 10,000 grid cells in the modeling domain, and added each assigned land cover (i.e., tree taxon, grass, soil, rooftop, pavement, asphalt) as tabular data to the shapefile. Because a low number of observations were found for individual tree species (e.g., only 5 shamel ash cells across the RV scenario domain) we assigned all cells containing trees, regardless of taxon, to a generic "tree" class. Upon completion of the two modeling runs, we extracted atmospheric and surface outputs for each of the 26 time steps using the results-extraction tool LEONARDO (packaged with ENVI-Met 3.1) into a flat-file text format. We then used a relational database operation ("join") to correlate observations for each of the two output parameters for each modeling hour to the shapefile representing each modeling scenario. The results are two shapefiles of identical spatial extent (one for each scenario), which are suitable for comparison at each modeling hour time step and throughout the modeling area. For analysis purposes, we eliminated modeling cells

containing rooftops because model outputs remained constant throughout the modeling run in these cells.

Spatial autocorrelation and estimation of the extent of the park cool island (PCI)

We estimated both the potential magnitude and extent of the potential PCI by conducting a cluster analysis on modeled air temperature differences (*dTa*) using the local indicator of spatial autocorrelation method (LISA, Anselin 1995). LISA is a statistic computed for each observation in a spatial dataset that estimates the degree of significant spatial clustering of values in a variable in neighboring observations. Individual LISA components disaggregate the global indicator of spatial autocorrelation, Moran's I, which can be mapped to estimate the degree of local spatial autocorrelation within a study area (Anselin 1995; de Smith et al. 2007). The degree of spatial autocorrelation is expressed as a value that indicates the presence of clusters (high or low similar values in proximity, categorized as "high/high" or "low/low" outcomes), or dispersion (no high or low similar values in proximity, categorized as "high/low" or "low/high" outcomes). Computed p-values associated with each observation describe the statistical significance of LISA scores. Mapping the high/high outcomes of air temperature differences between the RV and LA (*dTa*) scenarios provides an estimation of the spatial extent of the potential PCI effect.

5.6 Results

Diurnal Air Temperature Differences (dTa) and the Spatial Extent of the Park Cool Island

An ensemble time-series of differences in air temperature (*dTa* = LA *Ta* – RV *Ta*) between the two model scenarios over different surface cover types is shown in Figure 5.3. Throughout the modeled environment, LA *Ta* was always lower than RV *Ta* (negative *dTa*) over all surfaces throughout the duration of the simulations, with air above the vegetated (tree and grass) and pervious (soil) surfaces showing the most negative *dTa*. Whereas the most negative *dTa* between the two model scenarios occurred in the late afternoon over all surface covers (e.g., -1.9 °C at 1500 hours over tree surfaces), negative *dTa* between -0.3 °C and -1.3 °C also occurred over all surface cover types post-sunset and persisted until sunrise.

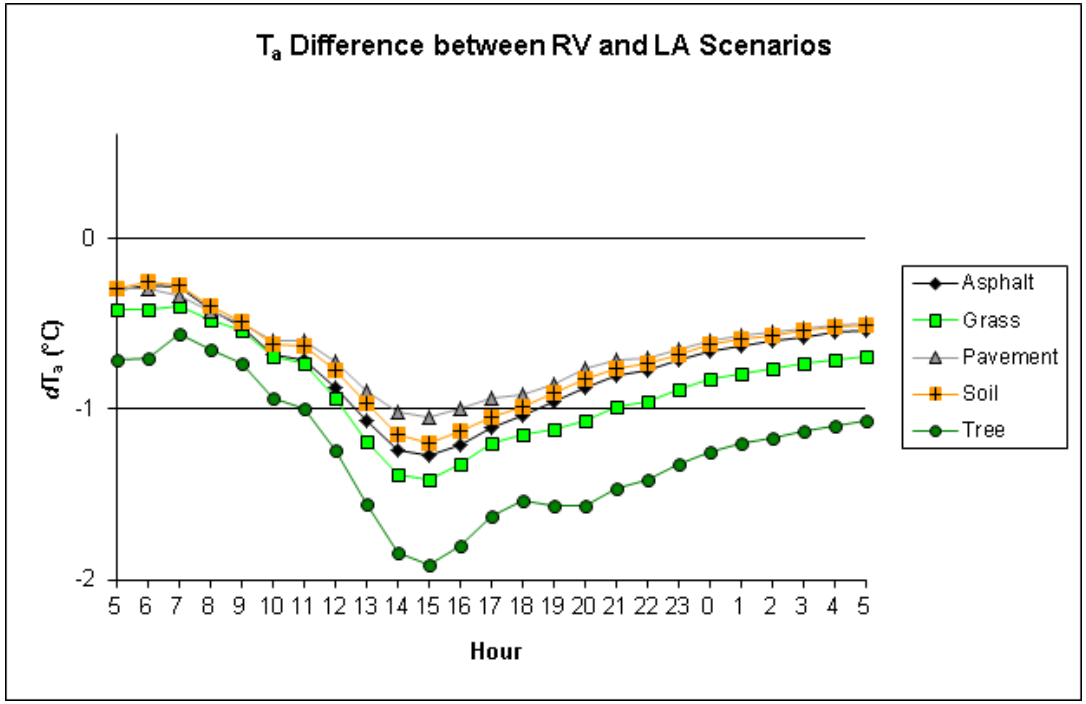

Figure 5.4: 24-hour profile of mean differences in air temperature (*dTa*) by surface cover between RV and LA scenarios.

We mapped the spatial distributions of *dTa* values for 0500 and 1700 hours (Figures 5.5a and 5.6a). We focused on these two timings because they typically equate to daily minimum and maximum air temperatures, respectively. These maps show significant differences in air temperature (*dTa*) between the LA and RV scenarios. At 0500 hours, *Ta* reductions typically in the -0.5 to -1.5 °C range occurred around the LA canopied surfaces, whereas the remaining non-canopied and unaltered surfaces experienced modest reductions of up to -0.5 °C (Figure 5.5a). At 1700 hours (Figure 5.6a), there were larger *Ta* reductions around surfaces with canopied vegetation, ranging from -1.0 to -3.1 °C. In addition, remaining impervious and unaltered surfaces experienced cooling in the -0.5 to -1.0 °C range, which was the likely result of greater vegetative evapotranspiration under the LA scenario. Near-surface humidity and latent heat for the entire model domain were higher in the LA scenarios.

We also mapped the potential extent of the PCI according to the calculated *dTa* (0500 and 1700 hours) between the RV and LA scenarios (Figures 5.5b and 5.6b). We used modeled *Ta* as an indicator of the PCI's spatial extent. We estimated the spatial extent of the PCI by calculating a Moran's I statistic, LISA cluster categories, and the statistical significance for each value of *dTa* in each cell in the modeling domain. The Moran's I statistic for *dTa* observations indicated a high degree of positive spatial autocorrelation among the grid cells (0.83 at 0500 hrs, 0.75 at 1700 hrs, $p<=0.05$), suggesting that, in general, similar values of *dTa* are clustered together at both time steps. This global statistic, however, does not describe the spatial distribution of high or low values in the modeling domain, and can, therefore, tell us little about the localized effects of vegetation on air temperatures.

a. T_a difference between RV and LA vegetation scenarios at 0500 hours (°C). Arrows show wind direction.

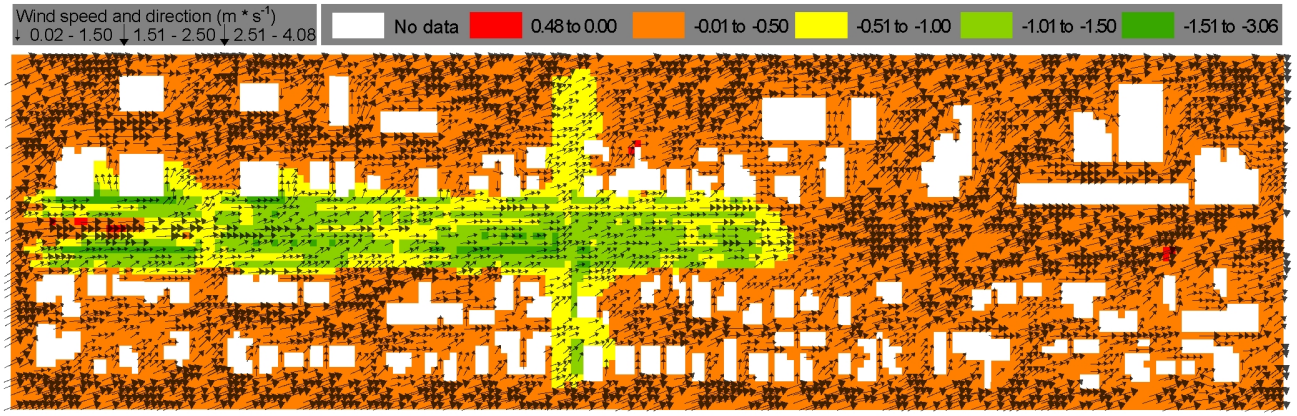

b. LISA analysis of T_a difference between RV and LA vegetation scenarios at 0500 hours (°C)

Figure 5.5: (a) *dTa* between RV and LA Vegetation Scenarios (°C) at 0500 hours, and (b) LISA Analysis of *dTa* between RV and LA Vegetation Scenarios (°C) at 0500 hrs. High/high and low/low LISA results are significant at the 95 percent confidence interval.

a. T_a difference between RV and LA vegetation scenarios at 1700 hours (°C). Arrows show wind direction.

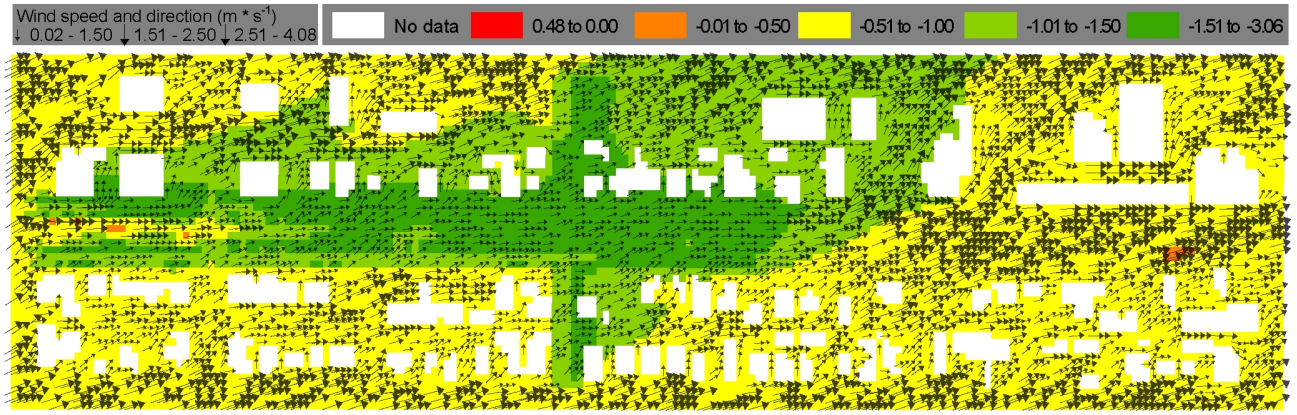

b. LISA analysis of T_a difference between RV and LA vegetation scenarios at 1700 hours (°C)

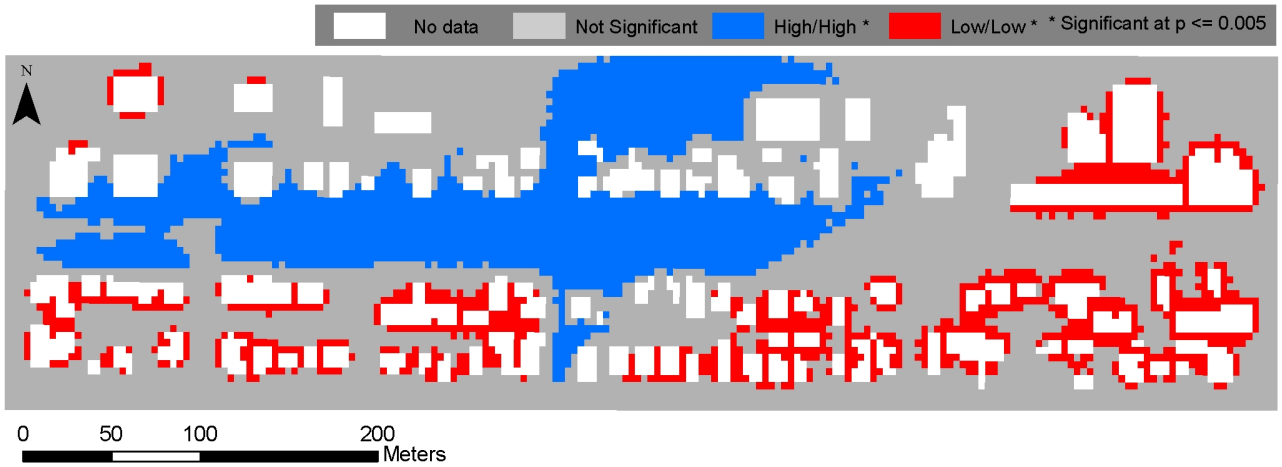

Figure 5.6: (a) *dTa* between RV and LA Vegetation Scenarios (°C) at 1700 hours, and (b) LISA Analysis of *dTa* between RV and LA Vegetation Scenarios (°C) at 1700 hours. High/high and low/low LISA results are significant at the 95 percent confidence interval.

LISA analysis disaggregates Moran's I into the local score calculated for each cell. Statistically-significant clusters (p<=0.05) were assigned by the LISA procedure based on one of four possible outcomes: high/high, low/low, high/low, low/high. Assignment of a cell to either of the first two categories indicates spatial clustering of high or low *dTa* at and around that cell. The latter two categories indicate that a cell had a high (low) *dTa* surrounded by low (high) values, suggesting no spatial clustering of extreme values around that cell. For our purposes, LISA outcomes of interest were high/high and low/low clusters that represented statistically significant (p<=0.05) large *Ta* differences surrounded by similar large differences or small differences surrounded by similar small differences, respectively.

The high/high outcome indicated that the largest differences of *dTa* were spatially clustered, suggesting a cooling effect that followed the pattern of canopied vegetation in the LA scenario (Figures 5.5b and 5.6b). Clustering of high *dTa* values outside modeling cells with canopied vegetation indicated a PCI effect, where the shading and transpirational cooling potential of the canopy extended beyond the location of trees into adjacent areas. The mean *dTa* of observations at 1700 hours in the high/high category was -1.63 °C, whereas for those in the low/low category it was -0.72 °C. These differences were reduced at 0500 hours, with a high/high mean *dTa* of -1.02 and a low/low mean of -0.21. The low/low values at 0500 hours were clustered around areas with little vegetation and surrounding rooftops, a spatial pattern that was reduced around asphalt but extended to the exposed soil land covers at 1700 hours.

Surface temperature differences and surface covers

Increased vegetation in the LA scenario showed significant mean surface temperature reductions from RV conditions for the model simulation period (dT_s = LA T_s - RV T_s, Figure 5.7). There were insignificant variations in *dTs* during the first 2-3 simulation hours (which could be attributed to model spin-up) but significant cooling for all surfaces commenced from noon and was most pronounced during late afternoon. Similar to Figure 5.4, vegetated and pervious surfaces decreased in mean *dTs*, but the magnitude of surface cooling for all types of surfaces was much larger compared to near-surface ambient temperatures (e.g. -8.2 °C vs. -1.9 °C for tree surfaces at 1500 hours, see Figure 5.4). The greater surface cooling suggested a strong influence of vegetated canopy shading that reduced direct insolation. Magnitudes of nocturnal mean *dTs*, however, were smaller for all surfaces compared to their corresponding values of *dTa*.

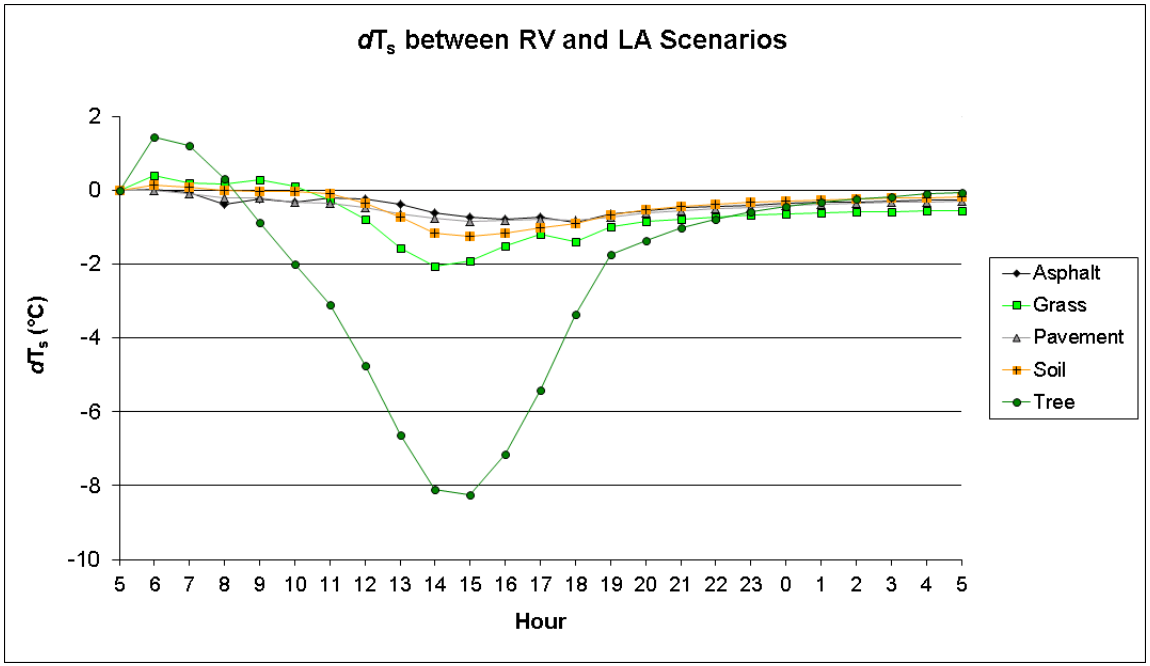

Figure 5.7: 24-hour profile of mean differences in surface temperature (*dTs*) by surface cover between RV and LA scenarios.

The statistical and spatial distributions of absolute surface temperatures at 1700 hrs varied considerably among the RV and LA scenarios. Linked-window maps of surface temperature highlight the sharp differences in the statistical distribution and correlation with surface covers in the EV (Figure 5.8) and LA (Figure 5.9) scenarios. Histogram bins for both RV and LA results were grouped into three distinct distributions observable in the RV and LA histograms (Figures 5.8b and 5.9b). *Ts* observations in increasing order of magnitude were color-coded blue, yellow, and red and linked in GIS to a surface cover map overlay to highlight surface temperature differences. In both histograms, observations coded in blue, yellow, and red generally corresponded to vegetated, bare soil, and impervious surface covers, respectively. There were, however, deviations from this pattern which suggested a cooling effect especially pronounced in the LA scenario. Areas in the low range of the distribution (blue, 25.3 °C >= Ts < 37.6 °C) in the RV scenario were located at or near modeling cells with tree canopy surface covers. In the LA scenario, the low range of temperatures expanded to cells at or near canopied cells, creating a cooling effect that extended to the impervious surface covers surrounding trees (Figure 5.9). Although impervious covers had the highest *Ts* values in both distributions, asphalt close to tree canopies in the LA scenario (west and central areas of the park) belonged to the (yellow) midrange, indicating net reductions in surface temperature.

a. Representative Vegetation Scenario

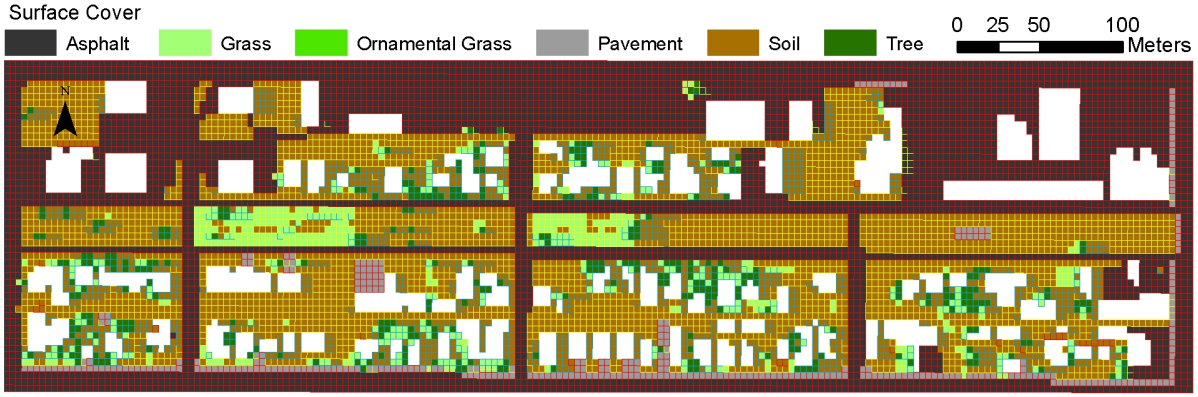

b. Linked Histogram of T_s for Representative Vegetation Scenario. Observations in blue (25.3 °C >= T_s < 37.6 °C), yellow (37.7 °C >= T_s < =40.2 °C), and red (40.3 °C >= T_s < 55.3 °C) , correspond to similarly-colored outlines in map. Surface covers are shown in the background to illustrate the relationship between surfaces and temperatures.

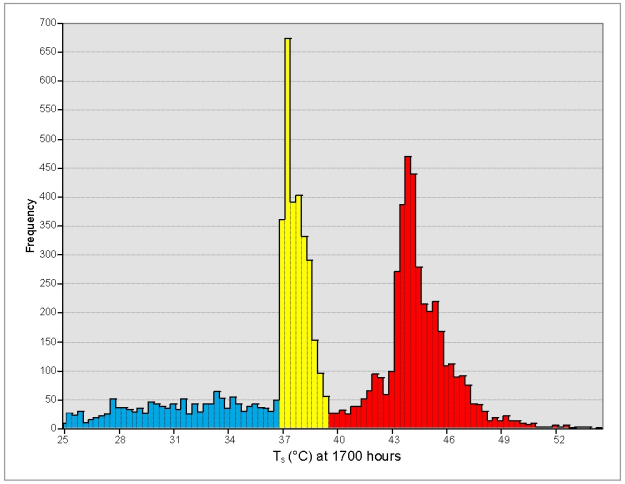

Figure 5.8: (a) Surface Covers, and (b) Linked-Histogram of *Ts* (°C) for RV Scenario at 1700 hours.

a. Landscape Architecture Scenario

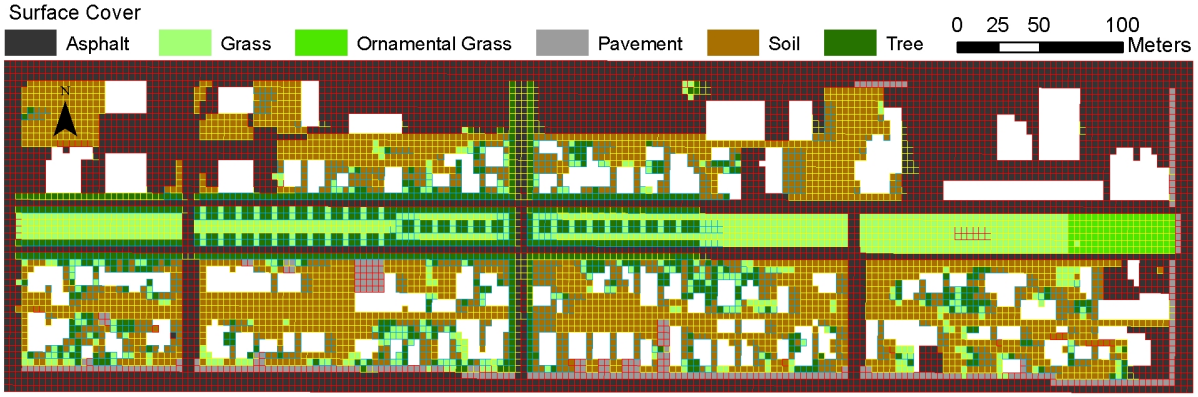

b. Linked Histogram of T_s for Landscape Architecture Scenario. Observations in blue (25.3 °C >= T_s < 35.2 °C), yellow (35.3 °C >= T_s < =39.6 °C), and red (39.7 °C >= T_s < 54.5 °C) , correspond to similarly-colored outlines in map. Surface covers are shown in the background to illustrate the relationship between surfaces and temperatures.

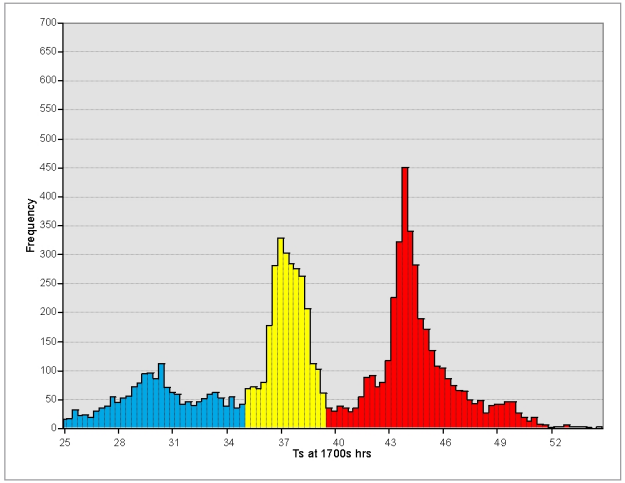

Figure 5.9: (a) Surface Covers, and (b) Linked-Histogram of *Ts* (°C) for LA Scenario at 1700 hours.

Although the surface temperatures were very high even in the low range (< 37.6 °C), the linked-window displays illustrate the potential for *Ts* reductions if the RV scenario were transformed into the LA vegetation conditions: 1452 cells in the blue bin in RV increased to 1827 in the LA scenario. Conversely, the number of cells in the high range (> 39.7 °C), decreased from 4212 (RV) to 3825 (LA), suggesting that surface temperatures in and around cells with tree canopies were reduced due to a cooling effect (Figure 5.9b).

5.7 Discussion and Conclusions

Our analyses of modeled air and surface temperatures showed that increasing vegetation in parks can mitigate local effects of the UHI by creating localized PCIs where extreme temperatures are lowered, sometimes significantly. The LISA analysis of air temperature indicated that for hours of typical daily minimum (0500 hours) and maximum (1700 hours) *Ta*, the largest reductions (i.e., most negative *dTa* values) for the Landscape Architecture (LA) park scenario compared to the Representative Vegetation (RV) scenario (Figures 5.6 and 5.7) were spatially clustered around canopied vegetation and immediately adjacent to non-vegetated surfaces. Conversely, the smaller temperature reductions (i.e., least negative *dTa* values) were clustered around areas with exposed soil, asphalt, or other impervious surfaces that were not immediately contiguous to vegetative surfaces. The 24-hour profile of mean *Ta* also showed the significant cooling effects of vegetation in the LA scenario through shading and transpirational cooling. These negative *dTa* values suggested a distinct PCI effect that we estimated to have the potential to cool the air (underneath or surrounded by canopied vegetation) by as much as 1.9 °C during the warmest time of the day.

The greatest reductions in surface temperatures between the LA and the RV scenarios occurred in grass (1400 hours) and tree surface covers (1500 hours), with mean *dTs* =-2.1 °C and -8.2 °C, respectively. A spillover effect of vegetation, similar to that observed in the diurnal profile for *Ta*, occurred in *Ts* values for impervious covers (asphalt and pavement), which registered mean *dTs* =-0.8 °C. The linked window analysis of *dTa* (Figures 5.8 and 5.9) illustrated the adjacent cooling effect of vegetation upon non-vegetated surfaces, namely that clusters of canopied vegetation can help cool impervious surfaces.

Anthropogenic changes of natural land covers into heat-retaining surfaces like roofs, pavement, or asphalt (e.g., through new housing development) are known to be related to increases in temperature (Brazel et al. 2007). *Ts* data are important in comparisons with remotely-sensed land cover data, usually in studies that evaluate the role of surface material changes in heat island mitigation. In

our study, the degree of coupling between these two variables was dependent on factors such as scale, land cover type and atmospheric stability. Although air and surface temperatures are usually correlated under low wind speeds, atmospheric turbulence conditions can decouple surface-air temperatures (Stoll and Brazel 1992). In our study, however, simulated values of *Ts* and *Ta* correlated well, (r=0.69 for the LA scenario; r=0.75 for EV at 1700 hours) largely due to the small geographic scale of the study area, and atmospheric stability during our modeling period (wind speed = 3.58 m/s, see Table 5.3).

Comparison of the RV and proposed LA scenarios demonstrated that increasing vegetation is one strategy through which extreme heat can be mitigated in arid cities. Providing adequate green spaces in the inner city is a critical component of UHI mitigation during the hot season, especially during EHEs. This is made difficult, however, by ongoing contestations over adequate urban amenities like parks and the resources necessary to provide them (e.g., water, tax dollars, local government will, regular maintenance). Contestations about the allocation of resources resonate with claims of environmental injustice that "ecologies of fear" (Brownlow 2006) often arise in neglected green spaces as legacies of environmental and racial discrimination, inner-city decay, and a continuing urban planning focus on fringe development. Indeed, in Phoenix, Guhathakurta and Wichert (1998) have shown that although inner-city areas bear higher property tax burdens in comparison with the suburbs, the former receive significantly fewer tax dollars than the latter for parks, recreation, and water supply.

Minority and low-income communities are increasingly addressing such disparities by demanding more equitable distribution of urban amenities, such as parks and clean air. Their desire for more vegetation is often framed as a means for neighborhood beautification and improving the quality of parks as community anchors and points of pride. Parks in low-income (but not exclusively) Hispanic communities often are the only available public gathering places that also embody a historical and cultural sense of place due to ties of past and present residents. Disparities in the distribution of fiscal and natural resources also translate into inequalities in ecosystem services, such as shading and transpirational cooling, that have significant and measurable outcomes in UHI impacts (Heisler et al. 1995; Perkins et al. 2004). Although the community in this study did not frame their arguments for park improvement explicitly around the heat mitigation benefits demonstrated in our research, this service may become more important in the future as the trend of increasing temperatures continues.

Green spaces can provide social, cultural, and—more directly for extreme heat mitigation—human health and ecological benefits (Boone et al. 2009; Oke 1998; Wolch et al. 2005).

Microclimate modeling combined with localized knowledge of vegetation, GIS, and spatial autocorrelation helps to close existing gaps in understanding ecological relationships between vegetation and extreme heat mitigation in low-income, urban core neighborhoods. One direction for future research is to validate modeled results with observed atmospheric data, which is a component of atmospheric modeling we did not engage in our scenario-building. Future research should investigate seasonal variability of the UHI, not only during EHE episodes but also during the cold season because the increased heat storage characteristic of the UHI can potentially mitigate the intensity of winters.

One aspect of extreme heat not addressed directly in our study was human thermal comfort. ENVI-Met can estimate Median Radiant Temperature (MRT) and Predicted Mean Vote (PMV), two indicators of human thermal comfort. BOT World, an agent-based modeling system for thermal comfort is also available with ENVI-Met. Additionally, Matzarakis et al. (2010) have implemented RayMan, a bodily-scale human-energy balance model. Understanding human thermal comfort requires further research and input data to implement at the microscale in complex urban environments such as our study area. For example, assessing thermal comfort in arid climates requires evaluation of radiant heat flux because it is a more important determinant of human thermal comfort than air temperature (Shashua-Bar et al. 2010; Pearlmutter et al. 2006).

Water consumption for vegetation in Phoenix plays a critical role in urban planning and policy-making because tradeoffs in using water and energy to produce ecosystem services are unavoidable in a water-scarce region. Water consumption for outdoor landscaping in Phoenix accounts for roughly 45 to 70 percent of total residential water use (Gober et al. 2009). Generally, there is higher irrigation in landscapes dominated by turf grass than landscapes comprised of desert-adapted trees and shrubs (Martin et al. 2004) but water consumption for irrigation is highly variable. For example, Martin and Stabler (2002) reported that the range of supplemental water for residential landscape irrigation in Phoenix can vary from 0 to 233 L/m ^{2} /month. These data suggest that microclimate cooling created by localized PCIs might require substantial inputs of water resources to irrigate—especially turf grass—underscoring the paradox of conflicting ecosystem services in arid regions of water conservation and UHI mitigation through evapotranspirational cooling (Jenerette et al. 2011). Vegetation scenarios focused on microscale UHI mitigation in arid cities should explore the spatial and temporal variability of irrigation in relation to cooling. ENVI-Met's treatment of irrigation conditions is currently limited to soil moisture and temperature variables differentiated vertically among three layers,

but not horizontally among modeling cells. Thus the model did not allow us to explore cooling differences from irrigation regimes among land covers.

Another important point to consider is the potential tradeoff between irrigation water and UHI mitigation, which suggests the potential for greatest temperature reductions exists in neighborhoods with small amounts of vegetation (Gober et al. 2009) such as our low-income study area. It is also of interest to evaluate the cost-benefit ratio of water application vs. temperature reductions (see Jenerette et al. 2011). In this regard, Shashua-Bar et al. (2010) have suggested that the reconciliation of these conflicting ecosystem services might best be realized through landscape design modalities consisting of shade trees alone, while Zhou et al. (2011) have found that the composition and configuration of vegetated landscape has significant impacts on UHI mitigation.

In this study, we applied ENVI-Met to assess the potential benefits of the LA scenario to the surrounding microclimate. ENVI-Met allows researchers to model the climate of a spatially discrete urban area (i.e. individual buildings, gardens, green spaces, canals etc.) and to test the effects of architectural and planning design scenarios on microclimates. ENVI-Met has been applied to scenario-testing in other cities at a building and neighborhood spatial scale (e.g., Emmanuel and Fernando 2007), and is one of the few urban computational fluid dynamics models that is relatively user-friendly for planners and architects. It has the capabilities to model several aspects of microscale urban climates (e.g. temperature, wind field and thermal comfort variations) that are not possible with other numerical or scale models. Like all models, however, ENVI-Met has its limitations. For instance, the inability of the model to account for albedo variations among buildings within its model domain (i.e. all modeled structures have the same assigned wall and roof albedo magnitude) possibly affects its accuracy in heterogeneous urban areas with different wall/roof colors and materials (see Chow et al. 2011 for further discussion of model limitations). Despite such limitations, the model can still be a very useful tool for urban planners, landscape architects, and other practitioners, provided that users are cognizant of the model's limitations and have initialized the model with accurate parameters (e.g. local vegetation and soil conditions).

This study contributed to a microscale understanding of energy fluxes among vegetated, non-vegetated, and impervious surfaces in an arid urban area that is demonstrably getting hotter. Through the scenario building exercise presented here, our research engaged in an interdisciplinary

effort to understand the localized impacts of climate change and to inform strategies to mitigate the effects of the UHI through the creation of park cool islands in low-income, inner-city neighborhoods.

Chapter 6

SYNTHESIS OF INTERDISCIPLINARY APPROACH

6.1 Summary of findings from the three case studies

This dissertation is an interdisciplinary attempt at understanding the socio-ecological drivers, antecedents, human health consequences, and potential mitigation of human vulnerability to extreme heat. The work is organized within a hazards vulnerability framework, which explicitly addresses the social and ecological dimensions imbricated in the production, distribution, and impacts of socio-environmental hazards in cities. In Chapter 1, I outlined three research questions that illustrate the contemporary, historical-geographical, and potential mitigation aspects of heat hazards. In the second chapter, I presented a model of heat hazards vulnerability that harnesses the risk-hazards, social vulnerability, and ecological resilience traditions in hazards research, articulating how these traditions help to describe the three dimensions of exposure, sensitivity, and coping capacity (Figure 2.1). I argued that theories and methods usually outside of those represented in the vulnerability research traditions have much to say about how heat hazards are produced, experienced, and potentially mitigated. In the subsequent three chapters, I wielded the explanatory power of diverse fields and methods to empirically evaluate different dimensions of extreme heat hazards: urban geography, spatial epidemiology, and public health (Chapter 3); environmental history, Marxist geography, historical-geographical materialism (Chapter 4); and urban climatology, microclimate simulations, and environmental justice (Chapter 5).

In the first case study, I assessed the sensitivity and exposure dimensions of present heat vulnerability conditions, compared them to heat health outcomes, and identified at-risk populations and neighborhoods, finding that urban core, low-income minorities and the suburban elderly have the most elevated risks of adverse heat health outcomes in Maricopa County. In the second case study, I uncovered the historical geography and environmental history of the Phoenix metro region to describe the production of differential extreme heat vulnerability among low-income minorities and wealthy elites. In doing so, I unpacked how capitalist urban development, via agricultural, industrial, and suburban development transitions, shaped the landscape of risk–what I term the riskscape–since the onset of the late 19th century modern settlement of Phoenix. The narrative revealed how land use changes and marginalization of minorities have created the spatial concentration of extremely high temperatures (along with other environmental hazards) and impoverished minorities in the central city core urban heat island, while affluent whites largely enjoyed the benefits of successive waves of economic

development. In the final case study, I focused on the potential for a vegetation-based intervention in reducing extremely high temperatures in a Phoenix urban core neighborhood park. Computational simulations of surface-air energy exchanges showed that shading vegetation can achieve significant reductions of extremely high temperatures, reducing exposure and increasing coping capacity of populations there. The case study also responds to environmental justice claims of poor urban core populations who are increasingly demanding equality in the provision of ecological services like those provided by urban parks and shading vegetation.

6.2 The metabolic transformation of the socio-ecological system in Phoenix

A challenge in this kind of interdisciplinary research is how to bring together the variety of research venues into a coherent framework that addresses the narrowness of focus of the social and physical sciences research deployed here. As I argued in Chapter 2, hazards and their human impacts emerge out of highly complex, multi-scalar and dynamic, socio-ecological processes. The vulnerability framework provides the "socio-ecological system" concept as a spatio-temporal container of anthropogenic practices and biogenic processes that comprise the key social (human) and ecological (non-human) transformations that shape landscapes. I use the term "container" because in the vulnerability tradition, the socio-ecological system is thought of in Cartesian space terms, that is, as an a priori space that exists independently of human or biophysical environment activity. Certainly, in this dissertation it has proven useful to 1) partition the contributions of various research disciplines to understanding heat hazards through the three vulnerability traditions, and 2) quantify the sensitivity, exposure, coping capacity, and health outcomes dimensions of vulnerability. However, this framework does not problematize the discursive and material production of space that characterizes urban development under the contemporary dominant mode of urban transformation: capitalist social relations. This is critical because, embedded within the processes of socio-environmental transformation that the vulnerability model in this dissertation describes, urban landscapes are shaped symbolically and materially by capitalist urban development. Understanding the symbolic and physical production of the process of urban development illuminates the fundamental dialectical tension between exchange values and social values: privileging the former (i.e., production of agricultural commodities or real estate profits) marginalizes the latter (e.g., clean environments and cooler temperatures), and is the fundamental metabolic (i.e., transformative) process that creates socio-spatial unevenness in the production of urban spaces and environmental amenities and hazards (Smith 1990).

The Marxist urban political ecology approach problematizes the transformations alluded above by locating socio-ecological dynamics within a unified field of "socio-environmental metabolic circulation" (Swyngedouw 2006, 13). The Marxist framing engages head-on the socio-ecological relations that unfold as nature is metabolized for human consumption (Heynen 2006), as has been the case in the uneven production of the urban environment in general, and heat hazards in particular, in Phoenix. The concept of "metabolization" is borrowed here from Marx's notion of labor performed on the landscape as the fundamental relationship that humans engage in with externalized nature, as an integral part of their socio-ecological reality (Marx 1992). Metabolization encompasses the physical and chemical circulation of materials like water, land, and seed into agricultural commodities, but also has a discursive dimension that imbues human practices like land use/land cover change and racial segregation with meaning. Concretely, metabolization is labor done on the landscape, or "purposeful activity aimed at the production of use-values" (Marx 1992, 290). The fundamental dialectical tension involved in the production of exchange and social values–the two kinds of use-values recognized by Marx–points to the class-based struggles that unfold in the process of capitalist uneven urban development:

> *[U]rban political ecology more explicitly recognizes that the material conditions that comprise urban environments are controlled, manipulated, and serve the interests of the elite at the expense of marginalized populations.* (Heynen et al. 2006, 6)

The historical-geographical materialist analysis thus framed proceeds by "untying" the "interwoven knots of *social process*, *material metabolism*, and *spatial form*" (Swyngedouw and Heynen 2003, 906, emphasis in original) that shape urban landscapes. Separated conceptually–although not analytically–these "knots" are not independent elements; they are dialectically enmeshed within each other, as human agents deploy socio-spatial practices of land use/land cover change and marginalization, transform material characteristics of landscapes, and alter or create new spatial forms such as those that generate urban heat islands.

The circulation of capital shapes the specific spatial forms, material metabolisms, and social processes of urban environments through displacement in *circuits of capital* (Harvey 1985). In the primary circuit, capital circulates for production of basic commodities. Success in this circuit–overaccumulation–requires displacement of capital into a secondary circuit, which Harvey identifies as the built environment: "a vast, humanly created resource system, comprising use values embedded in the physical landscape, which can be utilized for production, exchange, and consumption"

(2006, 233). Displacement of capital into the secondary circuit configures an urban built environment composed of multiple commodities, but that is itself a complex and composite commodity:

> *The built environment comprises a whole host of diverse elements: factories, dams, offices, shops, warehouses, roads, railways, docks, power stations, water supply and sewage disposal systems, schools, hospitals, parks, cinemas, restaurants–the list is endless. Many elements–churches, houses, drainage systems, etc.–are legacies from activities carried on under non-capitalist relations of production. At any one moment the built environment appears as a palimpsest of landscapes fashioned according to the dictates of different modes of production at different stages of their historical development. Under the social relations of capitalism, however, all elements assume a commodity form.* (Harvey 2006, 233)

Outlays of capital in the built environment are directed as fixed-capital elements that enable production, such as factories, freeways, and railroads, and also towards the "consumption fund" of consumable features of the urban environment: houses, sidewalks, or trees.

In Phoenix, the specific process of uneven urban development generalized above began in the late 1860s through the metabolization of land, water, solar energy, and labor into capitalist social relations to create agricultural commodities for sale to nearby military outposts and mines. The Hohokam irrigation canals were the material preconditions for Anglo-European settlement, the legacy of pre-capitalist relations existing in the Salt River Valley landscape. These abandoned canals were reconstructed by settlers and brought into capitalist circulation along with land, solar energy, and labor to generate a local agricultural economy. The surplus extracted from agricultural commodity production in the primary circuit drove displacement of capital towards the secondary circuit of urban development. Development took the form of federally-funded dams, residential quarters, spillways, and irrigation canals, warehouses, railroads, produce processing plants, shading trees, and the like, to support continued accumulation not just in the primary circuit, but also through production and consumption in the secondary circuit.

Floods around the end of the 19th century set the initial socio-spatial marginalization of minorities in South Phoenix while wealthy, White elites relocated to more desirable areas. Changes in the global political economy, namely the Great Depression and Second World War precipitated a shift in the dominant form of economic growth in Phoenix towards industrial development centered in the segregated, poor neighborhoods of South Phoenix. The postwar influx of population to the Sunbelt accelerated growth in Phoenix, signaling the third transition towards suburban expansion and the coalescing of Phoenix and adjacent communities into the continuous metropolitan region it is today.

Throughout this process, the substitution of desert land covers with the urban built environment altered the metabolism of surface-air energy exchanges, creating the intense urban heat island characteristic of Phoenix. Today, extreme heat risks–as measured by heat-related hospitalizations–are highest in neighborhoods in the Phoenix urban core, which encompass South Phoenix. This reflects the enduring legacy of the social processes of land use change and racial marginalization, and the uneven distribution of the UHI spatial form created in the formative decades of Phoenix. However, other areas of concern are apparent also: minority neighborhoods in smaller historical urban cores of second-tier municipalities, and also elderly people in suburban fringe retirement communities. This contrasts sharply with the lower heat risks found in wealthier, whiter areas of the metro region. One way in which the urban core inequalities in extreme heat exposure can be addressed is by creating neighborhood green spaces. This kind of intervention is shown to be not only ecologically effective in inner city neighborhoods, but also in line with low-income communities' demands of redressing historical environmental injustices.

Trees, as elements in the consumption fund, are especially relevant to the discussion of unevenness in the distribution of ecological services because, as Heynen has said, urban trees act as markers of power and wealth, while their absence "exposes spaces of marginalization" (2003, 983). In addition to trees, the location of other elements of the consumption fund like industry adjacent to residential land uses and freeways that contribute to environmental hazards (e.g., UHI, air pollution) also help locate spaces of socio-environmental marginalization like the Latino Urban Core (LUC) neighborhood (Chapter 5). In Phoenix, the marginalization of spaces like the LUC can be tied concretely to two main forces that characterize uneven development in the production and reproduction of the built environment: a historical regional focus on suburban fringe expansion subsidized by siphoning off urban core tax dollars to developers (Guhathakurta and Wichert 1998), and the sustained neglect of the South Phoenix urban core (Bolin et al. 2000; Bolin et al. 2002; Bolin et al. 2005). The microclimate computational modeling presented in Chapter 5 is an attempt at a vegetation-based intervention that seeks to redress ecological outcomes of socio-spatial uneven development. Admittedly, the intervention at the intersection of landscape architecture, environmental justice, and urban climatology does not address the structural socio-spatial practices of land use/land cover change and marginalization, or the specific regional political economy focused on increasing the Phoenix spatial footprint through suburban development. From the Marxist geography perspective, increasing the shading vegetation potential in the LUC neighborhood is a quantitative addition to the consumption

fund that constitutes a spatial fix (Harvey 2001). The fix consists of displacement of capital (trees, water, municipal labor) to create as-of-yet unrealized ecological social values like lower temperatures and cleaner air, but also exchange values related to the reproduction of labor via municipal construction projects, developer contracting, and parks maintenance. From the ecological and climatological standpoints, the proposed intervention has a demonstrated potential for providing valuable ecological services that address immediate socio-ecological inequalities, but neither address the fundamental structural relations of hegemonic domination that create socio-ecological disparities deployed historically against the neighborhoods of South Phoenix. Nevertheless, I find it important to bring disciplines traditionally outside vulnerability research and Marxist interpretations of the urban into the conversation about environmental hazards. Marx intimated the importance of understanding historical change in a dialectical fashion, that is, through the philosophy of internal relations that posits that history oscillates between quantitative and qualitative forms. The quantification of ecological benefits, or, more concretely, the specific, geostatistically-significant temperature reductions that can be achieved by the Park Cool Island in the LUC neighborhood can help identify the dialectical progression under which the addition of shading and transpirational cooling can precipitate qualitative changes in urban environments towards generally cooler ecosystems. Retroactively, we can understand the formation process of the Urban Heat Island in an analogous way, as the quantitative, progressive addition of heat-retaining land covers during the early years of the Phoenix townsite. The cumulative effect of impervious land covers on absolute temperatures was such as to create a qualitative shift towards the identification of a new signal in the urbanized landscape of Phoenix, the rural-urban temperature gradient described as early as 1921 (Gordon 1921).

Recently, scholars are linking the socio-ecological transformation paradigm–usually deployed through qualitative narratives–to quantitative assessments of environmental change. Heynen (2003) has used remotely-sensed land cover data to quantify changes in urban tree canopy covers as a methods-laden basis to engage a narrative of metabolization of the urban environment in Milwaukee. From the sociological perspective, Elliot and Frickel (2013) analyzed longitudinal data on hazardous waste accumulation, arguing that current methods do not take into account the "historical accumulation" of hazardous materials, and making a call for deeper understanding of the processes that create hazardous environments. These two examples show there is promise in increasing the interdisciplinary conversation across research and scholarly disciplines to improve understanding of heat hazards.

6.3 Future prospects for decreasing socio-ecological hazards inequality through interdisciplinary research

This dissertation contributes to unraveling the complex socio-ecological dynamics through which urban landscapes are created and heat inequalities are created. By framing it from the outset within socio-environmental hazards vulnerability research, I have brought into view multiple theoretical and methodological research insights that illuminate climatological, historical, geographical, and epidemiological facets of the totality of socio-ecological heat hazards in cities. In the course of doing so, questions not explored here arise. In the context of the empirical quantitative case studies, heat-related coping capacity (Chapter 3) and the role of irrigation in regulating the effects of the Park Cool Island (Chapter 5), have been left for future research. Taking the three case studies as a whole, two broad questions remain to be answered: First, in the face of impending increasing temperatures driven by climate change, what future mitigation and prevention of adverse human health outcomes can be created? This question is receiving the attention of public health and global climate change scientific communities. These communities are developing sophisticated climatic models, mapping spatially-explicit indicators, and projecting future temperature conditions under urban development planning scenarios. Increasingly, these communities are talking to each other, to scholars of urban inequality, and to the marginalized residential communities most burdened by impacts. Scientists of the biophysical environment are becoming interested in the social and environmental histories of places burdened with hazards like extreme heat, and urban scholars are recognizing that insights from empirical assessments of hazards can provide adequate data-based support for socio-ecological explanations for unequal outcomes. Continuing collaboration and conversations among these communities can help increase understanding of heat hazards and holistically integrate the contributions from each discipline.

The second question is related to articulating the pathways through which more equal landscapes of heat risk can be imagined. What should equality in heat hazards vulnerability look like? Viewed purely in distributional terms, does it mean spatially shifting "surplus" exposure away from more sensitive neighborhoods or simply increasing the ecological services footprint through shading trees? In procedural justice terms, does it mean more inclusiveness of marginalized communities in the decision-making processes of land use change? Marxist scholars have argued that the way forward in redressing uneven urban developments is an increased "right to the city" (Mitchell 2003b), a "greater

democratic control over the production and utilization of the [urban] surplus" (Harvey 2008, 37). Future interdisciplinary research should explore the ways in which decisions about urban development should be made in order to achieve greater equality in socio-ecological conditions.

The Marxist engagement focused on production and consumption of urban environments can help dig deep into the all-encompassing structural relations that create urban heat islands and marginalized populations, not just the proximate ones more readily identified by specific research disciplines. It is my hope that this dissertation serves to contribute to integrative, interdisciplinary framings of the three research questions presented here, but also go beyond those towards discussions on how to mitigate environmental hazards and reduce inequalities.

Adger, N. (1999). Social vulnerability to climate change and extremes in coastal Vietnam. *World Development 27*, 249–269.

Adger, N. (2006). Vulnerability. *Global Environmental Change 16*(3), 268–281.

Adger, W. N. (1996). Approaches to vulnerability to climate change. *CSERGE GEC working paper*.

Adger, W. N., S. Agrawala, M. M. Q. Mirza, C. Conde, K. O'Brien, J. Pulhin, R. Pulwarty, B. Smit, and K. Takahashi (2007). Assessment of adaptation practices, options, constraints and capacity. *Climate change*, 717–743.

Alwang, J., P. B. Siegel, and S. L. Jorgensen (2001). Vulnerability : a view from different disciplines. Social Protection Discussion Papers 23304, The World Bank.

Anderson, G. B. and M. L. Bell (2011). Heat waves in the United States: Mortality risk during heat waves and effect modification by heat wave characteristics in 43 US communities. *Environmental Health Perspectives 119*(2), 210.

Anselin, L. (1995). Local indicators of spatial association - LISA. *Geographical Analysis 27*(2), 93–115.

Applegate, W., J. Runyan Jr, L. Brasfield, M. Williams, C. Konigsberg, C. Fouche, et al. (1981). Analysis of the 1980 heat wave in Memphis. *Journal of the American Geriatrics Society 29*(8), 337.

ASTER Science Project (2010). Characteristics of ASTER sensor. http://www.science.aster.ersdac.jspacesystems.or.jp/en/about_aster/sensor/tokutyou.html. Last accessed 17 April 2013.

Autobee, R. (2013). Salt River Project. http://www.usbr.gov/projects//ImageServer?imgName=Doc_1305577664538.pdf.

AZMET (Arizona Meteorological Network) (2013). Raw hourly and daily data. http://ag.arizona.edu/azmet/az-data.htm. Last accessed 17 April 2013.

Balbus, J. M. and C. Malina (2009). Identifying vulnerable subpopulations for climate change health effects in the United States. *Journal of Occupational and Environmental Medicine 51*(1), 33–37 10.1097/JOM.0b013e318193e12e.

Balling, R. C. and S. W. Brazel (1987). The impact of rapid urbanization on pan evaporation in Phoenix, Arizona. *Journal of Climatology 7*(6), 593–597.

Balogun, A. A., I. A. Balogun, and Z. D. Adeyewa (2010). Comparisons of urban and rural heat stress conditions in a hot–humid tropical city. *Global Health Action 3*.

Bankoff, G. (2001). Rendering the world unsafe: 'vulnerability' as western discourse. *Disasters 25*(1), 19–35.

Bankoff, G. (2003). Vulnerability as a measure of change in society. *International Journal of Mass Emergencies and Disasters 21*(2), 30–50.

Barradas, V. L., A. Tejeda-Martinez, and E. Jauregui (1999). Energy balance measurements in a suburban vegetated area in Mexico City. *Atmospheric Environment 33*(24-25), 4109–4113.

Basu, R., W. Feng, and B. Ostro (2008). Characterizing temperature and mortality in nine California counties. *Epidemiology 19*(1), 138–145.

Basu, R. and J. M. Samet (2002). Relation between elevated ambient temperature and mortality: a review of the epidemiologic evidence. *Epidemiologic reviews 24*(2), 190–202.

Berkes, F., C. Folke, and J. Colding (2000). *Linking social and ecological systems: management practices and social mechanisms for building resilience*. Cambridge: Cambridge University Press.

Blaikie, P. (1994). *At risk: natural hazards, people's vulnerability, and disasters*. London; New York: Routledge.

Bohle, H. G., T. E. Downing, and M. J. Watts (1994, March). Climate change and social vulnerability: Toward a sociology and geography of food insecurity. *Global Environmental Change 4*(1), 37–48.

Bolin, B., S. Grineski, and T. Collins (2005). The geography of despair: Environmental racism and the making of South Phoenix, Arizona, USA. *Human Ecology Review 12*(2), 156–168.

Bolin, B., E. Matranga, E. J. Hackett, E. K. Sadalla, K. D. Pijawka, D. Brewer, and D. Sicotte (2000, January). Environmental equity in a sunbelt city: the spatial distribution of toxic hazards in phoenix, arizona. *Environmental Hazards 2*(1), 11–24.

Bolin, B., A. Nelson, E. J. Hackett, K. D. Pijawka, C. S. Smith, D. Sicotte, E. K. Sadalla, E. Matranga, and M. O'Donnell (2002). The ecology of technological risk in a sunbelt city. *Environment and Planning A 34*, 317–339.

Boone, C., G. Buckley, J. Grove, and C. Sister (2009). Parks and people: An environmental justice inquiry in Baltimore, Maryland. *Annals of the Association of American Geographers 99*(4), 767–787.

Bouchama, A. and J. Knochel (2002). Medical progress - heat stroke. *New England Journal of Medicine 346*(25), 1978–1988.

Brazel, A., P. Gober, S. J. Lee, S. Grossman-Clarke, J. Zehnder, B. Hedquist, and E. Comparri (2007). Determinants of changes in the regional urban heat island in metropolitan Phoenix (Arizona, USA) between 1990 and 2004. *Climate Research 33*(2), 171.

Brazel, A., N. Selover, R. Vose, and G. Heisler (2000). The tale of two climates - Baltimore and Phoenix urban LTER sites. *Climate Research 15*, 123–135.

Bronstert, A. (2003). Floods and climate change: interactions and impacts. *Risk Analysis 23*(3), 545–557.

Brooks, N., W. Neil Adger, and P. Mick Kelly (2005). The determinants of vulnerability and adaptive capacity at the national level and the implications for adaptation. *Global Environmental Change 15*(2), 151–163.

Browning, C. R., D. Wallace, S. L. Feinberg, and K. A. Cagney (2006). Neighborhood social processes, physical conditions, and disaster-related mortality: The case of the 1995 Chicago heat wave. *American Sociological Review 71*(4), 661–678.

Brownlow, A. (2006). An archaeology of fear and environmental change in Philadelphia. *Geoforum 37*(2), 227–245.

Bruneau, M., S. E. Chang, R. T. Eguchi, G. C. Lee, T. D. O'Rourke, A. M. Reinhorn, M. Shinozuka, K. Tierney, W. A. Wallace, and D. von Winterfeldt (2003). A framework to quantitatively assess and enhance the seismic resilience of communities. *Earthquake spectra 19*(4), 733–752.

Bruse, M. and H. Fleer (1998). Simulating surface-plant-air interactions inside urban environments with a three dimensional numerical model. *Environmental Modeling & Software 13*(3), 373–384.

Burton, I., R. W. Kates, and G. F. White (1978). *The environment as hazard*. New York: Oxford University Press.

Buscail, C., E. Upegui, and J.-F. Viel (2012). Mapping heatwave health risk at the community level for public health action. *International Journal of Health Geographics 11*(1), 1–9.

Buyantuyev, A. and J. Wu (2012). Urbanization diversifies land surface phenology in arid environments: Interactions among vegetation, climatic variation, and land use patterns in the Phoenix metropolitan region, USA. *Landscape and Urban Planning 105*(1-2), 149–159.

Byrne, J., J. Wolch, and J. Zhang (2009). Planning for environmental justice in an urban national park. *Journal of Environmental Planning and Management 52*, 365–392.

Canada, H. (2008). Human health in a changing climate: A Canadian assessment of vulnerabilities and adaptive capacity. Technical report, Health Canada.

Carnesale, A. and W. Chameides (2011). America's climate choices. Technical report, RC/NAS USA Committee on America's Climate Choices.

Centers for Disease Control and Prevention (2009). Extreme heat: a prevention guide to promote your health and safety. http://emergency.cdc.gov/disasters/extremeheat/heat_guide-page-3.asp.

Central Arizona Phoenix-Long Term Ecological Research (2003). Land use change: 1912 to 1995. http://caplter.asu.edu/data/?id=69.

Chen, F., K. W. Manning, M. A. LeMone, S. B. Trier, J. G. Alfieri, R. Roberts, M. Tewari, D. Niyogi, T. W. Horst, S. P. Oncley, et al. (2007). Description and evaluation of the characteristics of the ncar high-resolution land data assimilation system. *Journal of applied Meteorology and Climatology 46*(6), 694–713.

Chow, W., W. Chuang, and P. Gober (2011). Vulnerability to extreme heat in metropolitan Phoenix: Spatial, temporal, and demographic dimensions. *The Professional Geographer 64*(2), 286–302.

Chow, W. T. L., R. L. Pope, C. A. Martin, and A. J. Brazel (2011). Observing and modeling the nocturnal park cool island of an arid city: horizontal and vertical impacts. *Theoretical and Applied Climatology 103*(1-2), 197–211. WOS:000285780900015.

Collins, T. W. (2010). Marginalization, facilitation, and the production of unequal risk: The 2006 Paso del Norte floods. *Antipode 42*(2), 258–288.

Committee on Increasing National Resilience to Hazards and Disasters (CINRHD), Committee on Science, Engineering, and Public Policy, Policy and Global Affairs (PGA); The National Academies (2012). Disaster resilience: A national imperative. http://www.nap.edu/openbook.php?record_id=13457.

Cooney, C. M. (2012). Downscaling climate models: Sharpening the focus on local-level changes. *Environmental Health Perspectives 120*(1), a22.

Cromley, E. K. and S. McLafferty (2012). *GIS and public health*. Guilford Press.

Currie, B. and B. Bass (2008). Estimates of air pollution mitigation with green plants and green roofs using the UFORE model. *Urban Ecosystems 11*(4), 409–422.

Cutter, S. (2002). *American Hazardscapes: The Regionalization of Hazards and Disasters*. Natural Hazards and Disasters. National Academies Press.

Cutter, S. and C. Finch (2008). Temporal and spatial changes in social vulnerability to natural hazards. *Proceedings of the National Academy of Sciences of the United States of America 105*(7), 2301–2306.

Cutter, S. L. (1995). The forgotten casualties: women, children, and environmental change. *Global environmental change 5*(3), 181–194.

Cutter, S. L. (1996). Vulnerability to environmental hazards. *Progress in Human Geography 20*(4), 529–539.

Cutter, S. L., L. Barnes, M. Berry, C. Burton, E. Evans, E. Tate, and J. Webb (2008). A place-based model for understanding community resilience to natural disasters. *Local evidence on vulnerabilities and adaptations to global environmental change 18*(4), 598–606.

Cutter, S. L., B. J. Boruff, and W. L. Shirley (2003). Social vulnerability to environmental hazards. *Social Science Quarterly 84*(2), 242–261.

Cutter, S. L., C. G. Burton, and C. T. Emrich (2010). Disaster resilience indicators for benchmarking baseline conditions. *Journal of Homeland Security and Emergency Management 7*(1).

Cutter, S. L., J. T. Mitchell, and M. S. Scott (2000). Revealing the vulnerability of people and places: A Case Study of Georgetown. *Annals of the Association of American Geographers 90*(4), 713–737.

de Groot, R., R. Alkemade, L. Braat, L. Hein, and L. Willemen (2010). Challenges in integrating the concept of ecosystem services and values in landscape planning, management and decision making. *Ecological Complexity 7*(3), 260–272.

de Smith, M. J., M. F. Goodchild, and P. A. Longley (2007). *Geospatial Analysis*. Troubador Publishing Ltd.

Dean, D. R. and J. A. Reynolds (2006). Hispanic Historic Property Survey. http://www.ciudaddephoenix.com/webcms/groups/internet/@inter/@dept/@dsd/documents/web_content/pdd_hp_pdf_00043.pdf.

Department of Commerce (2011). Urban Area Criteria for the 2010 Census. http://www.census.gov/geo/reference/pdfs/fedreg/fedregv76n164.pdf.

Diffenbaugh, N., J. Pal, R. Trapp, and F. Giorgi (2005). Fine-scale processes regulate the response of extreme events to global climate change. *Proceedings of the National Academy of Sciences of the United States of America 102*(44), 15774–15778.

Dooling, S., G. Simon, and K. Yocom (2006). Place-based urban ecology: A century of park planning in Seattle. *Urban Ecosystems 9*(4), 299–321. 10.1007/s11252-006-0008-1.

Eakin, H. and L. A. Bojorquez-Tapia (2008). Insights into the composition of household vulnerability from multicriteria decision analysis. *Global Environmental Change 18*(1), 112–127.

Eakin, H. and A. Luers (2006). Assessing the vulnerability of social-environmental systems. *Annual Review of Environment and Resources 31*(1), 365–394.

Ebi, K. L., N. D. Lewis, and C. Corvalan (2006). Climate variability and change and their potential health effects in small island states: information for adaptation planning in the health sector. *Environmental Health Perspectives 114*(12), 1957.

Elliott, J. R. and S. Frickel (2013). The historical nature of cities a study of urbanization and hazardous waste accumulation. *American Sociological Review 7*(4), 521–543.

Emmanuel, R. and H. J. S. Fernando (2007). Urban heat islands in humid and arid climates: role of urban form and thermal properties in Colombo, Sri Lanka and Phoenix, USA. *Clim Res 34*(3), 241–251.

Environmental Protection Agency (2011). Natural disasters and weather emergencies: Extreme heat. http://www.epa.gov/naturalevents/extremeheat.html.

Famisa, Z. S. (1977). *The conversion of agricultural land to non-agricultural uses in the Phoenix-Tucson corridor, 1940-75*. Ph. D. thesis, Arizona State University.

Farish, T. E. (1918). *History of Arizona*, Volume 1-6. Filmer Bros. Electrotype Company.

Feiden, P. (2011). Adapting to climate change: Cities and the urban poor. http://intlhc.org/wp-content/uploads/2011/09/Climate-Change-and-the-Urban-Poor.pdf.

Fothergill, A. and L. A. Peek (2004). Poverty and disasters in the United States: A review of recent sociological findings. *Natural Hazards 32*(1), 89–110.

Fry, J., G. Xian, S. Jin, J. A. Dewitz, C. G. Homer, L. Yang, C. A. Barnes, N. D. Herold, and J. D. Wickham (2011). Completion of the 2006 National Land Cover Database update for the conterminous United States. *Photogrammetric Engineering and Remote Sensing 77*(9), 858–864.

Füssel, H.-M. (2007). Vulnerability: a generally applicable conceptual framework for climate change research. *Global Environmental Change 17*(2), 155–167.

Gallopín, G. C. (2006). Linkages between vulnerability, resilience, and adaptive capacity. *Global Environmental Change 16*(3), 293–303.

Garcia-Cueto, O. R., E. Jauregui-Ostos, D. Toudert, and A. Tejeda-Martinez (2007). Detection of the urban heat island in Mexicali, B. C., Mexico and its relationship with land use. *Atmosfera 20*(2), 111–131.

Georgescu, M., M. Moustaoui, A. Mahalov, and J. Dudhia (2012). Summer-time climate impacts of projected megapolitan expansion in Arizona. *Nature Climate Change 3*(1), 37–41.

Gober, P. (2005). *Metropolitan Phoenix: place making and community building in the desert*. University of Pennsylvania Press.

Gober, P., A. Brazel, R. Quay, S. Myint, S. Grossman-Clarke, A. Miller, and S. Rossi (2009). Using watered landscapes to manipulate urban heat island effects: How much water will it take to cool Phoenix? *Journal of the American Planning Association 76*(1), 109–121.

Goldberg, R. B. (1973). Michael Wormser, Capitalist. http://americanjewisharchives.org/publications/journal/PDF/1973_25_02_00_goldberg.pdf.

Golden, J. S. (2004). The built environment induced urban heat island effect in rapidly urbanizing arid regions – a sustainable urban engineering complexity. *Environmental Sciences 1*(4), 321–349.

Gordon, J. H. (1921). Temperature survey of the Salt River Valley, Arizona. *Monthly Weather Review 49*(5), 271–274.

Grimmond, C., C. Souch, and M. Hubble (1996, January). Influence of tree cover on summertime surface energy balance fluxes, San Gabriel Valley, Los Angeles. *Climate Research 6*(1), 45–57. WOS:A1996UB31600004.

Grineski, S., B. Bolin, and C. Boone (2007). Criteria air pollution and marginalized populations: Environmental inequity in metropolitan Phoenix, Arizona. *Social Science Quarterly 88*, 535–554.

Grossman-Clarke, S., J. a. Zehnder, T. Loridan, and C. S. B. Grimmond (2010). Contribution of land use changes to near-surface air temperatures during recent summer extreme heat events in the Phoenix Metropolitan Area. *Journal of Applied Meteorology and Climatology 49*(8), 1649–1664.

Grossman-Clarke, S., J. A. Zehnder, W. L. Stefanov, Y. B. Liu, and M. A. Zoldak (2005). Urban modifications in a mesoscale meteorological model and the effects on near-surface variables in an arid metropolitan region. *Journal of Applied Meteorology 44*(9), 1281–1297.

Guhathakurta, S. and P. Gober (2010, July). Residential land use, the urban heat island, and water use in Phoenix: A path analysis. *Journal of Planning Education and Research 30*(1), 40–51.

Guhathakurta, S. and M. Wichert (1998). Who pays for growth in the city of Phoenix? An equity-based perspective on suburbanization. *Urban Affairs Review 33*(6), 813–838.

Harlan, S., L. Larsen, T. Rex, S. Wolf, E. Hackett, A. Kirby, R. Bolin, A. Nelson, and D. Hope (2003). The Phoenix Area Social Survey: Community and Environment in a Desert Metropolis. Technical report, Central Arizona – Phoenix Long-Term Ecological Research Contribution No. 2, Center for Environmental Studies, Arizona State University, Tempe.

Harlan, S. L., A. J. Brazel, L. Prashad, W. L. Stefanov, and L. Larsen (2006). Neighborhood microclimates and vulnerability to heat stress. *Social Science & Medicine 63*, 2847–2863.

Harlan, S. L., M. Budruk, A. Gustafson, K. Larson, D. Ruddell, V. K. Smith, S. T. Yabiku, and A. Wutich (2007). 2006 highlights: Phoenix area social survey community and environment in a desert metropolis. Technical report, Central Arizona – Phoenix Long-Term Ecological Research Contribution No. 4, Global Institute of Sustainability, Arizona State University, Tempe.

Harlan, S. L., J. H. Declet-Barreto, W. L. Stefanov, and D. B. Petitti (2013). Neighborhood effects on heat deaths: Social and environmental predictors of vulnerability in Maricopa County, Arizona. *Environmental Health Perspectives 121*(2), 197.

Harlan, S. L. and D. M. Ruddell (2011). Climate change and health in cities: impacts of heat and air pollution and potential co-benefits from mitigation and adaptation. *Current Opinion in Environmental Sustainability 3*(3), 126–134.

Harvey, D. (1973). *Social justice and the city*. Jonhs Hopkins University Press.

Harvey, D. (1985). *The urbanization of capital*. Blackwell Oxford.

Harvey, D. (1996). *Justice, nature, and the geography of difference*. Cambridge, Mass.: Blackwell Publishers.

Harvey, D. (2001). *Spaces of capital: Towards a critical geography*. Routledge.

Harvey, D. (2006). *The limits to capital*. University of Chicago Press Chicago.

Harvey, D. (2008). The right to the city. *53*, 23–40.

Hedquist, B., S. Di Sabatino, H. Fernando, and A. Brazel (2009). Results from the Phoenix Arizona urban heat island experiment. In *The seventh International Conference on Urban Climate*, Volume 29.

Heim, C. E. (2001, January). Leapfrogging, urban sprawl, and growth management: Phoenix, 1950-2000. *American Journal of Economics and Sociology 60*(1), 245–283.

Heisler, G., R. Grant, C. Grimmond, and C. Souch (1995). Urban forests—cooling our communities? *Proceedings of the Seventh National Urban Forestry Conference: American Forests*, 31–34.

Hewitt, K. (1983). *Interpretations of Calamity from the Viewpoint of Human Ecology*. Risks & Hazards Series. Allen & Unwin.

Hewitt, K. (1997). *Regions of risk: A geographical introduction to disasters*. Longman London.

Heynen, N. (2006). Green urban political ecologies: toward a better understanding of inner-city environmental change. *Environment and Planning A 38*(3), 499–516.

Heynen, N., M. Kaika, and E. Swyngedouw (2006). *In the nature of cities: Urban political ecology and the politics of urban metabolism*. Questioning cities series. London ; New York: Routledge.

Heynen, N. C. (2003, November). The scalar production of injustice within the urban forest. *Antipode 35*(5), 980–998.

Hill, T. and C. Polsky (2007). Development and drought in suburbia: A mixed methods rapid assessment of vulnerability to drought in rainy Massachusetts. *Global Environmental Change, Part B: Environmental Hazards 7*, 291–301.

Holling, C. S. (1973). Resilience and stability of ecological systems. *Annual Review of Ecology and Systematics 4*(1), 1–23.

Hondula, D. M., R. E. Davis, M. J. Leisten, M. V. Saha, L. M. Veazey, and C. R. Wegner (2012). Fine-scale spatial variability of heat-related mortality in Philadelphia County, USA, from 1983-2008: a case-series analysis. *Environmental Health 11*(1), 16.

Honker, A. M. (2002). "A terrible calamity has fallen upon Phoenix": The 1891 flood and Salt River Valley reclamation. *The Journal of Arizona History 43*(2), 109–132.

Horton, A. (1941). *An economic, political and social survey of Phoenix and the Valley of the Sun*. Southside Progress.

Huttner, S., M. Bruse, and P. Dostal (2008). Using ENVI-Met to simulate the impact of global warming on the microclimate in central European cities. *Ber Meteorol Inst Univ Freiburg 18*, 307–312.

IPCC Working Group I (2013). Fifth Assessment Report (AR5). Technical report, Intergovernmental Panel for Climate Change.

Jackson, J. E., M. G. Yost, C. Karr, C. Fitzpatrick, B. K. Lamb, S. H. Chung, J. Chen, J. Avise, R. A. Rosenblatt, and R. A. Fenske (2010). Public health impacts of climate change in washington state: projected mortality risks due to heat events and air pollution. *Climatic change 102*(1-2), 159–186.

Jenerette, G. D., S. L. Harlan, A. Brazel, N. Jones, L. Larsen, and W. L. Stefanov (2007). Regional relationships between surface temperature, vegetation, and human settlement in a rapidly urbanizing ecosystem. *Landscape Ecology 22*, 353–365.

Jenerette, G. D., S. L. Harlan, W. L. Stefanov, and C. A. Martin (2011). Ecosystem services and urban heat riskscape moderation: water, green spaces, and social inequality in Phoenix, USA. *Ecological Applications 21*(7), 2637–51.

Jennings, V., C. Johnson Gaither, and R. Schulterbrandt Gragg (2012). Promoting environmental justice through urban green space access: A synopsis. *Environmental Justice 5*(1), 1–7.

Jesdale, B. M., R. Morello-Frosch, and L. Cushing (2013). The racial/ethnic distribution of heat risk-related land cover in relation to residential segregation. *Environmental health perspectives 121*(7), 811–817.

Johnson, D. P., A. Stanforth, V. Lulla, and G. Luber (2012). Developing an applied extreme heat vulnerability index utilizing socioeconomic and environmental data. *Applied Geography 35*(1–2), 23–31.

Kalkstein, A. J. and L. S. Kalkstein (2004). The development of an evaporative cooler warning system for Phoenix, Arizona. http://www.udel.edu/SynClim/Evap_cooler.pdf.

Kasperson, J. X. and R. E. Kasperson (2013). *Global environmental risk*. Routledge.

Kates, R. W. (1985). The interaction of climate and society. In R. W. Kates, J. Ausubel, and M. Berberian (Eds.), *Climate Impact Assessment: Studies of the Interaction of Climate and Society*, pp. 3–36. John Wiley.

Kilbourne, E., K. Choi, T. Jones, and S. Thacker (1982). Risk-factors for heatstroke - a case-control study. *Journal of the American Medical Association 247*(24), 3332–3336. WOS:A1982NU01400022.

Kinney, P. L. (2008). Climate change, air quality, and human health. *American Journal of Preventive Medicine 35*(5), 459–467.

Klein, R. J., R. J. Nicholls, and F. Thomalla (2003). Resilience to natural hazards: How useful is this concept? *Global Environmental Change Part B: Environmental Hazards 5*(1), 35–45.

Klinenberg, E. (2003). *Heat Wave: A Social Autopsy of Disaster in Chicago*. University of Chicago Press.

Knowlton, K., C. Hogrefe, B. Lynn, C. Rosenzweig, J. Rosenthal, and P. Kinney (2008). Impacts of Heat and Ozone on Mortality Risk in the New York City Metropolitan Region Under a Changing Climate. *Advances in Global Change Research 30*, 143–160.

Konig, M. (1982). Phoenix in the 1950s: Urban Growth in the "Sunbelt". *Arizona and the West 24*(1), 19–38.

Kotlanger, M. (1983). *Phoenix, Arizona: 1920-1940*. PhD thesis, Arizona State University.

Kovats, S. and R. Akhtar (2008). Climate, climate change and human health in asian cities. *Environment and Urbanization 20*(1), 165–175.

Kupel, D. E. (2006). *Fuel for growth: water and Arizona's urban environment*. University of Arizona Press.

Lahme, E. and M. Bruse (2003). Microclimatic effects of a small urban park in densely built-up areas: Measurements and model simulations. Fifth International Conference on Urban Climate (ICUC5) Lodz. http://nargeo.geo.uni.lodz/~icu5/text/P_5_1.pdf.

Lalic, B. and D. Mihailovic (2004). An empirical relation describing leaf-area density inside the forest for environmental modeling. *Journal of Applied Meteorology 43*(4), 641–645.

Larsen, L. and D. Alameddin (2007). The evolution of early phoenix: Valley business elite, land speculation, and the emergence of planning. *Journal of Planning History 6*(2), 87–113.

Lefebvre, H. (1991). *The production of space*. Blackwell.

Leichenko, R. (2011). Climate change and urban resilience. *Current Opinion in Environmental Sustainability 3*(3), 164–168.

Lochner, K. A., I. Kawachi, R. T. Brennan, and S. L. Buka (2003). Social capital and neighborhood mortality rates in Chicago. *Social Science & Medicine 56*(8), 1797–1805.

Longino, C. F. and R. J. Manheimer (2006). *Retirement migration in America*. Vacation Publications.

Lowry, W. (1967). The climate of cities. *Scientific American 217*, 15–23.

Luckingham, B. (1989). *Phoenix: The history of a southwestern metropolis*. Tucson: University of Arizona Press.

Luers, A. L. (2005). The surface of vulnerability: An analytical framework for examining environmental change. *Global Environmental Change 15*(3), 214–223.

Luers, A. L., D. B. Lobell, L. S. Sklar, C. Addams, and P. a. Matson (2003). A method for quantifying vulnerability, applied to the agricultural system of the yaqui valley, mexico. *Global Environmental Change 13*(4), 255–267.

Maricopa Association of Governments (2009). Land use dataset.

Maricopa County Assessor's Office (2010). GIS parcels database.

Maricopa County Department of Public Health, Division of Disease Control, Office of Epidemiology (2012). Heat-associated deaths in Maricopa County, AZ: report for 2011. http://www.maricopa.gov/publichealth/Services/EPI/pdf/heat/2011annualreport.pdf.

Maricopa County Flood Control District (2013). ALERT system - single sensor data report generator. http://www.fcd.maricopa.gov/Rainfall/ALERT/ssdata.aspx.

Martin, C. and L. B. Stabler (2002). Plant gas exchange and water status in urban desert landscapes. *Journal of Arid Environments 51*, 235–254.

Martin, C., P. S. Warren, and A. P. Kinzig (2004). Neighborhood socioeconomic status is a useful predictor of perennial landscape vegetation in residential neighborhoods and embedded small parks of Phoenix, Arizona. *Landscape and Urban Planning 69*, 355–368.

Martin, C. A. (2009). Virtual library of Phoenix landscape plants. http://www.public.asu.edu/~camartin/Martinlandscapeplantlibrary.htm.

Marx, K. (1992). *Capital: A Critique of Political Economy Vol I*. Penguin Classics.

Matzarakis, A., F. Rutz, and H. Mayer (2010). Modelling radiation fluxes in simple and complex environments: Basics of the RayMan model. *International Journal of Biometeorology 54*(2), 131–139. 10.1007/s00484-009-0261-0.

Mawn, G. P. (1977). Promoters, speculators, and the selection of the Phoenix townsite. *Arizona and the West 19*(3), 207–224.

McCoy, M. G. (2000). *Desert metropolis: image building and the growth of Phoenix, 1940-1965*. Ph. D. thesis, Arizona State University.

McHugh, K., P. Gober, and D. Borough (2002). The Sun City Wars: Chapter 3. *Urban Geography 23*(7), 627–648.

McMichael, A. (2001). Impact of climatic and other environmental changes on food production and population health in the coming decades. *Proceedings of the nutrition Society 60*(02), 195–201.

McMichael, A. J., R. E. Woodruff, and S. Hales (2006). Climate change and human health: Present and future risks. *The Lancet 367*(9513), 859–869.

Meehl, G. and C. Tebaldi (2004). More intense, more frequent, and longer lasting heat waves in the 21st century. *Science 305*(5686), 994–997.

Merrifield, A. (2002). *Metromarxism: A Marxist tale of the city*. Psychology Press.

Mills, D. M. (2009). Climate change, extreme weather events, and US health impacts: what can we say? *Journal of Occupational and Environmental Medicine 51*(1), 26–32.

Mills, G. (2006). Progress toward sustainable settlements: A role for urban climatology. *Theoretical and Applied Climatology 84*, 69–76.

Milly, P., R. Wetherald, K. Dunne, and T. Delworth (2002). Increasing risk of great floods in a changing climate. *Nature 415*(6871), 514–517.

Mitchell, D. (2003a). Cultural landscapes: just landscapes or landscapes of justice? *Progress in Human Geography 27*(6), 787–796.

Mitchell, D. (2003b). *The right to the city: Social justice and the fight for public space*. Guilford Press.

Morello-Frosch, R., M. Pastor, and J. Sadd (2001). Environmental justice and Southern California's "riskscape" The distribution of air toxics exposures and health risks among diverse communities. *Urban Affairs Review 36*(4), 551–578.

Mustafa, D. (1998). Structural causes of vulnerability to flood hazard in Pakistan. *Economic Geography 74*(3), 289–305.

Mustafa, D. (2005). The production of an urban hazardscape in Pakistan: Modernity, vulnerability, and the range of choice. *Annals of the Association of American Geographers 95*(3), 566–586.

Mustafa, D., S. Ahmed, E. Saroch, and H. Bell (2011). Pinning down vulnerability: From narratives to numbers. *Disasters 35*(1), 62 – 86.

NASA Landsat Program (2010). Landsat TM scene l5037037_03720100813.

National Climatic and Oceanographic Administration (2013). National Climatic Center Land-Based Data. http://lwf.ncdc.noaa.gov/oa/land.html.

Neil Adger, W., N. W. Arnell, and E. L. Tompkins (2005). Successful adaptation to climate change across scales. *Global Environmental Change 15*(2), 77–86.

Niebur, J. E. (1967). *The Social and Economic Effect of the Great Depression on Phoenix, Arizona, 1929-1934*. Ph. D. thesis, Arizona State University, 1967–History.

Oberle, A. P. and D. D. Arreola (2008). Resurgent Mexican Phoenix. *Geographical Review 98*(2), 171–196.

Oke, T. (1981). Canyon geometry and the nocturnal urban heat island: comparison of scale model and field observations. *Journal of Climatology 1*(3), 237–254.

Oke, T. (1982). The energetic basis of the urban heat-island. *Quarterly Journal of the Royal Meteorological Society 108*(455), 1–24.

Oke, T. (1989). The micrometeorology of the urban forest. *Philosophical Transactions of the Royal Society of London Series B-Biological Sciences 324*(1223), 335–349. WOS:A1989AP05500009.

Oke, T. R. (1997). *The changing climatic environments: Urban climates and global environmental change.* New York: Routledge.

Oke, T. R. (1998). The thermal regime of urban parks in two cities with different summer climates. *International Journal of Remote Sensing 19*(11), 2085–2104.

O'Keefe, P., K. Westgate, and B. Wisner (1976). Taking the naturalness out of natural disasters. *Nature 260*, 566–567.

O'Neill, M. S., A. Zanobetti, and J. Schwartz (2005). Disparities by race in heat-related mortality in four US cities: The role of air conditioning prevalence. *Journal of Urban Health 82*(2), 191–197.

Ozkeresteci, I., K. Crewe, A. Brazel, and M. Bruse (2003, August). Use and evaluation of the ENVI-Met model for environmental design and planning: an experiment of linear parks.

Pachauri, R. K. and A. Reisinger (2007). *Climate Change 2007: Synthesis Report. Contribution of Working Groups I, II and III to the Fourth Assessment Report of the Intergovernmental Panel on Climate Change*. Cambridge University Press, Cambridge, United Kingdom and New York, NY, USA,.

Parry, M. L., C. Rosenzweig, A. Iglesias, M. Livermore, and G. Fischer (2004). Effects of climate change on global food production under SRES emissions and socio-economic scenarios. *Global Environmental Change 14*(1), 53–67.

Patz, J. A., M. A. McGeehin, S. M. Bernard, K. L. Ebi, P. R. Epstein, A. Grambsch, D. J. Gubler, P. Reither, I. Romieu, J. B. Rose, et al. (2000). The potential health impacts of climate variability and change for the United States: Executive summary of the report of the health sector of the US National Assessment. *Environmental health perspectives 108*(4), 367.

Payne-Sturges, D., G. C. Gee, K. Crowder, B. J. Hurley, C. Lee, R. Morello-Frosch, A. Rosenbaum, A. Schulz, C. Wells, T. Woodruff, and H. Zenick (2006). Workshop summary: Connecting social and environmental factors to measure and track environmental health disparities. *Environmental Research 102*(2), 146–153. WOS:000241172100002.

Pearlmutter, D., P. Berliner, and E. Shaviv (2006). Physical modeling of pedestrian energy exchange within the urban canopy. *Building and Environment 41*(6), 783 – 795.

Pelling, M. (2003). Toward a political ecology of urban environmental risk: The case of Guyana. In K. S. Zimmerer and T. Bassett (Eds.), *Political Ecology: An integrative approach to geography and environment-development studies*. New York: The Guildford Press.

Perkins, H., N. Heynen, and J. Wilson (2004). Inequitable access to urban reforestation: The impact of urban political economy on housing tenure and urban forests. *Cities 21*(4), 291–299.

Peterson, T. C., R. R. Heim, R. Hirsch, D. P. Kaiser, H. Brooks, N. S. Diffenbaugh, R. M. Dole, J. P. Giovannettone, K. Guirguis, T. R. Karl, R. W. Katz, K. Kunkel, D. Lettenmaier, G. J. McCabe, C. J. Paciorek, K. R. Ryberg, S. Schubert, V. B. S. Silva, B. C. Stewart, A. V. Vecchia, G. Villarini, R. S. Vose, J. Walsh, M. Wehner, D. Wolock, K. Wolter, C. A. Woodhouse, and D. Wuebbles (2013). Monitoring and understanding changes in heat waves, cold waves, floods, and droughts in the united states: State of knowledge. *Bulletin of the American Meteorological Society 94*(6), 821–834.

Pilkey, O. H. and J. A. G. Cooper (2004). Society and sea level rise. *Science 303*(5665), 1781–1782.

Pulido, L. (2000). Rethinking environmental racism: White privilege and urban development in southern California. *Annals of the Association of American Geographers 90*(1), 12–40.

Redman, C. L. and A. P. Kinzig (2008). Water can flow uphill: A narrative of central Arizona. In C. L. Redman and D. R. Foster (Eds.), *Agricultural landscapes in transition: comparisons of long-term ecological and cultural change.*, Long-Term Ecological Research Network, pp. 238–271. Oxford University Press, USA.

Reeves, W. C., J. L. Hardy, W. K. Reisen, and M. M. Milby (1994). Potential effect of global warming on mosquito-borne arboviruses. *Journal of Medical Entomology 31*(3), 323–332.

Reid, C. E., J. K. Mann, R. Alfasso, P. B. English, G. C. King, R. A. Lincoln, H. G. Margolis, D. J. Rubado, J. E. Sabato, N. L. West, B. Woods, K. M. Navarro, and J. R. Balmes (2012). Evaluation of a heat vulnerability index on abnormally hot days: An environmental public health tracking study. *Environmental Health Perspectives 120*(5), 715–720.

Reid, C. E., M. S. O'Neill, C. J. Gronlund, S. J. Brines, D. G. Brown, A. V. Diez-Roux, and J. Schwartz (2009). Mapping community determinants of heat vulnerability. *Environmental health perspectives 117*(11), 1730–6.

Rey, G., A. Fouillet, P. Bessemoulin, P. Frayssinet, A. Dufour, E. Jougla, and D. Hémon (2009). Heat exposure and socio-economic vulnerability as synergistic factors in heat-wave-related mortality. *European journal of epidemiology 24*(9), 495–502.

Robaa, S. M. (2003). Urban-suburban/rural differences over greater Cairo, Egypt. *Atmosfera 16*(3), 157–171.

Robbins, W. G. (1994). *Colony and empire: The capitalist transformation of the American West*. Development of western resources. Lawrence, Kan.: University Press of Kansas.

Romero Lankao, P. and H. Qin (2011). Conceptualizing urban vulnerability to global climate and environmental change. *Current Opinion in Environmental Sustainability 3*(3), 142–149.

Romero-Lankao, P., H. Qin, and K. Dickinson (2012). Urban vulnerability to temperature-related hazards: A meta-analysis and meta-knowledge approach. *Global transformations, social metabolism and the dynamics of socio-environmental conflicts 22*(3), 670–683.

Rosenzweig, C., G. Casassa, D. Karoly, A. Imeson, C. Liu, A. Menzel, S. Rawlins, T. L. Root, B. Seguin, P. Tryjanowski, et al. (2007). Assessment of observed changes and responses in natural and managed systems. In M. L. Parry, O. F. Canziani, P. J. P, P. J. van der Linden, and C. E. Hanson (Eds.), *limate Change 2007: Impacts, Adaptation and Vulnerability. Contribution of Working Group II to the Fourth Assessment Report of the Intergovernmental Panel on Climate Change,*, pp. 79–131. Cambridge University Press, Cambridge, UK.

Rosenzweig, C., W. D. Solecki, and S. A. Hammer (2011). *Climate change and cities: first assessment report of the Urban Climate Change Research Network*. Cambridge University Press.

Rosheidat, A., D. Hoffman, and H. Bryan (2008). Visualizing Pedestrian Comfort Using ENVI-Met. In *Third National Conference of IBPSA-USA*.

Roth, M. (2002). Effects of cities on local climates. *Proceedings of Workshop of IGES/APN Mega-City Project 33*, 23–25.

Ruddell, D. M., S. L. Harlan, S. Grossman-Clarke, and A. Buyantuyev (2010). Risk and exposure to extreme heat in microclimates of Phoenix, AZ. In *Geospatial techniques in urban hazard and disaster analysis*, pp. 179–202. Springer.

Sampson, R. J. (2009). Racial stratification and the durable tangle of neighborhood inequality. *The Annals of the American Academy of Political and Social Science 621*(1), 260–280.

Schellnhuber, H.-J. (1998). Discourse: Earth System analysis–The scope of the challenge. In *Earth System Analysis*, pp. 3–195. Springer.

Seager, R. and G. A. Vecchi (2010). Greenhouse warming and the 21st century hydroclimate of southwestern North America. *Proceedings of the National Academy of Sciences 107*(50), 21277–21282.

Semenza, J. C., J. E. McCullough, W. D. Flanders, M. A. McGeehin, and J. R. Lumpkin (1999). Excess hospital admissions during the July 1995 heat wave in Chicago. *American Journal of Preventive Medicine 16*(4), 269–277.

Sen, A. (1981). *Poverty and famines: An essay on entitlement and deprivation*. Oxford University Press, USA.

Shashua-Bar, L., O. Potchter, A. Bitan, D. Boltansky, and Y. Yaakov (2010). Microclimate modelling of street tree species effects within the varied urban morphology in the Mediterranean city of Tel Aviv, Israel. *International Journal of Climatology 30*(1), 44–57.

Sheffield, P. E. and P. J. Landrigan (2011). Global climate change and children's health: threats and strategies for prevention. *Environmental health perspectives 119*(3), 291.

Sheridan, T. E. (1995). Arizona: The political ecology of a desert state. *Journal of Political Ecology 2*(1), 41–57.

Simon, A. (2002). *Mixing Water and Culture: Making the Canal Landscape in Phoenix*. Ph. D. thesis, Arizona State University.

Smit, B. and J. Wandel (2006). Adaptation, adaptive capacity and vulnerability. *Global environmental change 16*(3), 282–292.

Smith, N. (1990). *Uneven development : nature, capital, and the production of space*. Ideas. Oxford, UK ; Cambridge, Mass., USA: B. Blackwell.

Smoyer, K. E., D. G. Rainham, and J. N. Hewko (2000). Heat-stress-related mortality in five cities in Southern Ontario: 1980–1996. *International Journal of Biometeorology 44*(4), 190–197.

Stabler, L. B., C. A. Martin, and A. J. Brazel (2005). Microclimates in a desert city were related to land use and vegetation index. *Urban Forestry & Urban Greening 3*, 137–147.

Stoll, M. J. and A. J. Brazel (1992). Surface-air temperature relationships in the urban environment of Phoenix, Arizona. *Physical Geography 13*(2), 160–179.

Stott, P. A., D. A. Stone, and M. R. Allen (2004). Human contribution to the european heatwave of 2003. *Nature 432*(7017), 610–614.

Swyngedouw, E. (1999). Modernity and Hybridity: Nature, *Regeneracionismo*, and the production of the Spanish waterscape, 1890–1930. *Annals of the Association of American Geographers 89*(3), 443–465.

Swyngedouw, E. (2006). Power, water and money: Exploring the nexus. http://hdr.undp.org/en/reports/global/hdr2006/papers/swyngedouw.pdf.

Swyngedouw, E. and N. Heynen (2003). Urban political ecology, justice and the politics of scale. *Antipode 35*(5), 898–918.

Terrain Group (2007). Government roles in climate change adaptation for urban infrastructure. Technical report, Canada: Natural Resources.

Theobald, D. M., W. R. Travis, M. A. Drummond, and E. S. Gordon (2013). Assessment of climate change in the Southwest United States: A report prepared for the National Climate Assessment. Technical report, National Climate Assessment.

Thomalla, F., T. Downing, E. Spanger-Siegfried, G. Han, and J. Rockström (2006). Reducing hazard vulnerability: towards a common approach between disaster risk reduction and climate adaptation. *Disasters 30*(1), 39–48.

Tobin, G. A. and B. E. Montz (1997). *Natural hazards: Explanation and integration*. The Guilford Press.

Tran, K. V., G. S. Azhar, R. Nair, K. Knowlton, A. Jaiswal, P. Sheffield, D. Mavalankar, and J. Hess (2013). A cross-sectional, randomized cluster sample survey of household vulnerability to extreme heat among slum dwellers in Ahmedabad, India. *International Journal of Environmental Research and Public Health 10*(6), 2515–2543.

Tuccillo, J. (2011). Path dependence as place dependence: Water allocation, settlement patterns, and urban trajectories in the Salt River Valley, 1914-1979. Arizona State University, Undergraduate Thesis.

Tucker, C. J. (1979, May). Red and photographic infrared linear combinations for monitoring vegetation. *Remote Sensing of Environment 8*(2), 127–150.

Turner, B. L., R. E. Kasperson, P. A. Matson, J. J. McCarthy, R. W. Corell, L. Christensen, N. Eckley, J. X. Kasperson, A. Luers, M. L. Martello, C. Polsky, A. Pulsipher, and A. Schiller (2003). A framework for vulnerability analysis in sustainability science. *Proceedings of the National Academy of Sciences 100*(14), 8074–8079.

Uejio, C., O. Wilhelmi, J. Golden, D. Mills, S. Gulino, and J. Samenow (2011). Intra-urban societal vulnerability to extreme heat: The role of heat exposure and the built environment, socioeconomics, and neighborhood stability. *Health & Place 17*(2), 498–507.

United States Bureau of Reclamation (2013). Dam details: Theodore Roosevelt Dam. http://www.usbr.gov/projects/Facility.jsp?fac_Name=Theodore+Roosevelt+Dam&groupName=General.

United States Census Bureau (2010a). 2006-2010 American Community Survey 5-year estimates.

United States Census Bureau (2010b). 2010 Census of Population and Housing.

United States Census Bureau (2010c). Phoenix-Mesa-Glendale, AZ Metro Area. Core Based Statistical Areas (CBSA - Metropolitan and Micropolitan Statistical Areas).

United States Department of Agriculture (2007). National agriculture imagery program (NAIP). http://datagateway.nrcs.usda.gov/.

Voogt, J. A. and T. R. Oke (2003). Thermal remote sensing of urban climates. *Remote Sensing of Environment 86*(3), 370–384.

Walker, B., C. S. Holling, S. R. Carpenter, and A. Kinzig (2004). Resilience, adaptability and transformability in social–ecological systems. *Ecology and society 9*(2), 5.

Walker, J. and T. Blaschke (2008). Object-based land-cover classification for the Phoenix metropolitan area: optimization vs. transportability. *International Journal of Remote Sensing 29*(7), 2021–2040.

Wenum, J. D. (1968). *Spatial Growth and the Central City: Problems, Potential, and the Case of Phoenix, Arizona*. Ph. D. thesis, Northwestern University.

Whitaker, M. C. (2000). The rise of Black Phoenix: African-American migration, settlement and community development in Maricopa County, Arizona 1868-1930. *The Journal of Negro History 85*(3), 197–209.

Whitaker, M. C. (2005). *Race work: The rise of civil rights in the urban West*. U of Nebraska Press.

White, G. F. (1974). *Natural hazards, local, national, global*. New York: Oxford University Press.

Wilhelmi, O. V. and M. H. Hayden (2010). Connecting people and place: A new framework for reducing urban vulnerability to extreme heat. *Environmental Research Letters 5*(1).

Wilson, S. M. (2009, March). An ecologic framework to study and address environmental justice and community health issues. *Environmental Justice 2*(1), 15–24.

Wisner, B. (1978). An appeal for a significantly comparative method in disaster research. *Disasters 2*(1), 80–82.

Wisner, B. (2004). *At risk: Natural hazards, people's vulnerability and disasters*. Psychology Press.

Wolch, J., J. Wilson, and J. Fehrenbach (2005). Parks and park funding in Los Angeles: An equity-mapping analysis. *Urban Geography 26*(1), 4–35.

Wolf, J., W. N. Adger, I. Lorenzoni, V. Abrahamson, and R. Raine (2010, February). Social capital, individual responses to heat waves and climate change adaptation: An empirical study of two UK cities. *Global Environmental Change 20*(1), 44–52.

Writers' Program of the Work Projects Administration in the State of Arizona (1940). *Arizona: A state guide*. Hastings House: New York.

Wutich, A. (2007). Vulnerability, Resilience, and Robustness to Urban Water Scarcity: A Case from Cochabamba, Bolivia. In K. Warner (Ed.), *Perspectives on Social Vulnerability*, Volume 6 of *Publication Series of the UNU-EHS*, Chapter 2.1, pp. 62–71. Studies Of the University: Research, Counsel, Education.

Yip, F., W. Flanders, A. Wolkin, D. Engelthaler, W. Humble, A. Neri, L. Lewis, L. Backer, and C. Rubin (2008). The impact of excess heat events in Maricopa County, Arizona: 2000-2005. *International Journal of Biometeorology 52*(8), 765–772.

Zarbin, E. (1995). Dr. AJ Chandler: Practitioner in land fraud. *The Journal of Arizona History 36*(2), 173–188.

Zarbin, E. (2001). Desert land schemes: William J. Murphy and the Arizona Canal Company. *The Journal of Arizona History 42*(2), 155–180.

Zhou, W., G. Huang, and M. L. Cadenasso (2011). Does spatial configuration matter? Understanding the effects of land cover pattern on land surface temperature in urban landscapes. *Landscape and Urban Planning 102*(1), 54–63.

APPENDIX A

NOTES ON MAXIMUM DAILY AIR TEMPERATURE ESTIMATION PROCEDURES

Assigning temperature to discrete locations (e.g., Census Block Groups, geocoded hospitalizations) is a common methodological challenge in heat risk research. The main difficulty lies in resolving spatial and temporal mismatches between temperature observations and the locations or events that require assignment of temperature values. Weather data with a high degree of both spatial and temporal resolution are often available as daily air temperature observations from weather station networks. The spatial distribution of observations is often sparse and irregular, making it necessary to estimate temperature for unsampled locations in a study area via kriging or other spatial interpolation methods. Other sources of spatially explicit temperature data are available as land surface temperature (LST), estimated from thermal remote sensing platforms, but the time periods available are limited to the day that a space or airborne sensor flies over the study area. The relationship between air and surface temperatures is well understood; hence air temperatures, a predictor of heat stress, can be estimated from LST (Jenerette et al. 2011)

Several methods were considered to assign *tmax* to locations where no observations were available. Although simple kriging of weather station observation data is commonly used in heat risk research, I discarded this method as inadequate because it assumes a linear relationship between observed data points, and does not take into account microclimate differences created by topographic or urban canopy spatial forms, which have been established as important determinants of variation in urban microclimates and urban heat island intensities (Oke 1981). I also considered co-kriging, a kriging variant that incorporates covariate sampled data available at the locations of observations of the variable of interest in a model to estimate a continuous field of predictions. Co-kriging is an effective interpolation technique when the covariates correlate with the variable of interest. I tested NDVI (Normalized Density Vegetation Index), an indicator of active vegetation, and percent imperviousness data available from Landsat (NASA 2010) and the 2006 National Land Cover Database (NLCD, Fry et al. 2011) for statistical correlations with observed *tmax* data for each day in the study period. I chose these two variables because the distributions of vegetation and impervious surfaces are known to be important regulators of air temperatures in cities (Jenerette et al. 2007). The mean correlation coefficients for the 920 days in the study period were -0.03 (mean *p*-value= 0.67) for NDVI and 0.18 for percent imperviousness (mean *p*-value=0.32). The low coefficients and the non-statistically significant text itp-values indicate that co-kriging based on these co-variates will not yield reliable results. This could be explained by temporal mismatches between the observed daily *tmax* data and the co-variates: NDVI was based on a Landsat image acquired on 8 August 2013, while the percent impervious NLCD data represents annual conditions for 2006.

APPENDIX B

PERMISSION TO USE COPYRIGHTED MATERIALS

ASU Libraries
ARIZONA STATE UNIVERSITY

September 6, 2013

Juan Declet-Barreto
438 W. Nopal Ave.
Mesa, AZ 85210

Dear Mr. Declet-Barreto:

Thanks for your communication of September 5th regarding permission to publish our photographs in your dissertation entitled *A Socio-Ecological Understanding of Extreme Heat Vulnerability in Maricopa County, Arizona*, forthcoming in December 2013. With this communication we hereby extend our permission for use of the physical property contained in the photos you have selected. This permission is issued solely for publication in the dissertation you've described. Any requests for further duplication or reuse of the photographs should be directed to Archives & Special Collections for additional permissions.

The copyright (or intellectual property) status and proper citation of our photographs varies with each collection, and in some cases each photograph. I'll review each case below:

FP FPC 1 Box 10, Folder 2 #6: This vintage mounted print depicting a canal in a Phoenix barrio is a copy of an undated print by Phoenix commercial photographer Hartwell. ASU does not own rights to Hartwell's photographs and cannot extend permission for use of this intellectual property. However, since Hartwell died in 1908 and the last known reference to Hartwell's Studio is dated 1913 (Rowe, *Photographers in Arizona*, 1997), it is likely the rights to this image have entered the public domain. Should you choose to use the photo please cite it from the Barry Goldwater Historic Photographs, Arizona Collection, Arizona State University Libraries.

FP FPC 1 Box 10, Folder 2 #18: This vintage mounted print bearing the inscription "irrigating canal" bears no information identifying the photographer who made it or the date of production. ASU does not own rights to this photo and so we cannot extend permission for use of this intellectual property. Should you choose to use the photo please cite it from the Barry Goldwater Historic Photographs, Arizona Collection, Arizona State University Libraries.

FP FPC 1 Box 9, Folder 5 #29: This vintage mounted print identified as Monroe Street in Phoenix bears no information identifying the photographer who made it or the date of production. ASU does not own rights to this photo and so we cannot extend permission for use of this intellectual property. Should you choose to use the photo please cite it from the Barry Goldwater Historic Photographs, Arizona Collection, Arizona State University Libraries.

Since the intended application is an ASU dissertation we hereby waive the applicable commercial use fees.

I hope this information is useful to you Mr. Declet-Barreto. Please contact me if you have additional questions about our collections and services.

Sincerely,

Robert P. Spindler
University Archivist & Head
Archives & Special Collections
480.965.9277
rob.spindler@asu.edu